#4563

CMHC SCHL

Helping to house Canadians

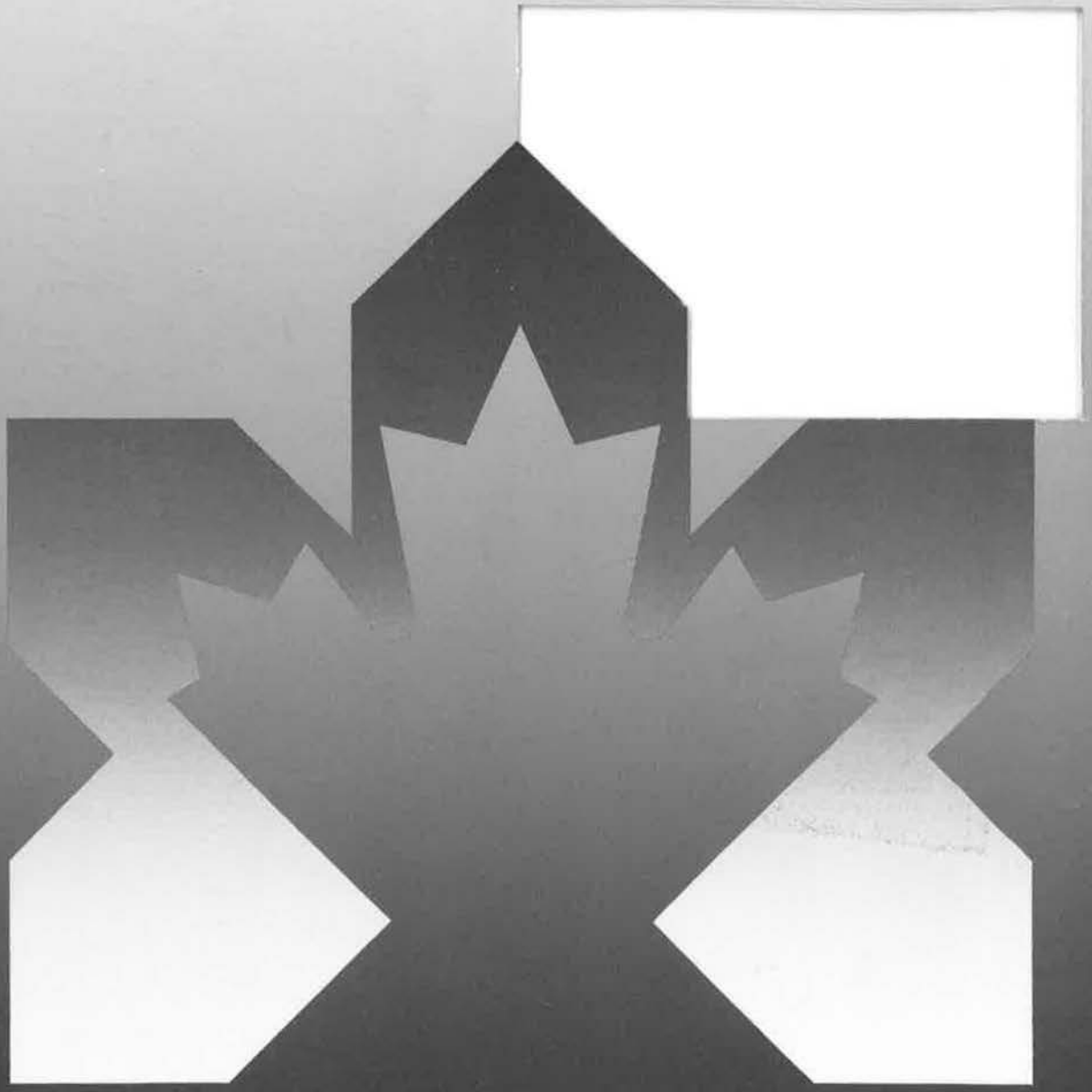

Canada

INDOOR AIR QUALITY TEST PROTOCOL FOR HIGHRISE RESIDENTIAL BUILDINGS

Final Report

Prepared for:

Mr. Jacques Rousseau
Project Manager
Project Implementation Division
Canada Mortgage and Housing Corporation
682 Montreal Road
Ottawa, Ontario

Submitted by:

Buchan, Lawton, Parent Ltd
5370 Canotek Road
Ottawa, Ontario
K1J 9E6

BLP File No: 2507
April 1990

Canada Mortgage and Housing Corporation, the Federal Government's housing agency, is responsible for administering the National Housing Act.

This legislation is designed to aid in the improvement of housing and living in Canada. As a result, the Corporation has interests in all aspects of housing and urban growth and development.

Under Part IX of this Act, the Government of Canada provides funds to CMHC to conduct research into the social, economic and technical aspects of housing and related fields, and to undertake the publishing and distribution of the results of this research. CMHC, therefore, has a statutory responsibility to make widely available, information which may be useful in the improvement of housing and living conditions.

This publication is one of the many items of information published by CMHC with the assistance of federal funds.

DISCLAIMER

This study was conducted by Buchan, Lawton, Parent Ltd for Canada Mortgage and Housing Corporation under Part IX of the National Housing Act. The analysis, interpretations and recommendations are those of the consultant and do not necessarily reflect the views of Canada Mortgage and Housing Corporation or those divisions of the Corporation that assisted in the study and its publications.

EXECUTIVE SUMMARY

This manual provides a protocol for the assessment of air quality in highrise residential buildings. The protocol is based on a three stage process: a preliminary assessment, simple contaminant measurements and, where warranted, complex measurements. The preliminary assessment consistes primarily of site inspections and occupant surveys. The second stage involves simple, usually inexpensive, contaminant measurements which, in most cases, identify the majority of problems. The final stage of the investigative process is requred only when careful evaluation during the first two stages has not identified both the causes and probable solutions to any detected problems.

Section 2.0 of the manual describes the preliminary assessment and specific contaminants of concern to air quality in highrise residential buildings. Section 3.0 provides a number of checklists to assist in the preliminary assessment process. Section 4.0 describes measurement techniques that a technologist could undertake to help identify a problem.

TABLE OF CONTENTS

1.0 INTRODUCTION

The investigation of indoor air quality in highrise residential buildings can be broken down into three basic stages:

- a preliminary assessment,
- simple measurements, and
- complex measurements.

The preliminary assessment consists primarily of site inspections and the investigation of potential problems or complaints. Essentially, it involves the application of common sense and observation in an attempt to identify the likely causes of problems.

Simple measurement techniques are those techniques which a reasonably knowledgeable, but not specially trained, technologist could undertake with the appropriate instruments and samplers. The results, in conjunction with information from the preliminary investigation, should identify the vast majority of problems.

The more complex measurement techniques may require the services of an expert in the field and are usually more costly. In most cases, they are necessary only if careful evaluation during the first two stages has not identified both the causes and likely solutions to the detected problems.

In general, achieving acceptable indoor air quality in a building requires:

- reducing, to as low as is practically possible, all contaminant sources;
- collecting and eliminating (exhausting) airborne contaminants as close as possible to their source;
- providing an adequate level of fresh air ventilation;
- using the space in a manner for which it was designed; and
- eliminating other environmental "stressors", physical or otherwise, to avoid confusing their effects with the effects of indoor air pollution.

In other words, it is not sufficient to ventilate a building according to recognized standards if there are particularly strong sources of contamination in the space; nor will ventilation be effective in removing odour if the flow path of ventilation air tends to spread odors rather than remove them at the source. No remedial action is likely to provide a cost-effective remedy if the right problem is not addressed. For example, there is no benefit at all to increasing ventilation rates if the root of an indoor air quality complaint lies with mould growth in a humidification system.

This manual provides a protocol for air quality assessments in highrise residential buildings based on a three stage process. Section 2.0 describes the preliminary assessment and specific contaminants of concern. Although this section contains little new information to people practicing in the field, it provides a good primer for those who are not familiar with Indoor Air Quality assessments.

Section 3.0 provides checklists to assist in the preliminary assessment process. This can be copied for use in individual buildings.

Section 4.0 describes measurement techniques that a technologist could undertake to help identify a problem. These have been categorized into simple and complex tests.

2.0 PRELIMINARY ASSESSMENT

2.1 General Procedure

The preliminary assessment consists of collecting information which could be helpful in identifying possible pollutants, locating their sources, assessing the effectiveness of ventilation systems, and defining the nature and severity of the problems experienced. Information can be obtained from building plans, complaint records, inspecting different areas of the building, and interviews with occupants, managers and others. No measurements involving instruments are made at this stage. The information collected will, however, enable the person conducting the investigation to choose appropriate locations for later testing.

The preliminary assessment provides the greatest single opportunity to find the true cause of an indoor air quality problem. Information gathering techniques normally employed at this stage include three steps: occupant response sampling, pollutant source identification, and general mechanical systems observation.

Useful tools include: a flashlight, a screwdriver, an adjustable wrench, a two metre step ladder, smoke pencils (to check air flow directions), and the checklists from Section 3.0.

Step 1: Occupant Response Sampling

This is often the first and most important source of information. Sources include: interviews, questionnaires, and records of complaints.

It is not possible to measure and observe everything at all times. Occupant feedback can greatly reduce the investigative effort required. Although the subjective judgement of the occupants may be in error concerning the true cause of an indoor air quality problem, their observations can be an important source of information concerning if, where, and when an indoor air quality problem exists. Determining whether there is a spatial, seasonal, or daily pattern to problems can assist greatly in pinpointing the cause of a pollution problem. As well, it should be determined whether the noted problems are individual to specific apartments or general to the building's common systems.

Step 2: Pollutant Source Identification

The second most important way to gather information is by observing possible air pollution sources during a building walk through. Visual observation, smell, breathing or eye discomfort, and common sense should provide the greatest clues to the type and size of pollutant sources which could be present.

Common sources that may be visually identified and associated with air pollutants include:

- garages (combustion byproducts),
- open sumps (radon and moulds),
- laundries (humidity, chemicals from cleaning products),
- garbage handling facilities (moulds, odors),

- condensate draining from air conditioners (moulds, fungi, bacteria),
- wet building materials (moulds, fungi, formaldehyde),
- humidifiers (moulds, fungi, treatment chemicals),
- new furnishings (formaldehyde and volatile organic compounds),
- occupant activities such as hobbies which use solvents, glues, or other strong sources,
- new paint, carpet glue, etc. (volatile organic compounds),
- outdoor air (a variety of pollutants),
- smokers (a great number of irritating and carcinogenic substances),
- fuel burning appliances (combustion products),
- swimming pools (chemicals, chlorine, humidity and associated biological growth),
- pets,
- cleaning agents, and
- cooking odors

In an apartment building, it is necessary to recognize that problems could be associated with sources in a specific unit or from common elements. It is necessary to access all units where problems have been noted.

Step 3: General Mechanical Systems Observation

If the previous two steps have not indicated a good reason for an air quality problem to exist, then the general condition and operation of the mechanical systems should be examined. This should include the determination of:

General Type

Constant Flow, Variable Air Volume, etc.

Air Flow Pattern

Most apartment buildings have simple ventilation systems where one or more fans pressurize the corridors and exhaust provisions are made in the individual units. The latter can be either individual fans or central exhaust fan(s) which service a number of units. This approach is supposed to establish a flow pattern which restricts pollutants and odors generated in a unit from spreading through the corridors. This "corridor-to-unit" flow pattern can be reversed by improper balancing of the corridor pressurization system or by environmental effects such as wind and stack forces and other mechanical systems. An example of this would be apartment buildings with central air conditioning systems in which the cool air supply to the unit is less than the removal rate through return grilles and exhaust systems.

Wherever strong sources exist, ventilation systems should be checked in order to ensure that they are performing in a reasonably satisfactory manner. In general, the ventilation system should exhaust strong sources directly outside.

Fresh air rates

- constant and economizer cycle;

Location of fresh air inlets

- and possible sources of exterior contaminants;

Local Exhausts

- where are they?
- what rules do they operate from?
- are they adjustable?

Controls

- type, mode of operation, general strengths and weaknesses, general condition and state of upkeep;

Details of operation

- hours of operation, strategy for operation of separate ventilation systems;

General condition and cleanliness

- of filters, humidifiers, cooling towers, air handling components;

Garage ventilation

- method, hours of operation, control, condition, operation against stack forces; and

Pool ventilation

- type.

Section 2.2 of this document describes some of the specific indoor air quality concerns potentially encountered in an apartment building. Section 3.0 provides checklists that can be used to organize the investigation process.

2.2 Specific Concerns

2.2.1 Carbon Dioxide

Carbon dioxide is produced both by the occupants of the building and by inadequately vented combustion devices. In office buildings, CO_2 is considered one of the prime indicators of a lack of adequate ventilation. In apartment buildings, population density is much less significant except perhaps in assembly areas which may have high "people loads" for relatively short periods of time. The CO_2 levels in most areas would not be expected to build up to the 800 - 1,000 ppm range common in offices. If it did, very restricted ventilation or another source of CO_2 would be expected.

Exhaust products from fuel-fired equipment could be a source of CO_2 if they are inadequately vented. If this is suspected refer to Subsection 2.2.2.

2.2.2 Carbon Monoxide/Combustion Products

CO, which is toxic, is primarily a product of incomplete combustion such as that which occurs in internal combustion engines. With clean burning flames, CO levels can be quite low and the primary product is CO_2. Nitrogen oxide is also formed in fuel burning operations. It has been noted as a problem with unvented appliances such as gas stoves.

The plans or discussions with the building operator and occupants will reveal the presence of possible problems in the building such as:

- internal parking garages,
- free standing fuel-fired heaters,
- kitchens with gas-fired stoves,
- furnace rooms for fuel-fired central heating systems and DHW systems,
- occupied areas close to any of the above, and
- air intakes close to other exhausts or to a street carrying heavy traffic.

2.2.3 Humidity

Health and Welfare Canada suggests that humidity levels be maintained between 30 and 80% RH in the summer and 30 and 55% RH in the winter.

Humidity levels below these ranges can result in symptoms of irritation, particularly in people who have respiratory problems. The primary concern with high humidity levels is that water can condense on cold surfaces, such as water pipes or poorly insulated walls and windows. This condensation can occur in concealed areas if air leakage leads to the cooling of exfiltration air in the building envelope. Water can damage the building in its own right, but it also provides one of the necessities for fungal growth. Constant wetting due to condensation can lead to mildew and other fungal growth. Some species of fungi are toxic, and a great variety of others cause allergic reactions in particular individuals.

The issue of biological contamination is dealt with in Subsection 2.2.8.

The level of humidity in individual apartments can be expected to vary a great deal depending on individual water generation rates and the level of ventilation. It is quite possible to have a localized problem affecting residents of individual units.

2.2.4 Formaldehyde

Plans or records of construction or renovation should indicate whether urea formaldehyde foam insulation (UFFI) may have been installed in the building envelope. If it was, the amount used should be determined and information obtained on efforts made to seal it from the indoor air. UFFI is potentially a strong source of formaldehyde.

Records should also indicate which parts of the building have been renovated (structural alterations, painting, replacement of ceiling tiles or carpets) in the past month. Formaldehyde is a component of many synthetic materials and adhesives. These areas should be inspected and the nearby residents should be interviewed.

Another potential source of formaldehyde is construction materials such as particleboard, particularly if it is wet. Sealing these materials can reduce emissions.

Normally, two coats of polyurethane varnish or vapour barrier paint are necessary for adequate protection.

Cleaning and maintenance procedures (such as washing walls and carpets or applying furniture polish) can also lead to the release of formaldehyde into the air. The timing of complaints should be checked to see if it coincides with activities of this type.

Symptoms of formaldehyde exposure include: difficulty breathing, eye, nose and throat irritation, headaches, coughing, fatigue, nausea and skin rashes. As these symptoms also occur with exposure to other organic compounds, they are not in themselves diagnostic of pollution due to formaldehyde.

Because many of the sources are building and furnishing materials, the emission rate should be fairly constant. Thus, if ventilation rates vary, symptoms will be worse in periods of low ventilation. If the timing of symptoms correlates with cleaning activities, this is reasonable evidence that the cleaning materials are responsible. However, chemicals other than formaldehyde in the cleaning materials could also be responsible.

In all likelihood, the only formaldehyde sources which are likely to be identified during the preliminary assessment are poorly sealed UFFI and large amounts of unsealed particleboard or plywood. It is much more probable that an apartment building will contain a myriad of weak sources. These can be difficult to identify. It is possible that the preliminary assessment will not provide evidence for a formaldehyde problem and the simple measurement techniques of Section 4.0 will be required.

2.2.5 Particulates

While particulates (dust and fibres) are not usually a problem in apartment buildings, an inspection (walk through) of recently renovated areas, the mechanical rooms, and any areas from which complaints have been received should be carried out.

The most likely sources of particulates inside a building are:

- renovations,
- outdoor air,
- ventilation ducts,
- humidifier deposits in areas with hard water, and
- smoking.

The evidence pointing to each of these sources is indicated below. As in the case of some other air pollutants, symptoms arising from exposure to particulates are non-specific and should not be used to identify sources in the absence of physical evidence for their existence.

- Renovations involving structural changes will almost certainly cause a particulate problem. However, since the particles tend to be large, the problem should not extend far beyond the space being altered (unless particles are carried by the ventilation system); nor should it persist for long after the renovations are completed.

- Outdoor air is unlikely to be the cause of particulate problems if properly maintained filter systems are installed in the air intakes. However, if there is

no filter system and any type of loose material is observed around the intake, then outdoor air may be implicated. Allergies appearing during the pollen season are also probably caused by outside air (pollen could be removed by a filter unit).

- Dirt around the diffusers indicates particulates are being introduced into the area by the ventilation system. These particulates may originate in the ventilation ducts if the building is old, if the ducts have never been cleaned or if there is insulation on the inside surface of the ducts.

- Chalky deposits around diffusers may be hard water minerals coming from humidification equipment. Observation of hard water deposits on humidifier vanes, complaints of dust, cement, or plaster-like odors when the humidifiers are operating or after they have been cleaned would provide additional evidence. Obviously, problems from this source will be most severe in winter.

Symptoms of particulate exposure include: dry eyes, nose, and throat, and the effects of dust irritation such as coughing, sneezing, and respiratory allergies.

2.2.6 Radon

Radon is an odorless gas originating in the soil. It can be introduced through below-grade air leakage and, under certain circumstances, dissolved in water. The following areas should be inspected for below-grade entry paths:

- basement or sub-basement areas
- rooms containing sump pumps
- areas where large volumes of air from the basement could be entering the above-grade portion of the building (such as through the top of the stairwell or through the elevator shafts).

During or after the inspection, the following questions need to be answered:

- Is there ventilation in these areas?
- Do people spend a significant part of the day in any of these areas?

There is a real possibility of problems with radon at a location if the following three conditions are met:

- The location has a potential strong source of radon, such as contact with the soil;

- Ventilation in that part of the highrise is minimal or absent, or there are odors (which are a useful indication of whether existing ventilation is operating properly); and

- People spend time in these areas, or nearby.

2.2.7 Volatile Organic Compounds

Many different chemicals can originate from building materials, furnishings, fixtures and the materials kept by occupants of a building. The concentrations of volatile organic compounds (VOCs) are likely to be low, however, unless there are major sources and/or very poor ventilation. Potential sources include:

- storage areas for chemicals such as pesticides, painting and solvents;

- cleaning and maintenance activities (including painting, recarpeting, structural changes and sealing); and
- occupant activities, such as hobbies, that use solvents.

Building records, maintenance schedules, and interviews of occupants should be used to obtain basic information about the building and the location of potential sources. These areas should then be inspected.

The symptoms experienced by people exposed to VOCs include: coughing, sore throat, faintness, nausea, fatigue, headaches, watery eyes, blurred vision, nervous stomach, skin irritation and allergies. These are non-specific and are not usually sufficient to identify individual chemicals. For this reason, the nature of the symptoms is less useful than information about when and where it was noticed.

2.2.8 Biological Contamination

Moulds and their spores are the most common type of biological contamination found in residential buildings. Some species of mould induce allergic reactions in a very broad spectrum of people, while other species are toxic to a select number of people only. Biological contamination is primarily found when suitable wet or damp breeding grounds exist. Therefore, one of the most important things to look for is signs of periodic wetting or an indication of a "water crisis" occurrence such as flooding or an overflow.

Fungal growth on surfaces like walls and ceiling tiles is usually dark brown or black. Green, white, blue-green and yellow colors can also occur with some species. Fungal colonies can be dense dark piles of spores that are slightly raised above the surface of their substrate. The spore of well developed colonies can be removed by rubbing. Examine the top side of removable ceiling tile. Things which could be mistaken for fungal growth include rust staining and burn marks (plumbing torches).

On carpets that remain damp and undisturbed (no traffic), fungus may develop as visible black, grey, or green patches on the surface. These patches can be circular in shape if they start at a point where they can radiate in all directions without being disturbed or interrupted. More likely, fungal colonies will form on the jute backing or underpad of the carpet. One should look for carpet stains that indicate water activity, such as evidence of stretching and rusty nails in the tack strip. If these are noticed, try to peel back the carpet at a convenient point and examine the jute backing and underpad for staining. Most species of fungus usually show as brown or black areas, but they can also appear as olive green, green, blue-green or yellow-green. Not all stains on the underside of a carpet will be fungal. Coffee and coke spills and other water stains are virtually indistinguishable from fungal colonies when viewed by the unaided eye. If the carpet was wet for more than a week, repeatedly soaked, or in a traffic area that brings in moisture on shoes and boots, fungal development is inevitable on carpets containing biodegradable fibres (i.e., jute) or on top of foam underpads.

A large number of fungi will rapidly colonize materials like cardboard boxes, clothes, and paper. First check for dampness on the surfaces in contact with the floor. Look for mould colonies as described above. Colonies growing across clothing may give it a peppered appearance. The "pepper" can be large spores of some fungus species.

In standing water, bacteria or algae (when visible) will add cloudiness to the water, form slime or accumulate in a bottom sludge. Only a few groups of fungi will develop

in water, but colonies are likely to occur just above the waterline as a black "tub" ring. Mineral precipitates could also form in water as a sludge and confuse the issue.

Some general guidelines for assessing the likelihood of microbial contamination in a building are indicated below:

- The presence of slime or mould in a humidifier or air-conditioning system or of mould in any of the ducts leading into or out of these units indicates a problem.
- Similarly, mould in ducts or on the surface of diffusers or exhaust louvres in an occupied area is a bad sign.
- The degree of contamination will increase if the ventilation is turned off for an extended period of time. The symptoms are likely to be more severe because of the lack of ventilation.
- Where there is a mouldy odour, there is probably also mould--although its location may not be immediately obvious.
- Damp spots on walls may be accompanied by fungal growth in the wall cavity.
- The temperature in the hot water tank should be maintained at a minimum of 75° C to eliminate legionnella bacteria.
- The spatial distribution of illness or complaints can be useful. If problems are widespread in the highrise, the contamination is probably in some part of the mechanical system.
- Problems are likely to be seasonal, involving humidifiers or condensation in winter and central air-conditioning systems in summer.

2.2.9 Ozone

Ozone can have significant, irritating effects on people. The primary source of ozone is arcing from high-voltage electrical systems; most notably from poorly operating electrostatic precipitators. These are not common in apartment buildings. If irritating symptoms are encountered where such units are operating, however, those units should be checked for cleanliness and a high level of arcing (snap and crackle on discharge). A second, relatively unlikely source of ozone is the high-voltage electric circuits in electrical vaults. Again, the problem is related to a dysfunction, and normally operating systems should not be producing ozone at significant levels.

2.2.10 Asbestos

Airborne asbestos fibres are a major air quality concern since asbestos is a known carcinogen. Asbestos was used as a high temperature pipe insulation and for fire protection of the structure. If it is fully contained so that fibres cannot escape into the air, it is of little concern unless renovations are planned. However, where coverings have degraded or were non existent, there certainly is potential for air contamination. Plans and inspections should determine if asbestos was used in construction and the potential for fibre release.

3.0 ASSESSMENT CHECKLISTS

This section contains two checklists. One for the building assessment and one for occupants to fill out.

The building assessment checklist has three sections:

I Building Common Areas
II Mechanical Systems and HVAC Operation
III Individual Apartment/Complaint Areas

Obviously, a number of the Section III checklists could be used in one building; and in some buildings, there may be enough of a separation of HVAC equipment to warrant use of separate Section II sheets.

The questions on the sheet are numbered 1 to 40. In many, there are supplementary questions noted as (a), (b), (c), etc. which are to be filled in if the answer to the main question is "YES".

In general, the "YES" answer implies there may be a source of air quality problems in this area.

Section 3.1 provides some advice on how to assess the response to individual questions.

I BUILDING COMMON AREAS

1. What year was the building constructed? _____
   a) Are the as-built design diagrams for this building missing? yes / no
   b) Are the current design diagrams for this building missing? yes / no
   c) Are the operating and maintenance manuals for the building's HVAC system missing? yes / no
   d) Is there no routine maintenance program for the HVAC system? yes / no

2. Have any areas been recarpeted recently? yes / no
   a) If YES, did odors persist for more than a week after carpet was laid? yes / no
   b) If YES, describe locations:

      _____

      _____

3. Have any areas been repainted recently? yes / no
   a) If YES, did odors persist for more than a week after the paint was applied? yes / no
   b) If YES, describe locations:

      _____

      _____

4. Has there been a recent or is there a regular cleaning process which uses large amounts of chemicals or solvents? yes / no
   a) If YES, what were the chemicals?

      _____

5. Is there a fuel-fired central heating unit or DHW system? yes / no
   a) Is there any physical evidence of leakage of combustion gasses from the furnace into the furnace or flue room or nearby areas? yes / no
   b) Is there the odour of combustion fumes in the room? yes / no

6. Is there an enclosed parking garage? yes / no
   a) Was the ventilation system found in an inoperative state? yes / no
   b) Is the ventilation system turned off for periods? yes / no
   c) Is the ventilation system controlled? yes / no
   d) Are there carbon monoxide sensors in the garage which control ventilation? yes / no
   e) If so, have they been recently calibrated? yes / no
   f) Are there obstructions in the exhaust or air inlets? yes / no
   g) Are stack forces sucking air from the garage into the building? (check at access doors) yes / no

7. Is there a garbage handling facility? yes / no
   a) Is the vent system off or ineffective? yes / no

b) Is there an air flow pattern from garbage rooms or chutes into the rest of the building? yes / no

c) Is there an unusually bad odour or mouldy smell associated with system? yes / no

8. Is there a pool, hot tub, sauna, or workout room? yes / no

a) Does maintenance and cleaning appear to be irregular or inadequate? yes / no

b) Are there any "mildew" stains on walls, ceilings, floors, fixtures or items such as like shower curtains yes / no

c) Is there any condensation on walls, floors, windows or ceiling? yes / no

d) Does humidity appear very high? yes / no

e) Do any biodegradable products (wood, etc.) get wet regularly? yes / no

9. Are there any basement or sub-basement areas or crawl spaces with dirt floors? yes / no

a) Are there occupied areas nearby? yes / no

If YES, describe locations:

_____

_____

b) Do these spaces lack ventilation? yes / no

Are there musty odors in these areas or nearby? yes / no

10. Are there rooms with sizeable holes in the walls or floor, such as sump pits, gas and water entrances, cracks, etc.? yes / no

a) If YES, describe location(s):

_____

_____

b) Do these spaces lack ventilation? yes / no

c) Are there musty odors in these areas or nearby? yes / no

11. Is there foam insulation in the walls of the building? yes / no

a) The type of insulation is polyurethane / polystyrene / urea formaldehyde / unknown.

12. Do drawings show asbestos insulation for pipes, fire protection of structure, etc.? yes / no

a) If YES, does inspection reveal loose fibre especially near air handling equipment and ducts? yes / no

13. Has there ever been a "water crisis" such as a flood or overflow? yes / no

14. Are there any signs of moisture problems such as:

a) stains or dampness on walls, floors or ceilings? yes / no

b) stained, streaked, or damp carpets? yes / no

c) mouldy odors, or musty smells? yes / no

II MECHANICAL SYSTEMS AND HVAC OPERATION

If the building contains two or more towers or wings, each controlled by a different HVAC system, a copy of this sheet should be filled out for each.

15. Describe ventilation system:

_____

_____

_____

_____

16. Is the amount of fresh air used by the ventilation system the same all year round? yes / no

17. Is the ventilation system of the recirculating type? yes / no
    a) Does the HVAC system use an economizer cycle? yes / no
    b) What is the maximum percentage of fresh air used? ____%
    c) What is the minimum percentage of fresh air used? ____%
    d) What is the fresh air percentage just now? ____%

18. Air supplied to the floors by:
    constant volume systems / variable air volume (VAV) system / heat pumps / other / unknown?

19. Is there a corridor pressurization system? yes / no
    a) Is the "corridor-to-apartment" flow reversed? yes / no

20. At what temperature is the tank supplying hot water to the building maintained? ____°C

21. Are there distinct fresh-air intakes for the building HVAC system? yes / no
    a) Are there intakes below third floor level and above a busy street? yes / no
    b) Are there intakes within 10 metres (30 feet) of the entrance or exit to a parking garage? yes / no
    c) Are there intakes within 10 metres (30 feet) of the exhausts of this or an adjacent building? yes / no
    d) Are intakes near standing water or a cooling tower? yes / no
    e) Is there a build up of organic debris near the intakes? yes / no
    f) Are there any other sources of pollution near any of the intakes? yes / no

22. Does this building have a particulate (dust) filter system installed in the fresh air intake? yes / no
    a) Are the filters missing? yes / no
    b) Are the filters changed less frequently than recommended by the manufacturer? yes / no
    c) Do the filters fit so poorly that air bypasses them at the edges? yes / no
    d) Are the filters matted or dirty? yes / no
    e) Are the filters wet? yes / no

23. Are spray humidifiers used in this building? yes / no
    a) Are the spray humidifiers supposed to operate at this time of year? yes / no
    b) Are the spray humidifiers operating now? yes / no
    If YES, answer the questions below:
    c) Are the spray humidifier pans plugged so that they are not draining properly? yes / no
    d) Is there slime in the humidifier pans? yes / no
    e) Are there mouldy odors? yes / no
    f) Is there mould in the ducts near the humidifiers? yes / no
    g) Is there evidence of foaming in the humidifiers? yes / no
    h) Is the water hard in this region? yes / no
    i) If so, are there hard water deposits on the vanes? yes / no
    j) Are the hard water deposits removed by scraping the vanes and blowing the dust into the ducts? yes / no

24. Are steam humidifiers used in this building? yes / no
    a) Are the steam humidifiers supposed to operate at this time of year? yes / no
    b) Are the steam humidifiers operating now? yes / no
    If YES, answer the questions below:
    c) Are chemicals used in the boiler or the pipes to protect against corrosion? yes / no
    If YES, state names of chemicals:

    _____

    _____

    _____

25. Does this building have an air-chilling system? yes / no
    a) Is the chilling system supposed to operate at this time of year? yes / no
    b) Is the chilling system operating now? yes / no
    If YES, answer the questions below:
    c) Are the condensate trays cleaned less often than once a week? yes / no
    d) Is there slime or growth in the condensate trays? yes / no
    e) Is there dirt on the cooling coils? yes / no
    f) Are there mouldy odors in the system? yes / no

26. Are the ventilation ducts or plenums insulated? yes / no
    a) Is the insulation on the inside and directly exposed to the moving air? yes / no
    b) Is it more than five years since the ducts or plenums were last cleaned? yes / no

27. Are there any signs of condensation in ducts? (Check cold spots such as near inlets and after cooling coils first.) yes / no

III INDIVIDUAL APARTMENT/COMPLAINT AREA OBSERVATION SHEET

No:_____

Where in the building do these observations apply? Please give the floor, room or apartment number or briefly describe (e.g. main lobby, everywhere):

_____

_____

Please answer all questions by circling or filling in the answers as required.

28. General Observations
    a) Are there damp spots or mould on the walls or ceiling? yes / no
    b) Are any of the carpets, curtains, etc. damp? yes / no
    c) Are there many potted plants in this area? yes / no
    d) Is there mould on the plants or their pots or soil? yes / no
    e) Do mites appear to be on the plants? yes / no
    f) Are there pets in the unit? yes / no
    g) Are there odors here? yes / no
    h) Which of the following best describes the odour?
    auto exhaust / diesel fumes / furnace room / heating system / pet odors / body odour / mouldy or musty / chemical / like solvent / (wet) cement or plaster / dusty / chalky
    i) Are people using fans to create more air movement? yes / no
    j) Is there much dust visible on flat surfaces? yes / no
    k) Is there evidence of condensation on windows or walls? yes / no

29. Are there **air supply diffusers**? yes / no
    a) Can you see any of the following around the diffusers?
    mould / chalky dust / dirt marks yes / no
    b) Are any of the air supply diffusers blocked by furniture, paper, or other obstructions? yes / no

30. Are there any **air exhaust fans** or **louvers** in unit or complaint area? yes / no
    a) Do they have a poor drain rate? yes / no
    b) Are there dirt marks around the air exhaust louvers? yes / no
    c) Are any of the air exhaust louvers blocked by furniture, papers or other obstructions? yes / no

31. Has carpeting or furniture been installed in the last three months? yes / no

32. Are there large areas of particleboard sheathing or furnishings? yes / no

33. Is there a gas stove? yes / no
    a) Are there exhausts to remove combustion gasses produced by the stoves? yes / no
    b) Are the stoves operated without exhaust fans on? yes / no

34. Is there a wood or gas fireplace in the area? yes / no
    a) Does it appear to be poorly vented? yes / no
    b) Does it appear to have inadequate supply air? yes / no

35. Is there a freestanding heater (gas or kerosene)? yes / no
    If YES,
    a) Are these heaters used in anything but well ventilated spaces? yes / no
    b) Is there an odour of combustion fumes in the room? yes / no
    c) Is the room exhaust recirculated rather than directly expelled outdoors? yes / no

36. Is there a refrigerator in the unit? yes / no
    a) Does anything in the fridge look mouldy? yes / no
    b) Is the refrigerator drain blocked? yes / no
    c) Is the drain pan wet and mouldy? yes / no
    d) Are the heat exchangers dusty? yes / no

37. Is there mould on bathroom tiles, walls or ceilings? yes / no

38. Are there humidifiers or dehumidifiers in the unit? yes / no
    a) Do the drip pans, coils, and water in these units have accumulation of dust, slime, sludge or mould? yes / no

39. Are there small but steady leaks in, around, under or behind sinks, toilets, tubs and/or sewers? yes / no

40. Are there poorly sealed mechanical/electrical chases or other entry paths for contaminants from outside the unit? yes / no

OCCUPANT COMPLAINT SHEET

Where in the building are your complaints worst? Please give the floor, room or apartment number or briefly describe (e.g., main lobby, everywhere):

_____

_____

Your answers to the questions below apply to this location. Where a choice is given, please circle the most appropriate answer. Enter your own answer where requested. Space for comment is provided.

1. Describe the usual temperature at this location:
   okay / too hot / too cold / sometimes too hot, sometimes too cold

2. How would you usually describe the air here?
   okay / drafty / stagnant / stuffy / stale / dry

3. Are you bothered by odour at this location? yes / no
   If YES, how often do you smell this odour?
   rarely / occasionally / frequently / all the time
   Which of the following best describes the odour?
   auto exhaust / diesel fumes / furnace smell / heating system / body odour / mouldy or musty / chemical / like solvent / (wet) cement or plaster / dusty or chalky smell
   What do you think causes the odour?
   _____

4. Can you "fix" any of the problems noted above? How? yes / no

5. Has there ever been a "water crisis", such as a flood or overflow, in this area or on the floor(s) above it? yes / no

6. Do you have a history of allergies? yes / no
   If YES, the type of allergy is:
   respiratory / skin / food / other
   Are your allergies worse while you are in this building? yes / no

7. From which of the following do you suffer that you think are due to the building?
   headache / tiredness / faintness / dizziness / nausea / stomach problems / skin irritation / dry eyes / itching eyes / watery eyes / blurred vision / stuffy nose / runny nose / sneezing / sore throat / dry throat / chest problems / coughing / asthma

8. What time of day are your complaints worst?
   morning / afternoon / evening / night / the same all the time
   What day of the week are your complaints worst?
   weekday / weekend / the same all week

9. Do the symptoms coincide with or occur soon after cleaning or maintenance activities in this area? yes / no

If YES, describe this activity:

Comments:

3.1 Assessment Summary

In general, three factors must be addressed before the decision is made whether an air quality problem warrants further investigation. They can be remembered as **PIP**--People, Inadequate Ventilation, and Pollutants. The presence of people is important; problems can sometimes be tolerated in unoccupied areas such as basement mechanical rooms. The level of ventilation provided to a space generally must balance the level of contaminants produced in that space; adequacy should be judged based on looking at both factors.

The assessment checklists are designed so that a 'YES' answer to a question implies that a problem is possible, not that there is one. With the subsidiary questions, the more yeses, the more likely a problem exists. The following notes refer to the question numbers of the assessment form and provide some guidance in this judgmental process:

Question No.

1	Clarifies the adequacy of the information on which the assessment is based
2 through 14	Assesses the pollution sources in the building. Specific possible concerns by question are as follows:
2 through 4	Volatile Organic Compounds
5	Combustion products related to heating systems
6	Carbon Monoxide from parking garages
7	Odors and biological contamination associated with garbage
8	Humidity and related fungal growth
9	Radon and humidity related fungal growth
10	Radon
11	UFFI
12	Asbestos
13 and 14	Fungal Growth

II Mechanical Systems and HVAC Operation

15 through 19	define what kind of controlled mechanical ventilation is provided in the building. Many highrise residential buildings do not have circulation systems, but are ventilated through natural driving forces through infiltration by a corridor pressurization system.
20	If the temperature is higher than 60°C, Legionnella bacteria are unlikely to survive and breed.

21 Carbon monoxide can be a problem if intakes are either just above a busy street or close to a loading dock or parking garage that has been identified as a potential problem source. Contaminated air from an exhaust can re-enter the building if intakes and exhausts are too close together. Organic debris or standing water can lead to biological contamination.

22 Particulates may be a problem if there are no filters or if they are poorly maintained. Constantly wet filters can be a breeding ground for fungi.

23 Biological contamination can be caused by spray humidifiers if the pans are not kept clean. If there is a high level of dissolved minerals in the water, particulate problems can also result.

24 Chemicals used to protect the boiler or steam pipes may enter the ventilation system and be distributed around the building.

25 Biological contamination can result if the air conditioning system is not cleaned regularly. This is related primarily to bacterial or biological growth in standing water from condensate.

26 Particulates or insulation fibres (especially dirt) originating in ducts can sometimes be accumulated if the ducts are insulated on the inside.

27 Biological growth can result from condensation. Odors are one external clue. Direct observation can be difficult.

28 General observations give clues that there may be a problem

29 Look for any indication of dirty duct work creating particulate problems of poor air distribution caused by blocked air inlets

30 Same as above only in the opposite direction

31 and 32 Primarily concerned with formaldehyde VOCs emitted from glues and solvents in the furniture

33 through 35 Combustion products

36 through 39 Common sources of fungal contamination

40 Looking for possible entry routes of contaminants produced outside of the unit.

4.0 MEASUREMENT METHODS

4.1 Suggested Measurement Capabilities

In most cases, the findings of the preliminary assessment would determine which contaminants to measure in a particular building. In situations where a test kit suitable for a broad range of buildings is desired, the following measurement capabilities are suggested. They have been selected for relevance, accuracy, level of simplicity and cost.

Temperature and **humidity** should be assessed in most cases. A variety of tools are available for sampling humidity. Buchan, Lawton, Parent Ltd. has had success with relatively simple aspirated psychrometers. As well, a number of electronic instruments, most notably the Vaisala HMI 31 series, are accurate and simple to use. We do not recommend the use of the manual, sling-type psychrometer because accuracy depends so much on the operator.

A GASTEC sampling pump and Colorimetric tubes for **carbon dioxide, carbon monoxide, ozone, formaldehyde** and **hydrocarbon solvents** can be good screening tools. The accuracy of these tubes is only ± 25% and the range of some tubes, particularly hydrocarbon solvents, does not detect down to the low levels of pollutants that may indicate concern about long-term exposure. They can, however, provide a simple to use, relatively inexpensive indicator of major problems.

An **Infrared Carbon Dioxide Analyser** (Buchan, Lawton, Parent Ltd uses the Nova 305 SBDL, but there are several others including the Fuji ZFP5, the Horiba APBA 210, and the GASTEC R1-411 which have been evaluated as satisfactory by Public Works Canada).

An electro-chemical **carbon monoxide detector**. (Buchan, Lawton, Parent Ltd. uses the dual purpose Nova 305 SBDL. Public Works Canada has judged the CO 260 monitor from Industrial Scientific Devices as satisfactory. This is available from at least one rental company).

A chemical sampler for **formaldehyde**. When limited time is available, Public Works Canada recommends the STC formaldehyde monitoring kit which uses a passive bubbling sampler and individual reagent tablets. This method is relatively simple and self-contained. For residential occupancies, longer term sampling is more appropriate. One suitable sampler is the Air Quality Research Incorporated PF 1 sampler which requires laboratory services and, therefore, can be relatively expensive to use in any quantity. It is well recognized, however, and very easily used.

A number of electronic measuring devices are available for measuring **respirable suspended particulates** which use either a light scattering or piezoelectric mass monitoring principle. These instruments are really not suited for the low level of particulates expected in an apartment. We would not, therefore, suggest measuring particulates as a normal activity unless a problem is suspected. If this is the case, it is usually simpler to use a gravimetric method involving the sampling of air through a filter. The filter is weighed before and after sampling to find the weight of the particulates collected. The sampling pumps are relatively expensive (about $1,500), but at least one rental company rents them individually or in groups of five for reasonable daily rates. The dust can be examined through a microscope to determine whether it contains asbestos or other specific materials.

Radon samplers come in a variety of forms. Charcoal canisters are most commonly used, but Buchan, Lawton, Parent Ltd. prefers the **R.A.D.** system involving an active sampling approach measuring radon daughters (output in working levels). The R.A.D. system is typically deployed for one week.

Measurement for airborne **biological contamination** cannot really be considered a simple measurement technique. A number of sampling methods (Anderson Sampler and Biotest RCS Unit) can provide an assessment of the level of airborne particles that can grow into fungal colonies on agar plates or strips. The results can be misleading and ultimately the species and source of innoculum should be determined. Samples of contaminated material should be sent to an expert for evaluation. (Buchan, Lawton, Parent Ltd. uses Residential and Industrial Fungal Detection Service, 4 Birkett Street, Nepean, Ontario K2J 2V8). If biological contamination is suspected, samples of the following sizes should be taken from the potential problem areas noted during the preliminary assessment.

Size and Type of Sample Required for a Biological Contamination Assessment

Standing water - a 30 ml sample collected in a sterile bottle.

Dust (from ducts etc.) - 2-5 ml samples collected in a sterile bottle.

Walls and Ceilings - the best sample is a 200 mm x 200 mm piece of the material itself. Where this is not possible, a number of 20 mm X 20 mm paint chips in a pill bottle or film cannister will do.

Carpet - If the carpet is to be discarded, several 200 mm X 200 mm pieces in separate envelopes is suggested. If this is not an alternative, use a sharp knife or scissors and tweezer to collect several stained fibers from the jute backing. Transport in a pill bottle or film canister.

The cost of sampling for **Volatile Organic Compounds** removes it from the "simple measurement" category. However, if arrangements are made with a laboratory which does airborne VOC analysis, collection of the samples can be done by "non-expert" personnel. If the laboratory is supplying sampling equipment, their instructions should be followed.

Another tool which can provide some information about the general "healthiness" of the indoor air, rather than measuring for specific contaminants, is a method called a **bioassay.** Bioquest International has developed one type of bioassay. Passive absorbent tubes are used to collect organic gases and particulates. The resulting mixture is introduced to colonies of nemotodes. Depending on how the colony grows in numbers compared to a control colony, a judgement can be made about the overall "healthiness" of the air.

More details on this equipment are provided later in this section, as well as information such as the target levels for gases measured, suppliers, range and accuracy.

4.2 Where and When to Measure

Assuming that potential air quality problems warranting investigation by measurement have been identified through the Building Checklists, the investigator would proceed to the second stage - measurement with simple instruments. When measuring pollutant concentrations, it is not enough to simply go to the areas indicated through the Checklist that may be the source of a problem and take measurements when it is convenient. Such data may be quite meaningless for a number of reasons:

- The severity of the problem may vary depending on the time of day and the day of the week.
- Outdoor air varies from place to place, and this is going to affect the air indoors.
- The equipment might not be working correctly.

For an effective assessment, it is important to choose the appropriate sampling time and to establish a baseline for the data by taking measurements at "control locations" for comparison to measurements made at the test locations. This approach allows adjustments for variations in outdoor air quality and compensates for some equipment malfunctions.

Suitable control locations are:

- the air intakes
- another outdoor location (if there is a chance that the intake air is being contaminated)
- places indoors assumed to be free of the pollutant being measured

Test locations should include:

- places the Checklist indicates may contain a source of the pollutant being measured
- complaint locations (pollutants can move around a building in surprising ways)
- the air exhausts

The monitoring of pollutants arising from the building structure, furnishings or ventilation (formaldehyde, some volatile chemicals, biological contamination, etc.) is not usually sensitive to time. However, pollutants generated by the occupants (such as carbon dioxide) or their activities (hobbies, cleaning, parking, etc.) are best checked when these activities have occurred.

The time of year also has to be taken into account. If the building has a variable air handling system, fresh air rates are likely to be less during very cold or very hot weather, the pollutant concentrations, therefore, will generally be higher in mid-winter and mid-summer. Some sources are also seasonal: humidifiers in winter, heating equipment in winter, air conditioning systems in summer, pollen in summer, etc.

The above discussion provides some general criteria to use when choosing where and when to make measurements. A more detailed examination of suitable locations for

taking control samples are listed in Table 4.1. Table 4.2 identifies suitable sampling locations and times for taking test samples. Table 4.2 refers to the pollutant sources and complaint locations identified in the Building Checklists.

Control locations are not used for temperature, relative humidity, and air movement measurements since these parameters are controlled by the mechanical systems of the building. Indoor values are expected to be different from outdoor values.

Usually, it is best to do the control and test measurements together, choosing a time appropriate for the test locations.

Table 4.1

SUITABLE CONTROL LOCATIONS FOR MEASURING POLLUTANTS

Pollutant	*Suitable Control Location*
Carbon Dioxide	- air intakes (if not contaminated) - outdoors - street level or roof - indoors - unoccupied area
Carbon Monoxide	- air intakes (if not contaminated) - outdoors - roof or upper floor - indoors - above second floor
Formaldehyde	- air intakes (if not contaminated) - outdoors - roof or upper floor on the building side of particulate filters - indoors - unoccupied area
Particulates	- air intakes (if not contaminated) - outdoors - roof or upper floor on the building side of particulate filters - indoors - unoccupied area
Radon	- outdoors - sheltered area (no wind or rain) - indoors - above second floor
VOC	- air intakes (if not contaminated) - outdoors - street level or roof - indoors - away from identified pollutant sources
Biological Contamination	- air intakes (if not contaminated) - outdoors - roof - indoors - area with no mould, water or plants

Table 4.2

TEST LOCATIONS AND IDEAL TIMES FOR MEASURING POLLUTANTS AND OTHER PARAMETERS

Pollutant or Parameter	*Test Locations*	*Time to measure*
Carbon Dioxide	- pollutant sources	- when heavily occupied - when fresh air rate low - when combustion products could be produced
Carbon Monoxide	- pollutant sources - complaint areas - stairwells linked to sources - elevators linked to sources - exhausts	- when fresh air rate low - when combustion products could be produced
Formaldehyde	- pollutant sources (building) - complaint areas	- when fresh air rate low
Particulates	- pollutant sources - complaint areas - exhausts	- when source is suspected
Radon	- pollutant sources	- when fresh air rate low
VOC	- pollutant sources (building) - complaint areas - exhausts	- when fresh air rate low
VOC	- pollutant sources (activity) - complaint areas - exhausts	- late morning - late afternoon - when fresh air rate low - after cleaning/ maintenance
Biological Contamination	- pollutant sources (building) - complaint areas	- when fresh air rate low - summer
Humidity	- supply air - complaint areas	- midwinter - midsummer
Air Movement	- near diffusers	- while the ventilation system is operating

4.3 Contaminants and Measurement Methods

The following pages provide information on the contaminants discussed in this report and the measurement methods suggestioned by the authors of this report and the Architectural and Building Services Division of Public Works Canada.

In general, a number of optional instruments or methods are provided. It is likely that the availability of a particular instrument or method will be a major factor in a user's final selection. With each contaminant, "user notes" provide some guidance on the use of the instrument or method for measuring indoor air contamination levels. In these instructions, it has been assumed that the user has obtained and read the operations manual of the instrument in question.

4.3.1 Simple Measurement Methods

Contaminant:	**TEMPERATURE and HUMIDITY**
Sources:	HVAC and enclosure problems
Permissible Exposure Limits: (Residential)	*Humidity:* Health and Welfare Canada 30 - 80% RH summer 30 - 95% RH winter ASHRAE RH 25 - 65% *Temperature:* Winter 20 - 24°C Summer 22 - 26°C
Instrumentation:	VAISALA HMI-31/HMP-31UT ($1,000)
Supplier:	Hoskins Scientific 1156 Speers Road Oakville, Ontario
Rental Suppliers:	
Principle of Operation:	Temperature: Platinum Thermistor RH: Thin film plymer capacitor
Range:	Temperature: -40°C to +80°C RH: 0-100% RH
Accuracy:	Temp: ± 0.3°C RH: ± 2% RH in 0 - 80% range, ± 3% in 80 - 100% range
Other Instruments/ Methods:	Solomat MPM Series Aspirated Psychrometers

Contaminant:	**CARBON DIOXIDE** (CO_2)
Sources:	Human metabolism, combustion
Permissible Exposure Limits:	Health and Welfare Canada - 3,500 ppm Suggested limit for offices - 1,000 ppm
Typical Residential Indoor Levels:	400 - 600 ppm
Health Effects:	Headache, dizziness, drowsiness
Instrumentation:	- NOVA 305 SBDL, 306, 390 (3,500) - Fuji ZFP5 ($3,300) - Horiba APBA 210 ($4,200) - GASTEC RI-411 ($3,400)
Suppliers:	NOVA, Analytical Systems Inc. 7 Lansdowne Avenue Hamilton, Ontario Safety Supply Canada Analygas System Ltd., Scarborough Levitt-Safety Ltd
Rental Suppliers:	
Principle of Operation:	Non Dispersive Infrared (NDIR) Air is sampled and passed through an infrared beam. The CO_2 concentration is measured by the detector and output to the meter in PPM
Range:	0 - 3000 PPM
Accuracy:	± 5% Full Scale
Time Until Results:	Immediate
Other Instruments/ Methods:	GASTEC or Drager Detector Tube/Hand Pump ($150) (tubes 10 for $25) accuracy approx. ±25%

User Notes:

Infrared carbon dioxide instruments have become the standard method of measuring ambient carbon dioxide levels. The user must be well aware of two cautions, however, when using the instruments. They require time to warm up, and they are subject to drift with time, temperature, and transportation. The instruments require careful calibration procedures.

For calibration, two "known" test points are required in order to set the "Zero" and the "Span." A "Zero" gas can be obtained in one of two ways: either by using dry nitrogen (which contains no $C0_2$) or by the using a "scrubber" which removes $C0_2$ from the air. The former is preferable for bench calibration, but the scrubber does have attractions for field use. The second test point requires a calibration gas with a known quantity of

carbon dioxide in dry nitrogen. The concentration of CO_2 in the calibration gas should be at the upper end of the expected measurement range--for indoor air quality studies, 1000 parts per million (ppm) is appropriate.

An instrument should be bench calibrated before and after each day of testing. Rechecking the "Zero" in the field is also necessary, and it is at that time that a scrubber is particularly useful.

While the specific calibration procedures may vary slightly with instruments, in general they consist of:

- Turn on the instrument and let it run for at least 15 minutes to warm up.
- Fill a plastic bag with 2 or 3 litres of "Zero" gas and attach this to the inlet line. Wait for instrument to stabilize. This will typically take 5 or 10 minutes.
- Use the "Zero" adjust knob on the instrument and adjust it so that it reads 0 ppm.
- Transfer 2 or 3 litres of the "calibration gas" to a plastic bag and attach this to an inlet line. Wait for the meter to stabilize and then use the "Span Adjust" knob or pot to adjust the reading to match the known quantity of CO_2 in the calibration gas.
- Run "Zero" gas through the meter again and readjust the "Zero" setting of the meter if necessary. If a fairly significant adjustment is required, it may be necessary to re-set the "Span" using the calibration gas and re-check the "Zero" again until the user is confident that the instrument is reading the 2 points with the desired accuracy.

In the field, it will be necessary to re-check the "Zero" using either a "Zero" gas or scrubber. It is desirable, but not absolutely necessary, to check the upper range using the calibration gas.

Remember that the instrument takes a long time to warm up even after a momentary shut-down. Most instruments come equipped with battery packs and a power cord. If a long day of testing is planned, it can be useful to do as many tests as possible using the power cord, but the instrument must be left on at all times under battery power to avoid the wait for the instrument to warm up again each time.

Contaminant:	**CARBON MONOXIDE** (CO)
Sources:	Car and truck exhaust, fuel-fired appliances, kerosene heaters
Permissible Exposure Limits:	Health and Welfare Canada 25 ppm - 1 hr, 11 ppm - 8 hrs
Typical Indoor Levels:	0.5 - 2 ppm
Health Effects:	Headache, impairment of visual acuity and brain functioning. Death at 1000 ppm.
Instrumentation:	- NOVA 305, 390 SBDL (3,500) - CO 260 Monitor ($1,125) - Industrial Scientific Devices
Suppliers:	NOVA, Analytical Systems Inc. 7 Lansdowne Avenue Hamilton, Ontario Safety Supply Canada
Rental Supplier:	C0260 Available from Hazco Canada Inc. 6567 Mississauga Road Mississauga, Ontario K5N 1A6
Principle of Operation:	CO passes through a diffusion medium and is absorbed on an electrocatalytic sensing electrode. This generates an electric current proportional to the gas concentration.
Range:	0 - 1000 ppm
Accuracy:	± 1 ppm
Other Instruments/ Methods:	GASTEC or Drager Colorimetric Tube/Hand Pump ($150) (tubes 10 for $25) accuracy approx. ± 25%

User Notes:

The electro-chemical carbon monoxide instruments suggested for use require calibration. They are less sensitive than the Infrared CO_2 sensors and normally are not adjusted for span, but should have their "Zero" checked periodically. A "Zero" gas (dry nitrogen) or a scrubber can be used. Many of these instruments also have a long warm-up time and should be left to warm up for 15 minutes to half an hour before taking readings. Since they draw very little electrical power, the instrument's internal battery can be left on all day with no problem.

Contaminant:	**FORMALDEHYDE** (CH_20)
Sources:	UFFI, off-gassing of building materials (carpets, particle board, fabrics) Cleaning fluids, adhesives
Permissible Exposure Limits:	Health and Welfare Canada Target level - .05 ppm Action level - .1 ppm ASHRAE - 0.1 ppm average over 8 hrs
Typical Indoor Levels:	0.02 - 0.1 ppm
Health Effects:	Irritation of eyes and upper respiratory passages
Instrumentation:	AQRI PF1 7 day samplers, $40 each
Suppliers:	ORTECH International Sheridan Park Research Community 2395 Speakman Drive Mississauga, Ontario L5K 1B3 Air Quality Research Inc. 901 Grayson Street Berkeley, CA 94710 Air Technology Labs Inc. 548 Mallard Circle Fresno, CA 93710
Rental Suppliers:	
Principle of Operation:	Formaldehyde vapours diffuse down the container to a paper medium impregnated with an absorbing chemical. This is extracted in a laboratory and the time-weighted average exposure is determined.
Range:	0.02 - 10.0 ppm
Accuracy:	± 25%
Other Instruments/ Methods:	STC Formaldehyde Monitoring Kit (100 samples - $750)

User Notes:

The suggested sampling method for most residential applications is the Air Quality Research Institute PF1 Passive Dosimeter. It looks like a pill bottle. The dosimeter is uncapped and left on-site for approximately one week, re-capped, and sent to an analysis lab. In Canada, the samplers are supplied and analyzed by a number of commercial labs including ORTECH International in Toronto.

The samplers come in kits of two. A label on each sampler provides space to mark the start and stop time, and the date, and a ribbon and pin permit the sampler to be hung from ceilings, fixtures, or furniture. Since the sampler works by an air diffusion

method, it should not be hung near heating or ventilation system outlets where there may be drafts and should not be placed within six inches of walls or near windows. Each kit comes supplied with instructions on deployment.

Contaminant: **RADON**

Sources: Decay product of uranium, rises from the soil and is often trapped in buildings. Building materials: bricks, stone.

Permissible Exposure Limits: (Residential)

Health and Welfare Canada
20 pCi/L or 0.1 WL
ASHRAE (EPA)
4 pCi/L or 0.02 WL

Typical Indoor Levels: N/A

Health Effects: Increased risk of lung cancer (Mesothelioma)

Instrumentation: M-1 R.A.D. pump - week-long sampling device

Supplier:

R.A.D. Service and Instruments Ltd.
Unit 208, 40 Silver Star Blvd
Scarborough, Ontario M1V 3L3

Rental Suppliers:

Principle of Operation: Air is drawn through a filter which traps particles to which radon daughters are attached. As the radon daughters decay, they leave tracks on an "alpha track" detector. These tracks are counted manually in a laboratory.

Range: N/A

Accuracy: ± 20%

Other Instruments/ Methods:

Long term (6 months) Alpha Tech Detectors ($35-50)

Barringer Laboratories
5735 McAdam Road
Mississauga, Ontario
L4Z 1N9

Bubble Technology Inc.
Highway 17
Chalk River, Ontario
K0J 1J0

R.A.D. Charcoal Canister ($20) - short term screening device.

Alpha Nuclear Co.
1125 Derry Road, East
Mississauga, Ontario L5T 1P3

Direct Reading ($3,000 - $5,000)

Pylon Electronic
147 Colonnade Road
Ottawa, Ontario K2E 7L9

Thomson & Nielsen Ltd.
4019 Carling Avenue
Phase I, Suite 202
Kanata, Ontario K2K 2A3

EDA Instruments Inc.
4 Thorncliffe Park Drive
Toronto, Ontario M4H 1H1

User Notes:

The R.A.D. measurement system for Radon daughters is preferred over charcoal cannisters because its active sampling method is less subject to very localized effects.

The R.A.D. system uses a small air pump similar to an aquarium air pump and is not, therefore, silent. The noise is relatively innocuous so there are few occasions where this creates a significant problem.

The R.A.D. system can be obtained directly from R.A.D. at the address shown on the previous page or through Buchan, Lawton, Parent Ltd. It is supplied complete with the pump and the measurement head. The pump is plugged into 110 volt outlet and the start date and time noted. Make sure it is not plugged into a switched outlet. At the completion of sampling--typically a week, but it can vary from three days to a month--the pump is unplugged, the stop date and time noted, and the entire unit sent to the supplier. Turnaround time for the results is usually two to three weeks.

4.3.2 Complex Measurement Techniques

The following notes concern measurements which normally require the services of an expert and would not be suggested for most applications. Because they do require these expert services, they are also relatively expensive to undertake on a building. They would normally only be used when a problem is suspected based on preliminary assessment.

Contaminant:	**RESPIRABLE SUSPENDED PARTICULATE** (RSP)
Sources:	Tobacco smoke, incomplete combustion, renovations
Permissible Exposure Limits:	Health and Welfare Canada 100 $\mu g/m^3$ - 1 hr 40 $\mu g/m^3$ - long term average
Typical Indoor Levels:	30 - 200 $\mu g/m^3$ non-smoking 20 - 30 $\mu g/m^3$
Health Effects:	Dependent on the chemical and physical nature of particulates Can increase risk of lung cancer
Instrumentation:	Gravimetrically with pump and filter ($1,800 for pump) filter 37 mm Cellulose Acetate
Suppliers:	Safety Supply Levitt Safety
Rental Supplier:	Hazco Canada Inc. 6547 Mississauga Road Mississauga, Ontario L5N 1A6
Principle of Operation:	Air is pumped through a filter at a known rate for 4 - 6 hours. The filter is weighed in a lab before and after sampling and then the mass of particulates is determined.
Range:	
Accuracy:	
Other Instruments/ Methods:	MDA-PDC-1 Digital Dust Counter ($8,700) Piezoelectric Mass Monitor (TSI model 3500; $7,000)

User Notes:

The gravimetric analysis of filter samples is easy to perform with the proper equipment. In principal, a known quantity of air is pumped through a pre-weighed filter. When the filter is re-weighed after sampling, the difference is the total mass of particulates filtered out of the air. The calibrated air pumps required are relatively sophisticated and expensive, but they are available for rent. The 37 mm cellulose acetate filters and cassette containers are available from most safety equipment suppliers. Air pumps need to be calibrated and set for an appropriate flow rate--typically, 2 litres per minute. Calibration equipment can be a simple bubble tube or special calibrators such as the "Mini-Buck" calibrator which speeds up the procedure because they eliminate the need for stop-watch timing and calculation of flow rates.

The appropriate sampling period depends on the particulate loading in the air. In most residential applications, sampling for less than four hours is not likely to yield a significant load of particulates.

The weighing of filters requires precision balances, but there are many laboratories that have the appropriate equipment. It is necessary to condition the filters before both weighings (before and after) by placing them in an environment of controlled humidity and temperature. This eliminates any variation in weight of the filter itse due to humidity related water gain.

The particulates collected by the filter can be examined through a microscope to determine whether they contain biological particles such as mould spores and polle and if they contain asbestos fibres or crystals. This is not normally required for ind air quality analysis in highrise buildings.

Contaminant:	**AIRBORNE MICROBIALS: FUNGI**
Sources:	Outdoor air and soil Improperly drained or maintained humidifiers Wet surfaces of HVAC systems Furnishings and ceiling tiles damaged by flooding
Permissible Exposure Limits:	ACGIH 1,000 cfu (colony forming units) per cubic metre of air 1,000,000 fungi per gram of dust 100,000 fungi per ml of stagnant water or slime AGRICULTURE CANADA <50 cfu/m^3, 2 species, or <150 cfu/m^3, 3 species, or <500 cfu/m^3
Typical Indoor Levels:	under 200 cfu/m^3, summer under 50 cfu/m^3, winter
Health Effect:	Allergic reaction to fungi can cause shortness of breath, coughing, sneezing, itchy eyes, or runny nose.
Instrumentation:	Biotest RCS Centrifugal Air Sampler ($2,300) with Rose Bengal Agar Strips (box of 50, $150)
Supplier:	Gelman Sciences 2535 Deminiac Street Montreal, Quebec H4S 1E5
Rental Suppliers:	
Principle of Operation:	Fungal spores drawn into the sampler are impacted by centrifugal force onto a strip of nutrient media (agar). After incubation, the number of colonies grown are counted and identified.
Range:	
Accuracy:	Sampled air volume ± 2%
Other Instruments/ Methods:	Andersen sampler for viable particles with pump

User Notes:

The Biotest RCS sampler is easy to use, but the data is difficult to interpret. Public Works Canada has used it for a number of years as a standard testing tool for airborne fungi spores in office buildings. The procedure recommended by PWC is:

- Sterilize fan blades and wipe them with an ethynol swab. This procedure should be done at the beginning of sampling and in major divisions, such as each floor of a large building.
- Open the Agar strip by pulling back the bubble pack cover a few centimetres. Without touching the Agar strip with your fingers, remove it from its covering and slide it, agar side in, into the drum of the instrument.
- Set sampling time switch to 4 minutes.
- Place the instrument in the required location and turn it on. Do not move the instrument while the sample is being taken. It stops automatically after the set sampling period.
- After sampling, remove the strip from the instrument and place it back in the original wrapper with the Agar side facing the raised surface of the bubble pack.
- Seal the opening with adhesive tape and mark the sample using a china marker for identification. Strips can be kept in a cooler for transport to the laboratory for incubation and examination for colony forming units and species identification.

The difficulty with the system is the need for qualified personnel to identify the species. Buchan, Lawton, Parent Ltd. uses the services of Residential Industrial Fungal Detection Services, 4 Birkett Street, Nepean, ON. There are also a number of university researchers who could perform this function.

In reality, assessing the significance of the biological testing results with this instrument is a job for experts. It cannot be classified as a "simple test" procedure.

Contaminant:	**VOLATILE ORGANIC COMPOUNDS**
Sources:	Building products, paints, sealants, glues, etc. Many cleaning products
Permissible Exposure Limits:	Not defined in Canada
Typical Residential Indoor Levels:	Under 2 mg/m^3 Total VOCs
Health Effects:	
Instrumentation:	Sampled pump air activated charcoal tubes analysed by gas chromatography.
Supplier:	Levitt-Safety Safety Supply
Rental Suppliers:	Hazco Canada (pumps only) 5667 Mississauga Road Mississauga, Ontario K5N 1A6.
Principle of Operation:	Air sample is pumped through an activated charcoal absorbant tube which is sent to a laboratory for analysis. Concentrated contaminants can be desorbed and analysed using gas chromatography or gas chromatography/mass spectrometry.
Range:	
Accuracy:	
Other Instruments/ Methods:	There are some infrared analysers which can give on-site readings of many volatile organic compounds; notably, the Moran 1B. This $30,000 instrument requires an expert operator.

User Notes:

Sampling for volatile organic compounds is not particularly difficult. The real complexity is in the analysis of results. A known volume of air is pumped through charcoal absorbant tubes that can be readily obtained from safety equipment suppliers. The tubes, along with information on the volume of air pumped through them, must be supplied to a laboratory with the capability to desorb and analyse the contents using either gas chromatography or gas chromatography/mass spectrometry. ORTECH International in Toronto is one lab offering these services, but there are a number of others.

Sample rates would be approximately 0.5 litres per minute and the sample time can vary. The longer the time, the more concentrated the sample and the easier it is to measure. Sample periods of as long as 20 to 30 hours are recommended, particularly if analysis is limited to gas chromatography. ORTECH will analyse samples with as little as 10 litres (20 minutes) at 0.5 litres per minute using GC/MS.

$$\frac{\Delta U}{U} \propto \left(\frac{R_B}{S}\right)^a \qquad (2\text{-}32)$$

where S is the distance downstream of the obstacle and

$$a = \left(\frac{3+p}{2+p}\right)$$

where p is the power law exponent of the boundary layer mean velocity profile (see section 2.5.3). For typical values of p of 0.12 to 0.47, "a" has a narrow range of values : $1.5 > a > 1.4$. Wind tunnel measurements in wakes behind structures in simulated atmospheric turbulent boundary layers by Peterka, Meroney and Kothari (1985) and Lemberg (1973) show that $a \approx 1.5$. Lemberg (1973) predicts $a = 1.5$ from his theory that determined wake centreline velocities based on the variable eddy viscosity model of Sforza and Mons (1970) and Hunt (1971). Because the range of a is small, for simplicity the wind shadow wake model will use a single value of $a = 1.5$. This corresponds to uniform flow with $p=0$ in Equation 2-32.

The separation distance, S, shown in Figure 2-10 is the distance from the centre of the surface being sheltered to the obstacle along a line parallel to the wind direction. If this line does not strike the obstacle then S is the distance to the projected plane of the nearest wall of the obstacle as shown in Figure 2-10. The shelter factor on the wake centreline, $S_{U,CL}$, is calculated individually for each wall as they each have a different distance to the obstacle. This is most important when the shielding obstacle is close to the building being studied. The assumption of self preservation means that all the velocity profiles measured downstream of an obstacle all have the same form when appropriately non-dimensionalised. This means that a single functional relationship between velocity and downstream distance, S, can be used to describe the wake. This is only true in the far field (where the wake decay has become independent of the obstacle geometry) which is at least three obstacle heights downstream for a three dimensional turbulent wake as shown by the results of Peterka, Meroney and Kothari (1985). In many cases shelter is provided by obstacles closer than three heights away. To account for this a virtual origin displacement can be introduced by rewriting Equation 2-32 as

$$\frac{\Delta U}{U}=\left(\frac{B_1}{\frac{S}{R_B}+B_2}\right)^a \qquad (2\text{-}33)$$

Combining Equations 2-28,2-29 and 2-32 yields the following relationship for the shelter factor $S_{U,CL}$:

$$S_{U,CL}=1-\left(\frac{B_1}{\frac{S}{R_B}+B_2}\right)^{\frac{3}{2}} \qquad (2\text{-}34)$$

where B_1 and B_2 must be found from measurements. Letting $B_1 \neq B_2$ accounts for possible flow reversals and non-zero velocities when S is close or equal to zero.

B_1 and B_2 have been estimated from the experimental results of Wiren (1985) who measured pressure coefficients on buildings of different separations. The value of $S_{U,CL}$ can be estimated by taking the square root of the ratio of the sheltered pressure coefficient to the unsheltered pressure coefficient. Using Equation 2-34 with the known building size and separation distance enables estimates of B_1 and B_2 to be made. Using measured pressure coefficients rather than velocities means that B_1 and B_2 will also include any static pressure changes. Given the limitations imposed by the limited quantity of data available it is reasonable to let $B_1 = B_2$. This implies that the mean windspeed is zero at the rear wall of the obstacle, which is a physically realistic assumption. The best fit to Wiren's data was found to be when $B_1 = B_2 = 3.3$. With more detailed Cp data better estimates of B_1 and B_2 could be made. A lower value of B_1 and B_2 results in a more rapid initial velocity recovery when S/R_B is small. $S_{U,CL}$ is calculated using Equation 2-35.

$$S_{U,CL}=1-\left(\frac{3.3}{\frac{S}{R_B}+3.3}\right)^{\frac{3}{2}} \qquad (2\text{-}35)$$

2.10 Accounting for Wake Spread

To account for the effect of turbulence on wake spread, as shown in Figure 2-11a and discussed earlier, a gaussian distribution of wind direction about the mean is assumed. The gaussian distribution is used to weight the calculated values of S_U

for each wind angle. This has the effect of smoothing out abrupt changes in wind shelter with wind angle that can result from the notch profile calculation of L_s and thus provides more realistic shelter estimates. To find the shelter factor for the mean wind angle θ, the shelter factors for wind angles, that deviate from θ by ϕ, are weighted by the gaussian distribution, f, given by

$$f(\phi,\theta,\sigma_\theta)=\frac{1}{\sqrt{2\pi}\sigma_\theta}\exp\left(-\frac{1}{2}\left(\frac{\phi-\theta}{\sigma_\theta}\right)\right) \qquad (2\text{-}36)$$

In the present study the standard deviation of wind direction was estimated by assuming a crosswind component atmospheric turbulence intensity of about 20%. This means that root mean square crosswind velocities perpendicular to the mean velocity are 20% of the mean velocity. This value of root mean square velocity is based on a summary of experimental results given by Panofsky and Dutton (1986) that shows that RMS crosswind velocities are typically 20%. The root mean square component of crosswind velocity from Panofsky and Dutton is for typical urban surroundings and a one hour time averaged velocities. The deviation in wind direction depends on the length of time average used. Time averages greater than about three hours should not be used because the deviation in wind direction will include the effects of changing weather systems. At shorter time averages all the scales of atmospheric turbulence may not be included. Wollenweber and Panofsky (1989) give a factor for correcting the deviation, $\sigma_{\theta 1}$, measured over the averaging time, t_{avg1}, to the deviation, σ_θ, measured over a different averaging time, t_{avg} as follows:

$$\sigma_\theta=\sigma_{\theta 1}\left(\frac{t_{avg}}{t_{avg1}}\right)^{0.2} \qquad (2\text{-}37)$$

Equation 2-37 allows for the increase in deviation with the increase in average time as a greater range of turbulent scales are included in the averaging process. The one hour time averages presented by Panofsky and Dutton are used in this study because the measured validation data was averaged over one hour and do not require the correction factor given by Equation 2-37.

For the wind shadow model the deviation in direction is found from the approximation $\sigma_\theta = \tan^{-1}(0.20)$ that is valid for small angles. This gives a standard

deviation of $\sigma_\theta \approx 11.3°$. To find S_U at the central wind direction, θ, sixty one deviations in wind angle, ϕ, are spread over $\pm 3\sigma_\theta$ (approximately one point per degree of wind angle). At each deviation angle ϕ the S_U calculated for that angle is multiplied by the weighting factor, f, calculated using Equation 2-36. The sum of the 61 points thus calculated gives S_U at the central wind direction, θ. This is an extremely tedious process requiring many trigonometric calculations for S_U and L_s.

For the validation of the ventilation model a computer programme was used to calculate S_U for all four walls of the test buildings at AHHRF every one degree of wind angle. The calculation of S_U is based on the empirically determined parameters that are summarised in Table 2-3.

Table 2-3. Summary of empirical parameters used to calculate shelter factor, S_U

Parameter	Value	Data Source
a Exponent for mean velocity decay	1.5	Peterka, Meroney and Kothari (1985) Lemberg (1973)
B_1 and B_2 Coefficients for mean velocity decay	$B_1 = B_2 = 3.3$	Based on pressure coefficients from Wiren (1985)
σ_θ Standard deviation of wind direction	11.3°	various sources listed in Panofsky and Dutton (1986)

The output of the computer programme is shown in Figures 2-15 and 2-16. When the walls are not sheltered $S_U = 1$ and complete shelter corresponds to $S_U = 0$. Figure 2-15 is for the north wall and shows the symmetry of its shelter with a maximum wind speed reduction factor of $S_U = 0.43$ for winds from 110 and 250 degrees. Figure 2-16 is for the east wall where the shelter is asymmetric since the sheltering building is much closer for east winds than west winds when the house is between the east wall and the upwind building. For east winds (90 degrees) the shelter effect is a maximum with $S_U = 0.25$. For west winds the shelter is less, with $S_U = 0.61$. Once these values of S_U are calculated they are stored in a data file as a lookup table thus reducing the calculations required by the ventilation model.

Localised leakage sites such as open windows or attic ventilators use the same Cp and S_U as the surface on which they are located. The attic surfaces (gable ends, soffits and the pitched roof slope) use the same shelter values as the house walls directly beneath them.

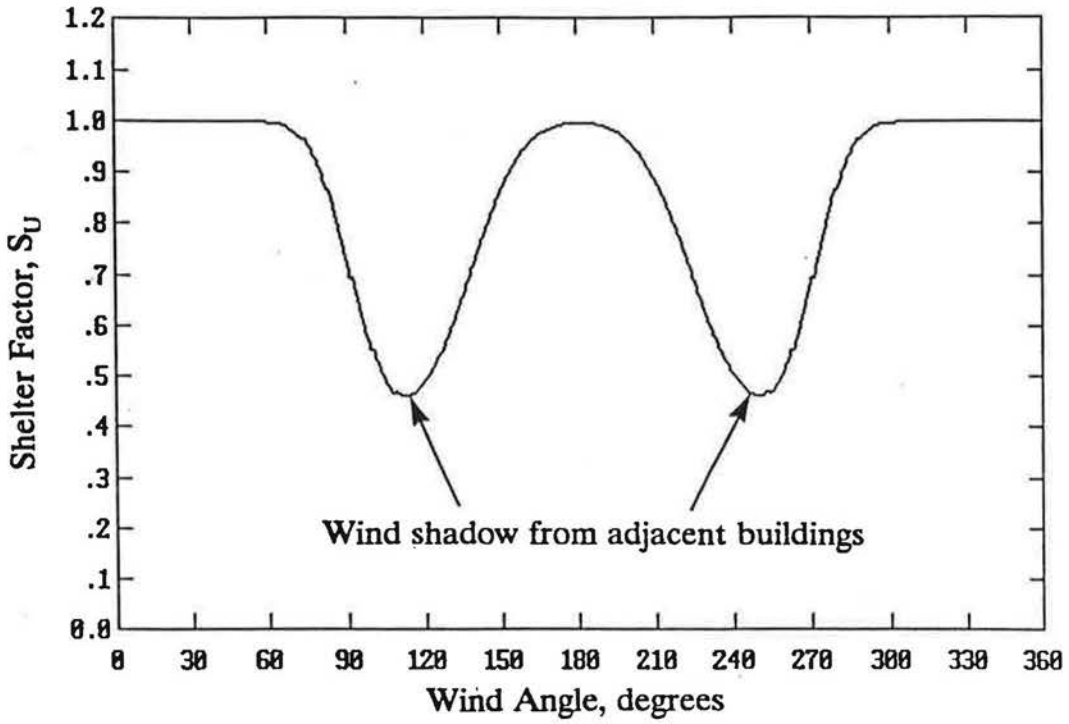

Figure 2-15. Wind angle dependence of wind speed reduction factor, S_U, for the north wall of a house at AHHRF. Calculated using data from Wiren(1985).

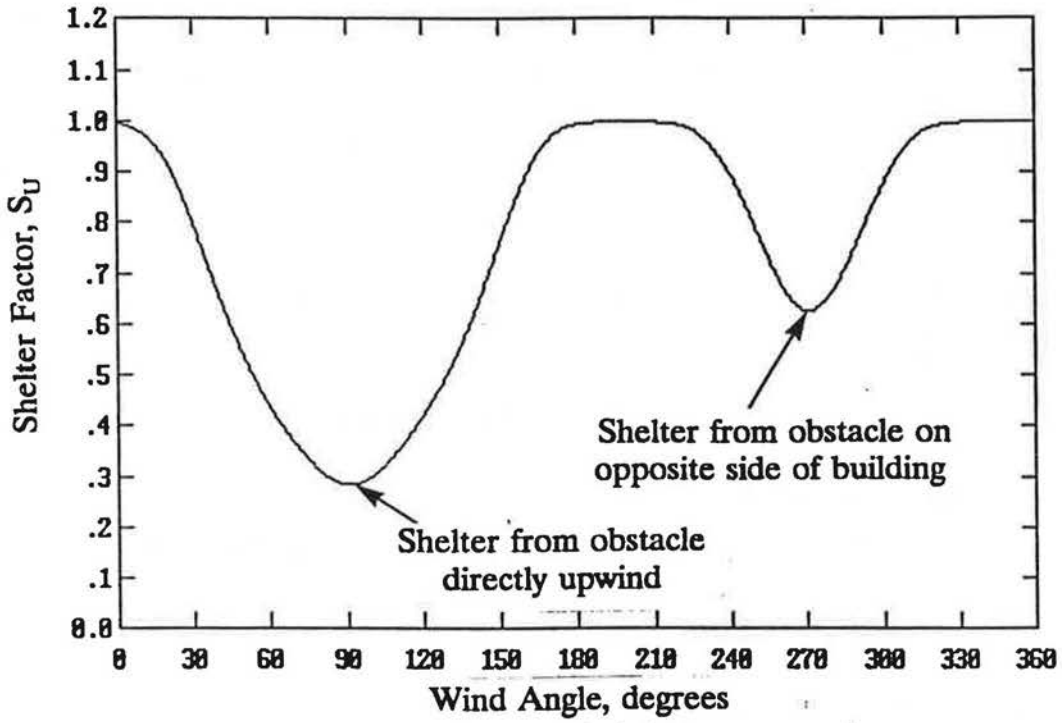

Figure 2-16. Wind angle dependence of wind speed reduction factor, S_U, for the east wall of a house at AHHRF. Calculated using data from Wiren(1985).

2.11 Combining Wakes

In some situations a building may be sheltered by more than one upwind obstacle. This complex flow situation is difficult to model using wake decay Equation 2-35 used in this study. For combined wakes, one wake is growing inside another wake. For the internal wake the external flow conditions are changing because they are a wake that is decaying. Equation 2-35 is based on the assumption that the flow external to the wake is not changing (i.e. U = constant) and therefore cannot be applied to the combined wakes. Wind tunnel studies by Wiren (1985) have shown that for multiple upwind obstacles the nearest obstacle will dominate the shelter effect. This only applies if the obstacles are of similar size. If the furthest upwind obstacle is a large building and the nearest obstacle is a lamp post then clearly the large building will have a greater sheltering effect. In this study the buildings where the measurements were made are sheltered by other buildings of the same size and the shelter is calculated based on the nearest building only, without the need to combine wakes.

2.12 Summary of Wind Shadow Shelter Model

The wind shadow shelter model has been developed to account for the sheltering effects of upwind obstacles on the surface pressures of houses and attics. The model uses a simple notched velocity profile with constant velocity deficit across the wake. For simplicity, the notch velocity profile does not include the three dimensional aspect of the wake flow including vortices and flow acceleration at the edges of the wake. The sheltering effect of the notch wake is flapped over a range of wind directions on either side of the mean wind direction with a gaussian weighting to account for wake spreading caused by atmospheric turbulence. Current wake theories only apply in the far field where velocity defects are assumed to be small and the specific geometry of the obstacle is no longer significant. The notched wake allows wake width and velocity close to the obstacle (where shelter effects are most significant) to be modelled. The model produces realistic shelter factors for a wide range of inputs and can be applied to many obstacle geometries because it relies on simple geometric construction to find the amount of shelter projected by an obstacle onto the building of interest. Static pressure changes in the wake are included indirectly in shelter factor coefficients developed from surface pressures measured by Wiren (1985).

2.13 Flow through Each Leak for the House

ATTICLEAK-1 has been developed to combine the ventilation from known ventilation sites such as fans, furnace flues, open windows and doors, and other passive vents with distributed background leakage. The distributed leakage, found from fan pressurization tests, is the unintentional leakage in a building envelope between the walls and foundation, in the ceiling, and around windows, doors and other holes in the vapour barrier. Following the work of Sherman (1980) and Sherman and Grimsrud (1980) at Lawrence Berkeley Laboratories the distributed leakage for the house is divided into user specified fractions at ceiling level, in the walls, and at floor level. This idea was modified in ATTICLEAK-1, where each of the four walls may have different amounts of leakage. As a further refinement the floor level leaks are further divided into four parts, one below each wall, for houses with basements. This allows different floor level leakage for each side of the building depending on plumbing penetrations and other leakage sites. It is assumed that the building has a rectangular floor plan so that there are four sides to the building, and that the flow exponent, n, in Equation 2-1, is the same for all distributed leaks. Because the flow exponent is assumed to be the same for all the distributed leaks, the flow coefficient, C_d, is equal to the sum of the user specified fractions. The total distributed leakage flow coefficient, C_d, and exponent, n_d, are best estimated from fan pressurization results. The flow coefficients for the ceiling, floor level leaks and walls are estimated as fractions of the total distributed leakage such that

$$C_d=\sum_{i=1}^{4} C_{f,i}+\sum_{i=1}^{4} C_{w,i}+C_c \qquad (2\text{-}38)$$

where $C_{f,i}$ is the floor level leakage below wall i, $C_{w,i}$ is the leakage in wall i and C_c is the ceiling leakage. The additional building leaks not included in C_d have different values of flow exponent so that the total building leakage cannot be found by simply adding the distributed and localised leakage coefficients.

The attic distributed leakage is divided into sloped roof pitch, soffit, gable end and attic floor areas. The attic floor leakage is the same as the ceiling leakage for the house by definition. Additional attic leakage sites include gable vents, roof vents and roof ridge vents. The flow through the attic leaks will be discussed later in section 2.14.

The following section deals with the particular flow through each leak. For

each leak C and n must be specified for use in the flow Equation 2-1, and Cp, S_U and z specified for the pressure difference Equation 2-18.

2.13.1 Furnace Flues and Fireplaces

Furnace flues and fireplaces are usually the largest openings in the building envelope and typically have a flow exponent, n_F, close to 0.5. In a previous study (Walker (1989)) the author measured the flow characteristics of a 6m length of flue made of 15cm diameter round galvanized steel, with a rain cap at one end. The results showed that $n_F = 0.54$ for both forward and backdraughting flow. The flue leakage coefficient, C_F, can be calculated from diameter, D_F, of the flue or fireplace assuming orifice flow. The values of C_F from Walker's (1989) experiments showed that the discharge coefficient of $K_D = 0.6$ should be used in the following orifice equation

$$C_F = K_D\left(\frac{\pi D_F^2}{4}\right)\sqrt{\frac{2}{\rho}} \qquad (2\text{-}39)$$

where ρ is the density of the airflow.

An estimate of the pressure coefficient to be used for furnace flues, Cp_F, can be found in Haysom and Swinton (1987). Haysom and Swinton measured Cp's at the top of flues with a range of flue caps and found a typical value of Cp = -0.5 in a uniform flow. Using this pressure coefficient, that is different from those used on other building leaks is important because the furnace flue is usually the largest single leakage site on a building. The change in wind velocity with height above grade may be significant for furnace flues that protrude above the reference eaves height. Equating the pressure produced by the increased velocity, U_F, at Cp = -0.5 to the pressure produced by the reference wind speed, U, (measured at the eaves height, H_e) and Cp_F using Equation 2-4 gives

$$U^2 Cp_F = U_F^2(-0.5) \qquad (2\text{-}40)$$

Rewriting this equation in terms of Cp_F gives

$$Cp_F = \left(\frac{U_F}{U}\right)^2(-0.5) \qquad (2\text{-}41)$$

The change in wind speed with height is found by assuming a power law wind velocity

such that:

$$\frac{U_F}{U}=\left(\frac{H_F}{H_e}\right)^p \tag{2-42}$$

where H_F is the height of the top of the flue above grade. The corrected Cp_F is then found by substituting Equation 2-42 in 2-41 to give

$$Cp_F=(-0.5)\left(\frac{H_F}{H_e}\right)^{2p} \tag{2-43}$$

Shelter for the flue, $S_{U,F}$, is the shelter factor at the top of the flue. If the surrounding buildings and other obstacles are below the flue height then it is assumed that $S_{U,F} = 1$. If the surrounding obstacles are higher than the flue then the flue is sheltered and $S_{U,F}$ is calculated using Equation 2-35. Now the general pressure difference Equation 2-18 can be written specifically for the furnace flue as

$$\Delta P_F=\Delta P_I-P'_T H_F+P_U S^2_{U,F} Cp_F \tag{2-44}$$

where P_U and P'_T are given by Equations 2-6 and 2-12 respectively.
The mass flow rate, M_F, for the flue is given by Equation 2-45.

$$M_F=C_F(\Delta P_F)^{n_F} \tag{2-45}$$

For a heated flue with the furnace on or a fire in the fireplace the temperature of the gas in the flue is T_F is used instead of the inside temperature, T_{in}. The flue temperature is used to find ρ_F in the mass flow rate Equation 2-1, correct C in Equation 2-3, and to change the driving pressure for flue flow. An extra term is added to Equation 2-44 that accounts for the difference in pressures between a flue full of air at T_{in} and air at T_F. The extra term is given by

$$-gH_F(\rho_{in}-\rho_F) \tag{2-46}$$

The density difference is expressed in terms of temperatures assuming that the air in the flue is an ideal gas so that

$$\Delta P_F=\Delta P_I+P_U\ S_{U,F}^2\ Cp_F-P_T'\ H_F-g\rho_{in}H_F\left(1-\frac{T_{in}}{T_F}\right) \qquad (2\text{-}47)$$

The extra term, from Equation 2-46, makes the flue flow driving pressure more negative and therefore increases the outflow through the flue. For a flue taken in isolation (with no ΔP_I or P_U) raising the flue temperature to 373K from 293K (typical T_{in}) will approximately quadruple the driving pressure and thus double the mass flow rate (with $n_F \approx 0.5$). This change in the flue temperature will also change C_F as shown by Equation 2-3.

2.13.2 Floor Level Leakage

The leakage at floor level, $C_{f,i}$, is estimated as a fraction of the total distributed leakage and n_f is the same as n for the other distributed leaks. There are two cases of floor level leakage that require different assumptions about wind pressure effects. The cases depend on house construction.

a. Basements and Slab on Grade

In this case the total floor level leakage is split into four parts, one for each side of the building. On each side the floor level leakage is given the same Cp and S_U as the wall above it. For the i^{th} side of the building

$$\Delta P_{f,i}=\Delta P_I+Cp_i\ S_{U,i}^2\ P_U-H_f\ P_T' \qquad (2\text{-}48)$$

where H_f is measured from grade level. For a house with a basement this is the height of the main level floor above grade and the leakage coefficient, $C_{f,i}$ includes the leakage around basement windows, dryer vents etc.

The mass flow rate for these floor level leaks is given by Equation 2-49.

$$M_{f,i}=C_{f,i}(\Delta P_{f,i})^{n_f} \qquad (2\text{-}49)$$

b. Crawlspaces

As an estimate of the wind pressure in a crawl space the shelter and pressure coefficients for the four walls of the building are averaged. The average is weighted for non square plan buildings by the length of each side, L_i, so that for the i^{th} side.

$$Cp_f=\sum_{i=1}^{4} S_{U,i}^2 Cp_i\left(\frac{L_i}{L_\pi}\right) \qquad (2\text{-}50)$$

where L_T is the perimeter of the building (the sum of the L_i's) and then the pressure across the crawlspace is given by

$$\Delta P_f = \Delta P_I + Cp_f P_U - H_f P_T' \quad (2\text{-}51)$$

The mass flow rate through the crawlspace leakage is given by Equation 2-52

$$M_f = C_f (\Delta P_f)^{n_f} \quad (2\text{-}52)$$

In the present study the houses where the measurements were made all had full basements and so the floor level leakage is divided into four parts and Equations 2-48 and 2-49 were used to find the floor leakage pressure differences and mass flow rates, respectively.

2.13.3 Ceiling Leakage

The ceiling flow coefficient C_c is estimated from the total distributed leakage and n_c is the same as n for the other distributed leaks. There are no wind pressures acting on the ceiling except indirectly through ΔP_I and $\Delta P_{I,a}$ as the ceiling is completely sheltered from the wind. $\Delta P_{I,a}$ is the equivalent of ΔP_I for the attic zone. The pressure across the ceiling includes the difference in attic and house buoyancy pressures

$$\Delta P_c = \Delta P_I - \Delta P_{I,a} - \rho_{out} g H_a \left(\frac{T_{in} - T_{out}}{T_{in}} - \frac{T_a - T_{out}}{T_a} \right) \quad (2\text{-}53)$$

When $T_a = T_{out}$ the buoyancy term is the same as for a house with no attic. When $T_a = T_{in}$ the buoyancy term vanishes and only the difference in internal pressures due to wind forces is acting across the ceiling.

The mass flow rate through the ceiling is given by Equation 2-54.

$$M_c = C_c (\Delta P_c)^{n_c} \quad (2\text{-}54)$$

2.13.4 Wall Leakage

For the i^{th} wall $C_{w,i}$ is estimated from the total distributed leakage and the flow exponent, n, for each wall is n_d, the same as for the other distributed leaks. The linear change in pressure with height due to stack effect means that when inflows and outflows are balanced there is a location where there is no pressure difference. This is called the neutral level, H_{NL} and is given by Equation 2-19. The location of the neutral level is shown in Figure 2-2, where $\Delta P = 0$. For $T_{in} > T_{out}$ flow is in below

H_{NL} and out above H_{NL}, with the flow directions reversed for $T_{out} > T_{in}$. If there is no stack effect and $P'_T = 0$, then the pressure is constant over the wall and H_{NL} is undefined. In this case the pressure difference across wall i is given by

$$\Delta P_{w,i}=\Delta P_I+S_{U,i}^2 Cp_i P_U \tag{2-55}$$

When $T_{in} \neq T_{out}$ the total flow through each wall must be found by integration because the pressure difference varies with height. This change in pressure and the change in mass flow rate with height is illustrated in Figure 2-17. The limits of integration for pressure are found at the top, ΔP_t, and bottom, ΔP_b, of the wall and are

$$\Delta P_t=\Delta P_I+S_{U,i}^2 Cp_i P_U-H_e P_T' \tag{2-56}$$

$$\Delta P_b=\Delta P_I+S_{U,i}^2 Cp_i P_U-H_f P_T' \tag{2-57}$$

The change in pressure with height, z, is given by Equation 2-18 such that

$$\Delta P_{w,i}(z)=\Delta P_I+S_{U,i}^2 Cp_i P_U-zP_T' \tag{2-58}$$

Thus the flow through the wall is also a function of height which must be integrated to find the total mass flow in and out of wall i.

$$M_{w,i}=\int dM_{w,i}(z)dz \tag{2-59}$$

where

$$dM_{w,i}(z)=\rho dC_{w,i}(\Delta P_{w,i}(z))^{n_i} \tag{2-60}$$

where $\Delta P_{w,i}(z)$ is given by Equation 2-58. Assuming evenly distributed leakage allows easy integration over the wall because the fractional leakage $dC_{w,i}$ is given by

$$dC_{w,i}=C_{w,i}\frac{dz}{(H_e-H_f)} \tag{2-61}$$

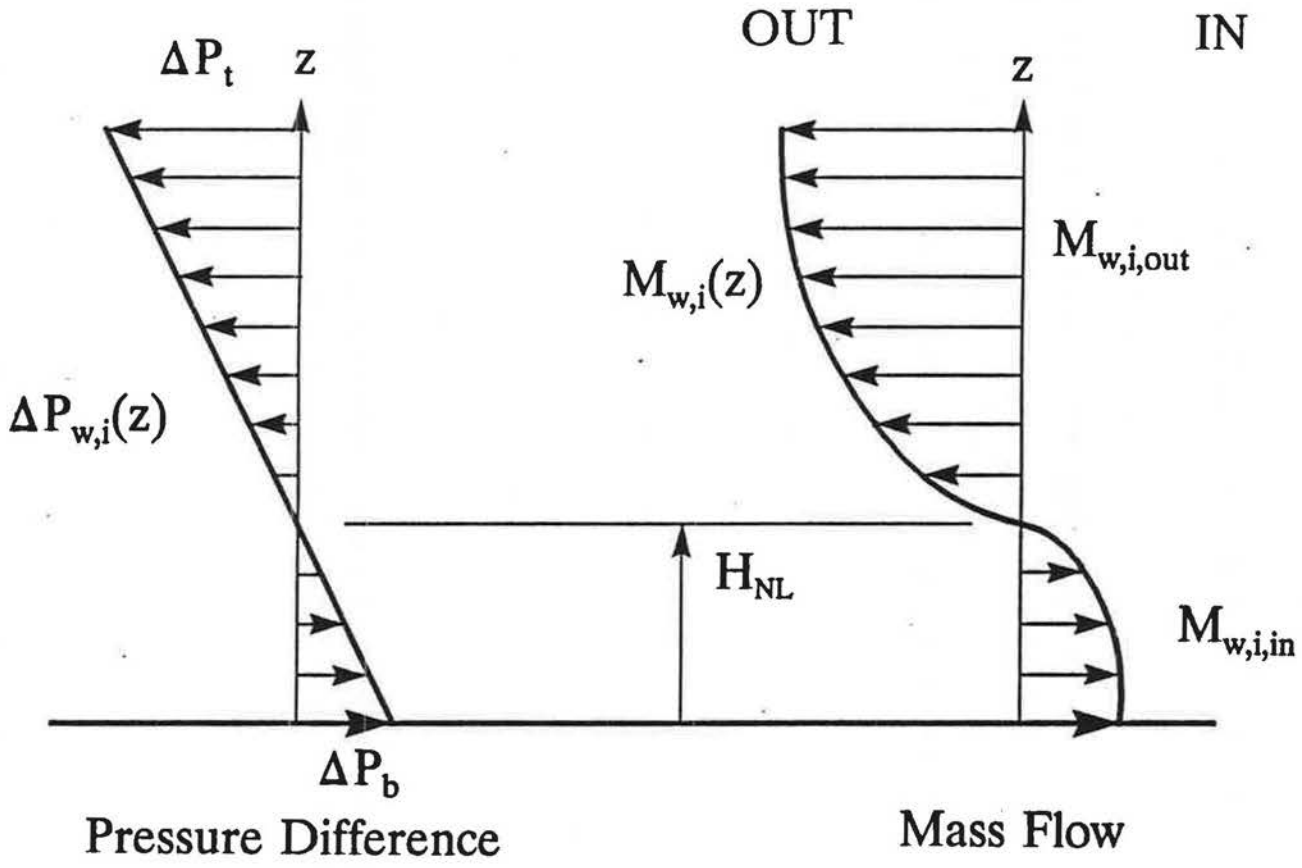

Figure 2-17. Variation of pressure difference and mass flows with height for a wall.

Substituting Equations 2-60 and 2-61 in 2-59 gives

$$M_{w,i}=\frac{\rho C_{w,i}}{(H_e-H_f)}\int \Delta P_{w,i}^{n_d} dz \qquad (2\text{-}62)$$

where the limits of integration depend on the neutral level height, H_{NL}, that is found for each wall using Equation 2-18. The next section shows how the limits of integration change depending upon H_{NL}. When H_{NL} is on the wall there is flow both in and out of the wall and upon integrating Equation 2-62 the masses flowing in and out are kept separate. This important for the total mass balance and for keeping track of all the flows through the building envelope.

There are six cases of wall flow, each with different integration limits, for Equation 2-62. There can be inflow, outflow or two-way flow for the wall with the flow direction determined by T_{in} and T_{out}. All of the cases are given in appendix A including an example derivation of Equation 2-63 and 2-64. The example case given here is for $T_{in} > T_{out}$ with H_{NL} on the wall with flow in below H_{NL} and flow out above H_{NL}, such that

$$M_{w,i,out}=\frac{\rho_{in} C_{w,i} \Delta P_t^{n_d+1}}{(H_e-H_f)P_T' (n_d+1)} \qquad (2\text{-}63)$$

$$M_{w,i,in}=\frac{\rho_{out} C_{w,i} \Delta P_b^{n_d+1}}{(H_e-H_f)P_T' (n_d+1)} \qquad (2\text{-}64)$$

2.13.5 Fan Flow

There can be multiple fans at different locations on the house envelope. Each fan may have its own fan characteristics of rated flow, Q_{rated}, and pressure difference, ΔP_{rated}. Fans at different locations will have different wind and stack pressures. Because the flowrate through a fan depends on the pressure difference across it the flow through a fan is found by using a fan performance curve. The operating point on the curve is determined by the pressure across the fan due to the wind, stack and internal pressure difference pressures. The stack and wind pressures across each fan are found by specifying which wall the fan is on and its height above grade, H_{fan}. Cp_{fan} and $S_{U,fan}$ are the same as the wall they are located in. The pressure difference across the fan is then given by

$$\Delta P_{fan}=\Delta P_I+S_{U,fan}^2 Cp_{fan} P_U-H_{fan} P_T' \quad (2\text{-}65)$$

A fan performance curve is used to find the effect that ΔP_{fan} has on the flowrate through the fan. Figure 2-18 shows a schematic of a fan curve illustrating this principle. The rated flowrate for the fan is Q_{rated} with no pressure drop and the maximum pressure that the fan can provide is ΔP_{rated} at no flow. Approximating the fan performance curve by a power law using p_{fan} gives the following equation for mass flow through the fan:

$$M_{fan}=\rho Q_{rated}\left(\frac{\Delta P_{rated}+\Delta P_{fan}}{\Delta P_{rated}}\right)^{p_{fan}} \quad (2\text{-}66)$$

where ρ is equal to ρ_{in} for outflow and ρ_{out} for inflow.

The flow direction is determined by the sign of the pressure term. A positive term means inflow and a negative term means outflow. ΔP_{rated} is positive for a supply fan and negative for an exhaust fan. The power, p_{fan}, depends on the type of fan being used. For the centrifugal fans used in this study it is assumed that $p_{fan} = 0.3$.

2.13.6 Vent Leakage

The vent leakage is attributed to deliberately installed leakage sites that are separate from the background leakage. These vents are assumed to be horizontal so that the temperature of air inside them does not change the pressure across the leak. ATTICLEAK-1 allows multiple vents to be installed, each with their own flow characteristics and each at a different location on the house envelope. Furnace and fireplace flues are treated separately as they may contain heated air that would produce a stack effect for that leak only. The flow characteristics, C_V and n_V must be known for each vent. These vents are assumed to exit through the walls at a height, H_V, with the same exterior shelter and pressure coefficients, S_U and Cp, as the wall they are located in. Vents exiting through the roof use the same Cp and S_U as the furnace flue. The pressure difference across a vent is

$$\Delta P_V=\Delta P_I+S_{U,V}^2\, Cp_V\, P_U-H_V\, P_T' \quad (2\text{-}67)$$

Q_{rated} = Maximum fan flowrate

ΔP_{rated} = Maximum fan pressure

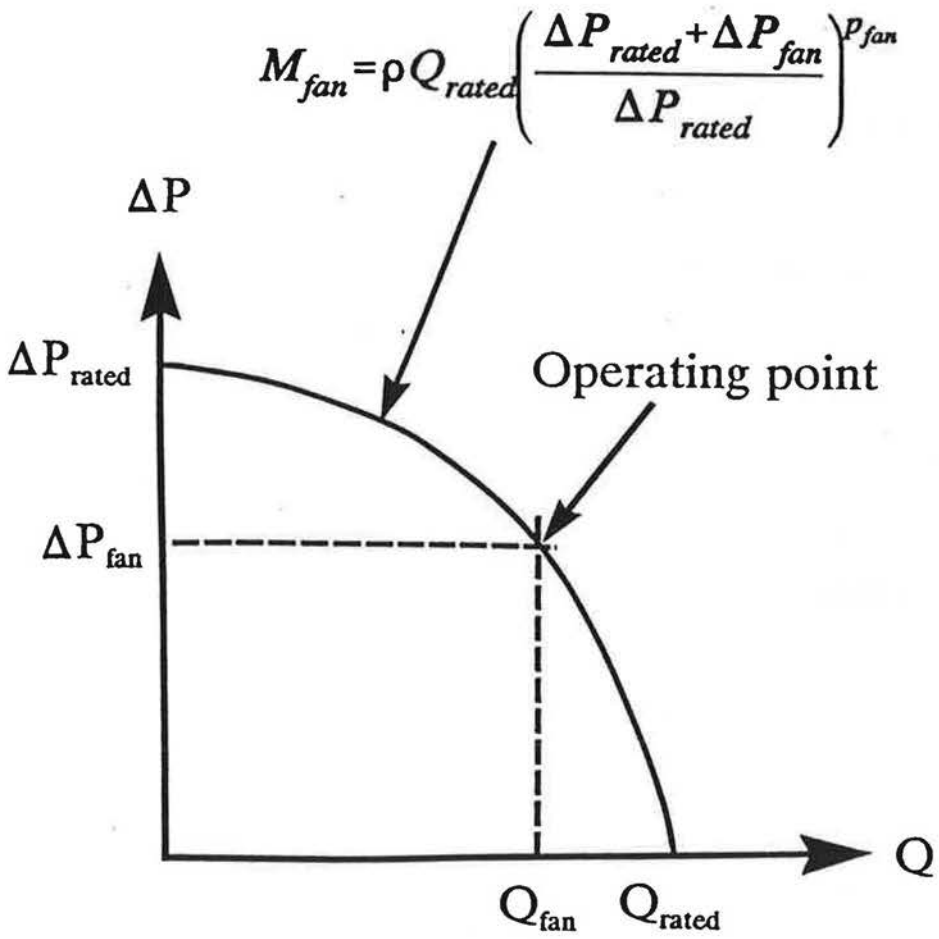

Figure 2-18. Schematic of fan performance curve

The mass flow through each vent is given by Equation 2-68.

$$M_v=C_v(\Delta P_v)^{n_v} \tag{2-68}$$

2.13.7 Flow through open Doors and Windows

Open doors and windows are both modelled the same way: as rectangular openings in the building envelope. The effect of specific door or window geometry (e.g. sliding windows or hinged windows) has been neglected for simplicity. Previous studies of flow through windows have concentrated on flows dominated by either temperature differences or wind effects, but little has been done with the combination of the two. Brown and Solvason (1962) developed flow relationships assuming stack effect only, and they assumed that exactly half of the opening area had inflow and half had outflow which implies equal volume flowrate and not equal mass flow. Shaw and Whyte (1974) studied the effects of additional forced airflow into a room combined with flow through an opening due to stack effect. They too assumed that exactly half of the opening area had inflow and half had outflow, which is unlikely for a room that is pressurized or depressurized due to forced ventilation.

The effects of wind pressure have been examined for flow through a single opening by Crommelin and Vrins (1988) and Cockroft and Robertson (1976). A major complication in determining flowrates due to wind pressure is the turbulent nature of the wind. Both the turbulence intensity and the energy spectra of the turbulence effect the flowrates. The various turbulent scales interact in different ways with both the building and the specific window geometry, e.g. the opening angle of hinged windows. Crommelin and Vrins found that the ventilation rates varied by a factor of two depending on the orientation of the open window to wind direction. An exact relationship is more complex as it depends on which turbulent scales are dominant in the atmospheric boundary layer. Cockroft and Robertson showed that a higher turbulence intensity resulted in greater ventilation rates and that a reasonable estimate of the amount of air entering a single opening that mixes completely with the internal air is approximately 1/3. This result applies to a building with a single opening in one wall with no net flow through the opening so that the air exchange is due to turbulence only. In a real building there will always be some net flow through the opening and this situation will not arise.

The mechanisms of ventilation outlined above are not well understood even for this simple single opening cases and are not included in this model. The factors neglected in estimating flow through open windows or doors in this model are:

• Window and door opening geometry. Crommelin and Vrins (1988) looked at the effect of hinged external windows on flow rate through the opening. Vertically hinged windows were tested by Crommelin and Vrins with the opening facing upwind and downwind. Their results showed increases in ventilation of up to a factor of three compared with the opening with no external hinged window. For sliding windows as used in the present study this effect does not occur.

• Interaction of turbulent scales in the wind with building and opening geometry. The mechanism of interaction is complex depending on the relationship between atmospheric turbulent scales, building scales and opening scales. This has been studied by Haghighat, Rao and Fazio (1991) for buildings with one and two openings. The two opening case is most like a real building with other leaks elsewhere on the building envelope. For the two opening case Haghighat et al. found that the turbulent flow through an opening was 84% of the mean flow.

The flowrates through door and window openings are determined by integrating the flow velocity profiles found by applying Bernoulli's equation along streamlines passing through the opening as shown by Kiel and Wilson (1986). For convenience the following parameters are defined

$$P_b = CpS_U^2U^2 - 2gH_b\left(\frac{T_{in}-T_{out}}{T_{in}}\right) + \frac{2\Delta P_I}{\rho_{out}} \qquad (2\text{-}69)$$

$$P_t = CpS_U^2U^2 - 2gH_t\left(\frac{T_{in}-T_{out}}{T_{in}}\right) + \frac{2\Delta P_I}{\rho_{out}} \qquad (2\text{-}70)$$

where Cp and S_U are for the surface that the opening is in

H_b = Height above grade of the bottom of the opening

H_t = Height above grade of the top of the opening

As with the integrated wall flows the mass flows in and out depend on H_{NL}, T_{in} and T_{out}. Figures 2-19a to 2-19c show the three different cases of neutral level location and flow pattern for $T_{in} > T_{out}$. All of the possible cases for flow above and below H_{NL} are given in appendix A. Appendix A also contains a derivation for the flow in below H_{NL} for the case where H_{NL} falls in the opening and $T_{in}>T_{out}$, such that

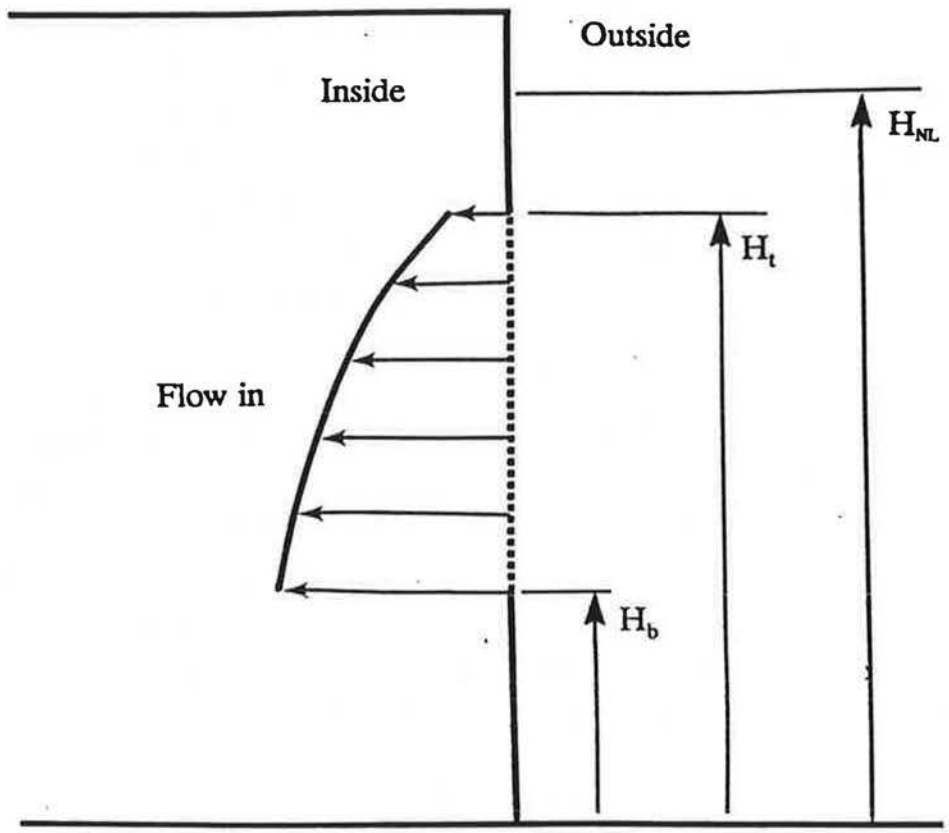

Figure 2-19a. Flow through window or door opening with the neutral level, H_{NL}, above the top of the opening, H_t, and all flow in.

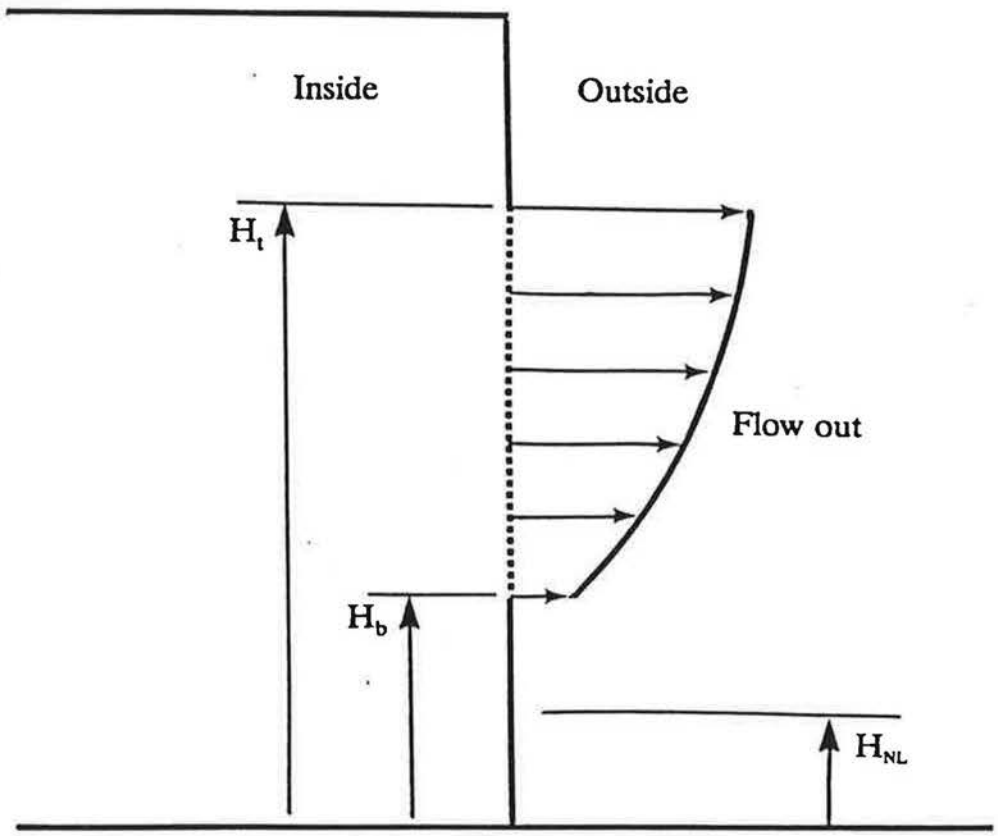

Figure 2-19b. Flow through window or door opening with the neutral level, H_{NL}, below the bottom of the opening, H_b, and all flow out.

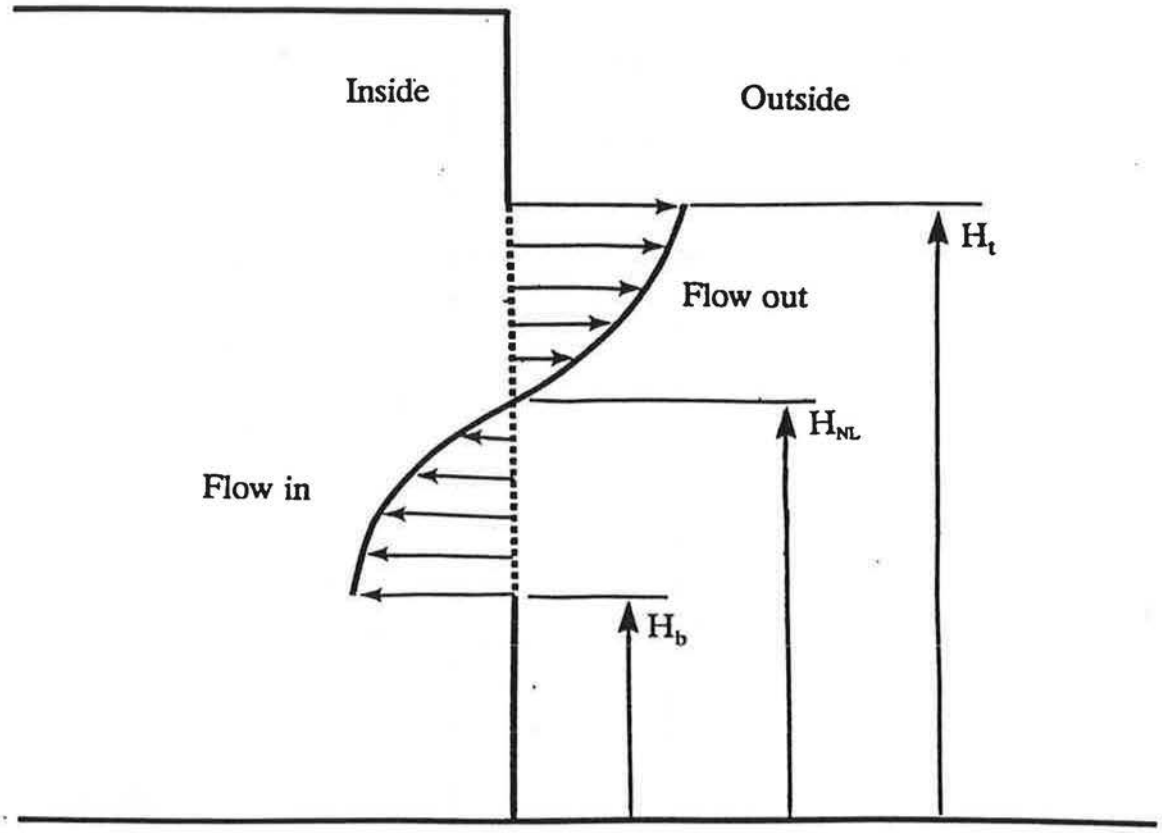

Figure 2-19c. Flow through window or door opening with the neutral level, H_{NL}, between the top, H_t, and the bottom of the opening, H_b. Flow is out above H_{NL} and in below H_{NL}.

$$M_{out}=(\rho_{out}\rho_{in})^{\frac{1}{2}}\frac{KWT_{in}}{3g(T_{in}-T_{out})}P_t^{\frac{3}{2}} \quad (2\text{-}71)$$

$$M_{in}=\rho_{out}\frac{KWT_{in}}{3g(T_{in}-T_{out})}P_b^{\frac{3}{2}} \quad (2\text{-}72)$$

2.13.8 Window and Door Flow Coefficient, K

The flow coefficient, K, accounts for reduction in flow due to flow contraction, viscous losses and interfacial mixing. An estimate for K that accounts for the variation in K due to interfacial mixing generated by atmospheric turbulence is given by Kiel and Wilson (1986) as

$$K=0.400+0.0045|T_{in}-T_{out}| \quad (2\text{-}73)$$

The flow coefficient must be altered when the interface is near the top or the bottom of the opening so that the iterative solution of flow for the whole building does not have the neutral level oscillating just above and below the top or bottom of the opening. A first order approximation is to let K vary linearly in the top and bottom 10% of the opening between the value of K with the neutral level at 10% or 90% of the opening height and K = 0.6 at the edges of the opening. This is physically realistic because when the interface is near the top or the bottom of the opening the edges of the opening will interfere with the interfacial mixing process. This will make the flow look more like one way flow with an assumed orifice discharge coefficient, K_D = 0.6.

2.14 Flow Through each Leak for the Attic

The attic ventilation section of ATTICLEAK-1 uses the same approach as for the house. The total leakage is divided into distributed leakage and localised leakage. The flow through each leak is then calculated using the pressure difference across each leak. The pressure difference uses the same relationship (Equation 2-18) as the house but with T_a replacing T_{in} in P'_T. For wind pressures, P_U is used together with the Cp's and S_U's for each leak location. The general pressure difference equation for attic leaks is given by

$$\Delta P(z)=CpS_U^2\rho_{out}\frac{U^2}{2}-gz(\rho_{out}-\rho_a)+\Delta P_{I,a} \qquad (2\text{-}74)$$

where $\Delta P_{I,a}$ is the internal pressure difference for the attic and is the equivalent of ΔP_I for the house.

Equation 2-74 can be written in terms of P_U and $P'_{T,a}$

$$\Delta P(z)=CpS_U^2P_U-zP'_{T,a}+\Delta P_{I,a} \qquad (2\text{-}75)$$

where

$$P'_{T,a}=\frac{\rho_{out}g(T_a-T_{out})}{T_a} \qquad (2\text{-}76)$$

The total distributed leakage flow coefficient $C_{d,a}$ and exponent $n_{d,a}$ are best estimated from fan pressurization results. All the distributed leakage sites are assumed to have the same flow exponent. The flow coefficients for the roof and soffit must be estimated as fractions of the total distributed leakage such that

$$C_{d,a}=\sum_{i=1}^{4}C_{s,i}+C_r \qquad (2\text{-}77)$$

where C_r is the total leakage in the two pitched roof surfaces and $C_{s,i}$ is the leakage in the soffit or gable ends above each wall. For the houses used in this study the north and south sides have soffits and the east and west sides have gable ends.

2.14.1 Pitched roof Leakage

The pitched roof leakage is treated the same way as house walls. The two pitched roof surfaces are assumed to have equal leakage. Therefore there is $C_r/2$ leakage in each surface. C_r is estimated from the total distributed leakage in the attic and n_r is the same as the n for the other distributed leaks. C_r is assumed to be evenly distributed over the pitched roof surfaces in the same way as wall leakage is evenly distributed. The same method of integrating the pressure difference over the height of the roof pitch can then be used to find the total mass flow. Equation 2-62 can be used with Equation 2-75 for attic pressure difference in place of the house pressure difference (Equation 2-58), and with $C_r/2$ in place of $C_{w,i}$.

Cp for the pitched roof surfaces is found using Equation 2-21 and Table 2-2. The pitched roof is assumed to have the same shelter factor as the furnace flue. This

means that if the surrounding obstacles are not higher than the flue top (which is close to roof peak height) then the pitched roof surfaces have no shelter and S_U = 1. If the surrounding obstacles are taller than the building in question then S_U for the pitched roof surfaces is estimated to be the same as the wall below them. For example, a south facing roof pitch would then have the same S_U as calculated for the south facing wall below it. For the attic roof the neutral level, $H_{NL,r}$, is calculated for the two roof pitches using the appropriate Cp and S_U values in

$$H_{NL,r}=\left(\frac{\Delta P_{I,a}+S_U^2 CpP_U}{P'_{T,a}}\right) \tag{2-78}$$

There are several different cases of flow through the pitched roof surfaces depending on the location of $H_{NL,r}$, T_a and T_{out}. The same combination of cases exist as for flow through walls. All of the cases are given in appendix A. The pressure differences at the eave height, ΔP_e, and at the roof peak, ΔP_p, are defined as follows and are convenient to use when calculating the mass flow rates.

$$\Delta P_p=\Delta P_{I,a}+S_U^2 CpP_U-H_pP'_{T,a} \tag{2-79}$$

$$\Delta P_e=\Delta P_{I,a}+S_U^2 CpP_U-H_eP'_{T,a} \tag{2-80}$$

An example case given by Equations 2-81 and 2-82 is for $T_a > T_{out}$ with $H_{NL,r}$ somewhere on the pitched roof surface between the eave height, H_e, and the peak height H_p. There is two way flow through the roof surface in this case with flow in below $H_{NL,r}$ and flow out above $H_{NL,r}$:

$$M_{r,out}=\frac{\rho_a \frac{C_r}{2}\Delta P_p^{(n_r+1)}}{(H_p-H_e)P'_{T,a}(n_r+1)} \tag{2-81}$$

$$M_{r,in}=\frac{\rho_{out} \frac{C_r}{2}\Delta P_e^{(n_r+1)}}{(H_p-H_e)P'_{T,a}(n_r+1)} \tag{2-83}$$

2.14.2 Soffit and Gable Leakage

The soffit and gable leakage are treated identically. The soffit and gable leakage is split into four parts, one for each side of the building. $C_{s,i}$ is the estimated fraction of the total attic distributed leakage in the soffit or gable on the i^{th} side of the building. H_s is the height of the leakage above grade and usually $H_s = H_e$ for soffits. For the gable leakage H_s can be assumed to be H_e plus half of the attic height (H_p - H_e). The wind pressure coefficient (Cp_i) and shelter factor ($S_{U,i}$) are assumed to be the same as for the wall below each soffit or gable. This simplifying assumption is made due to lack of data for wind pressure coefficients on soffits. There is little data because the additional complexity added to the building by including eave overhangs makes systematic wind tunnel measurements extremely time consuming. The pressure difference across each soffit or gable above wall i is then given by

$$\Delta P_{s,i}=\Delta P_{I,a}+Cp_i\ S_{U,i}^2\ P_U-H_s P'_{T,a} \qquad (2\text{-}83)$$

The flow through each soffit or gable is given by

$$M_{s,i}=C_{s,i}(\Delta P_{s,i})^{n_T} \qquad (2\text{-}84)$$

2.14.3 Attic Vent Leakage

Attic vents provide extra ventilation leakage area over the background distributed leakage. There can be multiple attic vents at different locations on the attic envelope, each with their own C_V and n_V. C_V and n_V are user specified leakage characteristics of each vent. Usually the vent can be assumed to act like an orifice with $n_V = 0.5$. In that case C_V can be estimated from the vent area multiplied by the discharge coefficient, K_D. The vent area should be corrected for any blockage effects e.g. by insect screens. $S_{U,V}$ and Cp_V for each vent are the same as for the attic surface they are on, either the gable ends (which have the same S_U and Cp as the wall below them) or the roof pitches. H_V is the height above grade of the vent and the pressure difference across each attic vent is given by

$$\Delta P_{V,a}=\Delta P_{I,a}+S_{U,V}^2\ Cp_V\ P_U-H_V\ P'_{T,a} \qquad (2\text{-}85)$$

$\Delta P_{V,a}$ is calculated for each attic vent and the flow through each attic vent is given by

$$M_{V,a}=C_V\,(\Delta P_{V,a})^{n_V} \tag{2-86}$$

2.14.4 Attic Floor Leakage

The mass flow rate through the attic floor is calculated by the house zone part of the ventilation model in Equation 2-54. The resulting $\Delta P_{I,a}$ from balancing the mass flows for the attic zone is returned to the house zone to be used in Equation 2-53 to calculate pressure across the ceiling, and then to recalculate the mass flow through the attic floor.

2.14.5 Ventilation Fans in Attics

Fans are included in the same way as for the house zone by using a fan performance curve. The operating point on the curve is determined by the pressure across the fan. The stack and wind pressures across each fan are found by specifying which attic surface the fan is located in and its height above grade, H_{fan}. Cp_{fan} and $S_{U,fan}$ are the same as the surface the fan is are located in. There can be multiple fans each with their own rated flowrates, Q_{rated}, and rated pressure differences, ΔP_{rated}. The pressure difference across each attic fan, $\Delta P_{fan,a}$, is given by

$$\Delta P_{fan,a}=\Delta P_{I,a}+S_{U,fan}^2 Cp_{fan} P_U - H_{fan} P'_{T,a} \tag{2-87}$$

Approximating the fan performance curve by a power law using p_{fan} gives the following equation for mass flow through each fan:

$$M_{fan,a}=\rho Q_{rated}\left(\frac{\Delta P_{rated}+\Delta P_{fan,a}}{\Delta P_{rated}}\right)^{p_{fan}} \tag{2-88}$$

where ρ is equal to ρ_a for outflow and ρ_{out} for inflow.

The flow direction is determined by the sign of the pressure difference term. A positive term means inflow and a negative term means outflow. ΔP_{rated} is positive for a supply fan and negative for an exhaust fan. The power, p_{fan}, depends on the type of fan being used. For the centrifugal fans used in this study it is assumed that $p_{fan} = 0.3$.

2.15 Solution Method

2.15.1 For Each Zone

All of the flow equations for the house contain the difference between the inside and outside pressure, ΔP_I, that is the single unknown (or $\Delta P_{I,a}$ for the attic).

To find ΔP_I all of the flow equations are combined into one equation that is the mass balance for air in the house

$$\sum M = M_F + M_f + M_c + \sum_{i=1}^{4} M_{w,i} + M_V + M_{fan} = 0 \qquad (2\text{-}89)$$

where M_f is the mass flow rate through all the floor level leaks, M_V is the mass flow rate through all of the vents and M_{fan} is the sum of the mass flow rates through all of the fans. This equation for mass balance is highly non-linear in ΔP_I. A Newton-Raphson iterative technique was used to attempt to solve this equation using the partial derivatives of all the flow equations with respect to ΔP_I. Unfortunately the shape of the solution curve of ΔP_I and ΣM makes this method unstable. A more robust iterative bisection technique was adopted because it is unaffected by the non-linearity of the function. This bisection search technique assumes that $\Delta P_I = 0$ for the first iteration and the mass inflow or outflow rates are calculated for each leak. At the next iteration ΔP_I is chosen to be +1000 Pa if total inflow exceeds total outflow and -1000 Pa if outflow exceeds inflow. These large initial pressure differences mean that even large high pressure fans may be included. Succeeding iterations use the method of bisection in which ΔP_I for the next iteration is reduced by half the difference between the last two iterations, thus the third iteration changes ΔP_I by $\pm$500 Pa. The sign of the pressure change is positive if inflow exceeds outflow and negative if outflow is greater then inflow. The limit of solution is determined by the number of iterations. After 17 iterations the change in ΔP_I is < 0.01 Pa, which gives mass flow imbalances on the order of 0.001 Kg/s (or 4Kg/hour).

For the attic the mass balance equation is given by

$$\sum M = M_r + M_c + \sum_{i=1}^{4} M_{s,i} + M_{V,a} + M_{fan,a} = 0 \qquad (2\text{-}90)$$

where M_r is the sum of the in and the out flows through the pitched roof surfaces, $M_{fan,a}$ is the sum of the mass flows through all the attic fans and $M_{V,a}$ is the sum of the flows through all the attic vents. As with the house all of the components of this mass balance equation contain the single unknown, $\Delta P_{I,a}$, the attic to outdoor pressure difference. The attic zone is solved using the same bisection technique as the house zone. The two zones interact through the ceiling flow that is common to both mass balance Equations 2-89 and 2-90.

2.15.2 Coupled Zones

The house and attic zones are coupled by the flow through the ceiling and pressure difference across the ceiling. The house zone uses $\Delta P_{L,a}$ to calculate the mass flow through the ceiling. This mass flow is used in the mass flow balance by the attic zone the calculate a new $\Delta P_{L,a}$. This is an iterative procedure that continues until the change in mass flow through the ceiling from iteration to iteration is less than 0.00001 Kg/s. A typical ventilation rate of 0.2 ACH for the houses in this study can be expressed in terms of mass flow as 0.0134 Kg/s. Thus the convergence criteria is about 0.075% of the total house flow.

2.16 Summary of important aspects of ATTICLEAK-1

ATTICLEAK-1 is a two-zone ventilation model that calculates ventilation rates for houses and attics. The flow through each leakage path (and the total flow for each zone) is found by determining the internal pressure in each zone that balances the mass flow rates in and out of each zone. The house and attic interact through the pressure difference and flowrate through the ceiling of the house, and the combined solution is found iteratively. The calculated ventilation rates are used in this study as inputs to the attic heat transfer model and the attic moisture transport model. The ventilation model and the heat transfer model are coupled because the ventilation rate effects the amount of outside and house air convected through the attic (as well as convective heat transfer coefficients) and the attic air temperature changes the attic air density. This change in density changes the mass flow rates and the stack effect driving pressures for ventilation. The combined ventilation and heat transfer model solution is found iteratively, with the ventilation rate being passed to the heat transfer model which then calculates an attic air temperature. This new attic air temperature is then used in the ventilation model to recalculate ventilation rates. The initial temperature estimate for the attic air used in the first iteration for the ventilation model is the outside air temperature. Most of the time the attic air is within a few degrees of the outside air temperature and the combined ventilation and heat transfer model requires only a few iterations (fewer than 5).

Some significant limitations and assumptions for ATTICLEAK-1 are listed below:

- There is assumed to be no valving action in the building and attic leakage so that flow coefficients are independent of flow direction.
- The building has a rectangular planform. The planform must not have the

longest side greater than about three times the shorter side because the wind pressure coefficients used in the model will be incorrect. In addition, both wall and floor level leakage is distributed among four walls and non-rectangular buildings (e.g. L-shaped) have more than four sides.

- The attic has two pitched roof surfaces and gable ends. This assumption affects the leakage distribution and the pressure coefficients applied to the attic leakage sites.
- The interior of both the house and the attic are well-mixed zones so that all of the air entering is completely mixed with the interior air.
- There are no indoor or outdoor vertical temperature gradients, so that the indoor and outdoor densities are independent of location.
- Air behaves as an incompressible ideal gas. This allows density and viscosity to be functions of temperature only.
- Wall and pitched roof leakage is evenly distributed so as to allow simple integration of height dependent mass flow equations.
- All wind pressure coefficients are averaged over a surface. This means that extremes of wind pressure occurring at corner flow separations are not included.
- The notch wake model does not include the three dimensional aspect of wake flow including vortices and flow acceleration at the edge of the wake. These are localised effects that are cannot be included in the model because leaks are not given specific horizontal locations. This can be an important factor for large openings in a wall that may experience much different wind pressures than that produced by the assumption of uniform wake effects for entire walls.
- Upwind obstacles are assumed to shade the entire wall height of the downwind building when calculating wind shelter.

Chapter 3. Attic Heat Transfer Model

The purpose of developing the attic heat transfer model is to determine the temperature of the attic air and the wood in the attic. These temperatures need to be known for the moisture transport model to calculate wood moisture content and to find saturation pressures. The saturation pressures are very important because they are used to calculate attic air relative humidity and to determine if mass is condensing. The moisture and heat transfer models are assumed to be uncoupled because the mass of water vapour transported in and out of the attic is very small (less than 1% of the air mass) and thus transports a negligible amount of energy. Later in this chapter it will be shown that condensation does release significant quantities of latent heat. The attic air temperature is also used to find the attic air density used in ATTICLEAK-1 to find the attic ventilation rates. The attic ventilation rate changes the energy balance for the attic air and the surface heat transfer coefficients. Fortunately this coupling of the ventilation model and the heat transfer model is weak because attic ventilation rates are not a strong function of attic air temperature, as will be shown later.

Some previous authors (Gorman (1987) and Burch and Luna(1980)) used simple steady-state energy balances in the attic that included the attic air, attic floor and the sheathing. These steady-state approaches do not capture the strong diurnal changes in attic temperature due to daytime solar gains or rapid changes in temperatures due to changing ventilation rates. As will be shown later by the attic simulations, these effects cannot be ignored if wood moisture content and condensed mass accumulation are to be predicted. Another approach taken by Peavy (1979) and Wilkes (1989) is to use response factors that include the effect of previous temperatures and heat fluxes to calculate a time dependent response for the attic temperatures. Neither Peavy or Wilkes separated the sheathing surfaces into north and south parts that receive different solar radiation gains or included conduction heat transfer losses through gable end walls. The most comprehensive model to date is that of Ford (1982). Ford (p.104) used a first order lumped heat capacity analysis where the change in energy at each node was equal to the sum of the heat fluxes at the node. The assumption of a lumped heat capacity analysis is improved here by splitting the wood into surface and inner layers. An option for further refinement of this model is to split the wood into more layers because this will improve the assumption of using a single temperature for each node. Ford also separated the north and south sheathing so that they may have different daytime solar gains and

included heat losses through gable ends. Because Ford's model is the most thorough it will be used as the basis of the heat transfer model for this study. A few refinements and simplifications to Ford's attic heat transfer model will be made as listed below:

- An additional node is used to account for the mass of wood in joists and trusses in the attic. This node effectively increases the thermal mass of the attic air.
- Attic ventilation and ceiling flow rates are calculated instead of being a required input. This results in an iterative procedure as the attic ventilation and ceiling flow rates depend on the attic temperature.
- Forced convection heat transfer coefficients are used inside the attic. In this study the ventilation rates are found using ATTICLEAK-1 and thus forced convection heat transfer coefficients may be calculated inside the attic. Ford did not have a ventilation model and so natural convection heat transfer coefficients were used.
- Radiation heat transfer inside the attic is simplified to three nodes: the attic floor and the two pitched roof surfaces. Ford also included gable ends and eaves but these components have small view factors and are neglected for simplicity in the present study.

The energy balance for the attic is based on Ford's lumped heat capacity analysis using the nodes shown in Figure 3-1 where:

T_1 = Temperature of the attic air
T_2 = Temperature of the underside of the North Sheathing
T_3 = Temperature of the outside of the North Sheathing
T_4 = Temperature of the underside of the South Sheathing
T_5 = Temperature of the outside of the South Sheathing
T_6 = Temperature of mass of wood in joists and trusses
T_7 = Temperature of the ceiling inside the house
T_8 = Temperature of the attic floor
T_9 = Temperature of the inside of the gable end walls
T_{10} = Temperature of the outside of the gable end walls

The pitched roof sheathing is labelled north and south so that the differences in solar radiation between north and south facing surfaces may be included. The test houses used in this study were in an east-west row so that they have north and south facing sheathing surfaces.

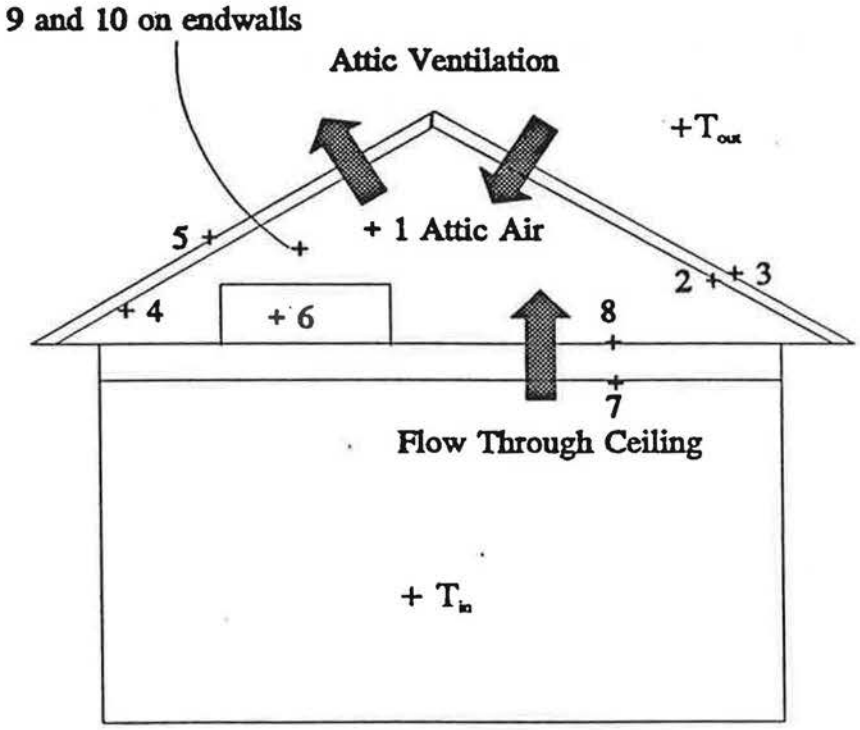

Figure 3-1. Node Locations for Heat Transfer Balance

1 = attic air
2 = underside of the North Sheathing
3 = outside of the North Sheathing
4 = underside of the South Sheathing
5 = outside of the South Sheathing
6 = mass of wood in joists and trusses
7 = ceiling inside the house
8 = attic floor
9 = inside of the gable end walls
10 = outside of the gable end walls

The rate of change of energy is equal to the sum of the heat fluxes for each node so that for node i

$$\rho_i V_i C_{sh,i} \frac{dT_i}{dt} = \Sigma q \qquad (3\text{-}1)$$

where ρ_i is the density [Kg/m^3] , V_i is the volume [m^3], $C_{sh,i}$ is the specific heat [J/KgK], T_i is temperature [K] and q are the heat fluxes [W]. The fluxes are due to convection, radiation and conduction heat transfer. The derivative in this equation is calculated using a finite difference approximation. Only the first term of the finite difference approximation is used so that the equation remains linear with temperature. This first order response assumes that temperatures change linearly with time so that the rate of change of energy with time at a node can be written as a linear equation in temperature as follows

$$\rho_i V_i C_{sh,i} \frac{T_i^j - T_i^{j-1}}{\tau} = \Sigma q \qquad (3\text{-}2)$$

were j refers to the current timestep and j-1 the previous timestep and τ is the length of the time step. Equation 3-2 is a backwards difference approximation to the derivative in Equation 3-1.

The error in approximating the derivative by the first term of the finite difference expansion is given by James, Smith and Wolford (1977) as

$$\text{Error} = \frac{5T^{\,i} - 18T^{\,i-1} + 24T^{\,i-2} - 14T^{\,i-3} + 3T^{\,i-4}}{6\tau} \qquad (3\text{-}3)$$

Using sheathing temperatures measured for this study Equation 3-3 has been used to estimate the errors for the finite difference approximation of Equation 3-2. The sheathing was chosen to evaluate the errors because it experiences the fastest temperature changes. The largest error will be for clear days when the sheathing temperature changes the fastest due to solar radiation gains. For a clear spring day the maximum error in rate of temperature change calculated using Equation 3-3 is about 1.75°C/hour. Over 24 hours the mean error is only 0.02°C/hour and the mean absolute error (where positive and negative errors do not cancel) is 0.6°C/hour. For other nodes whose temperatures change more slowly the errors would be reduced. The maximum error is 25% of the maximum measured temperature change rate of 7°C/hour for this day. This error would make a significant difference to the energy

Including the fact that the pitched roof surfaces and the floor have the largest surface areas of the attic nodes means that these three nodes dominate the internal radiation heat transfer in the attic. For simplicity the model developed for this study will neglect the eave overhangs and the gable ends because they have only a small area and the view factors for the floor and pitched roof surfaces are the largest. This reduces internal attic radiation heat transfer to a three surface problem that does not require numerical integration to find the view factors, F_{i-j}. The subscript i on the view factor indicates the surface that the radiation leaves and the subscript j the surface that the radiation reaches. The three surfaces are

1. Floor, node 8
2. Inner north sheathing, node 2
3. Inner south sheathing, node 4

and the node locations are illustrated in Figure 3-1. The following analysis does not use the complex numerical integration technique used by Ford (p.88) to find the view factors. For the simple three surface model used in this study the view factors have be determined as follows.

For a the test houses at AHHRF the roof slope is 1:3 and the attic floor is almost square (7.3m x 7.8m) if the eaves are included. From symmetry, the view factors for radiation between the floor and each of the two sheathing surfaces are the same. In addition, using a three surface model assumes that the floor only has radiant exchange with these two surfaces so that

$$F_{8-2}=F_{8-4}=0.5 \tag{3-4}$$

The calculated areas of the three surfaces (A_2, A_4 and A_8 where the subscripts refer to the node number) are A_2 = 30.3 m^2, A_4 = 30.3 m^2 and A_8 = 57 m^2. Using the reciprocity theorem and using these calculated areas the view factors for radiation from the sheathing (nodes 2 and 4) to the floor (node 8) are given by

$$F_{4-8}=F_{8-4}\frac{A_8}{A_4}=0.5\frac{57}{30.3}=0.94=F_{2-8} \tag{3-5}$$

The sum of the radiation view factors for each surface is unity, therefore the view factors for radiation between the sheathing surfaces are

$$F_{4-2}=F_{2-4}=0.06 \quad (3\text{-}6)$$

If only the attic floor is included in A_8 (i.e. not including the eaves) then A_8 is equal to 49 m^2 and the view factors become

$$F_{4-8}=F_{2-8}=0.81 \quad (3\text{-}7)$$

$$F_{4-2}=F_{2-4}=0.19 \quad (3\text{-}8)$$

For the purposes of verifying the model a nominal attic width of 7m was used which lies between these two extremes and the view factors then become

$$F_{4-8}=F_{2-8}=0.84 \quad (3\text{-}9)$$

$$F_{4-2}=F_{2-4}=0.16 \quad (3\text{-}10)$$

Radiation for Three Attic Surfaces

The calculation of radiation exchange inside the attic is based on heat exchange between non-blackbodies from Holman (1981, p.330-332). The final form of the internal attic radiation heat transfer to be used in the present study is given by Equations 3-22 and 3-23. These equations represent a linearised solution to the radiant heat transfer between three bodies: i, j and k. Equations 3-11 to 3-21 are given here to show how the linearised equations were developed by Holman.

The internal surfaces of the attic are assumed to be opaque bodies with no transmission of radiation. Based on this assumption the total radiation leaving the surface can be written as

$$J=\epsilon E_b+(1-\epsilon)G \quad (3\text{-}11)$$

where J = radiosity, the total radiation leaving per unit surface area [W/m^2]

ϵ = emissivity of surface

E_b = black body emissive power per unit surface area [W/m^2]

G = Irradiation, the total incident radiation per unit surface area [W/m^2]

The net energy radiant energy, q_R, leaving the surface is the difference between the radiosity and the irradiation

balance for that hour. Because the temperature is cyclic Equation 3-2 will sometimes overpredict the rate of change of temperature and sometimes under predict, and over 24 hours these effects will tend to cancel out. This is why the 24 hour averages errors are much smaller than the maximum error. The linear finite difference approximation of Equation 3-2 is used in this study for simplicity. The errors introduced by this approximation may be seen in errors in the time response of temperatures in the attic.

In the present study τ is equal to one hour because this is the time interval between measured data points. The energy balance is performed at each hour j with the previous hour's (j-1) temperatures used to calculate the rate of change of energy at each node. This results in a linear system of 10 equations and 10 unknowns (the temperatures) that can be solved using simple matrix solutions. A more complex analysis is unjustified because the rate of change of entered values such as outside temperature, T_{out}, are usually not known.

Figure 3-2 shows some typical heat transfer rates for a winter night and a winter day. The heat flows and attic air temperature were calculated during the simulations presented later in Chapter 7. The arrows indicate the direction of heat flow in each case. These results show that the heat flow through the ceiling is always an important contributor to the heat balance for the attic. During the day, when the solar gains heat the south sheathing, the ventilation flow cools the attic. At night, when the sheathing is losing heat by radiation to the night sky, the ventilation flow acts to heat the attic. This implies that it is important to include the attic ventilation rate and the external sheathing radiation exchanges in the heat transfer model.

3.1 Radiation Heat Transfer

3.1.1 Inside the Attic (Nodes 2,4 and 8)

View Factors

Ford (p.85) calculated view factors for an attic split into seven sections: floor, two gable end walls, two pitched roof surfaces and two eave overhangs (soffits). From Ford's analysis for a gable end attic the view factors from the attic floor and the pitched roof sheathing surfaces to the gable ends are about 0.03. From the pitched roof surfaces to the eaves the shape factors are about 0.11 for the eave directly below each pitched roof surface and about 0.003 for the eave across the attic from each pitched roof surface. The view factors from the pitched roof surfaces to the floor are about 0.76 and from the floor to each pitched roof surface about 0.47.

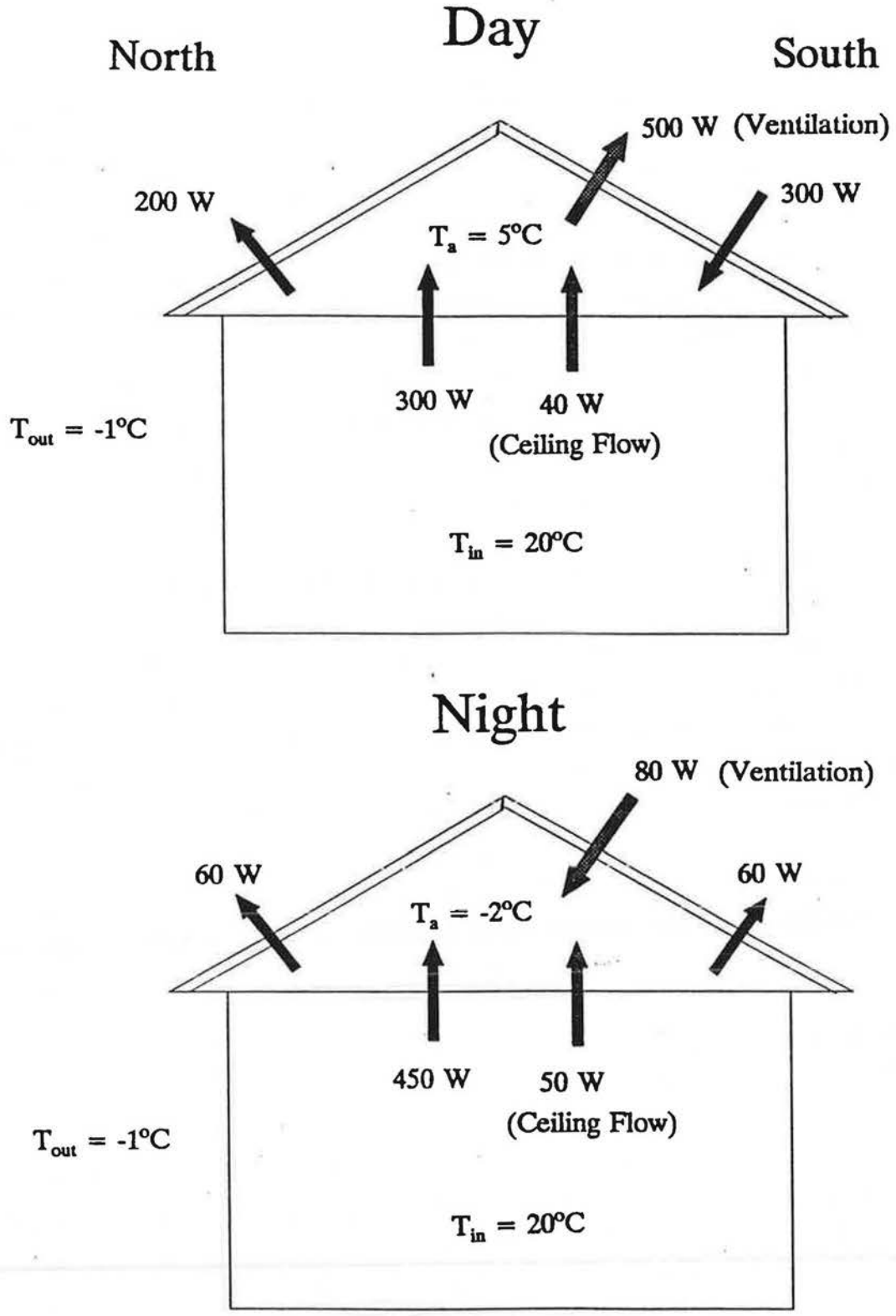

Figure 3-2. Typical attic heat fluxes for an attic with 7 ACH, clear skies, and an outdoor temperature of -1°C.

$$\frac{q_R}{A} = J - G \qquad (3\text{-}12)$$
$$= \epsilon E_b + (1-\epsilon)G - G$$

where A = Area [m^2] of the surface

q_R = rate of radiant energy leaving the surface [W]

Rearranging Equation 3-11 gives the irradiation

$$G = \frac{J - \epsilon E_b}{1-\epsilon} \qquad (3\text{-}13)$$

and substituting Equation 3-13 in 3-12 yields an equation for the rate of energy leaving the surface:

$$q = \frac{E_b - J}{\left(\frac{1-\epsilon}{A\epsilon}\right)} \qquad (3\text{-}14)$$

Of the total radiation leaving surface i the amount that reaches j is $J_iA_iF_{i-j}$ and the radiation leaving j that reaches i is $J_jA_jF_{j-i}$. The net exchange from surface i to surface j is then given by

$$q_{i-j} = J_iA_iF_{i-j} - J_jA_jF_{j-i} \qquad (3\text{-}15)$$

A_iF_{i-j} is equal to A_jF_{j-i} by reciprocity and Equation 3-15 can be written as

$$q_{i-j} = \frac{J_i - J_j}{\left(\frac{1}{A_iF_{i-j}}\right)} \qquad (3\text{-}16)$$

Using Equation 3-11 in Equation 3-16, the net radiation leaving surface i that reaches the surface j is given by

$$q_{i-j} = \frac{E_{b,i} - E_{b,j}}{\frac{1-\epsilon_i}{\epsilon_i A_i} + \frac{1}{A_iF_{i-j}} + \frac{1-\epsilon_j}{\epsilon_j A_j}} \qquad (3\text{-}17)$$

For the exchange between surfaces j and k Equation 3-17 may be written with k

substituted for j. Combining the exchange between the i and the other two surfaces j and k yields Equation 3-18.

$$q_i=\frac{E_{b,i}-E_{b,j}}{\frac{1-\epsilon_i}{\epsilon_i A_i}+\frac{1}{A_i F_{i-j}}+\frac{1-\epsilon_j}{\epsilon_j A_j}}+\frac{E_{b,i}-E_{b,k}}{\frac{1-\epsilon_i}{\epsilon_i A_i}+\frac{1}{A_i F_{i-k}}+\frac{1-\epsilon_k}{\epsilon_k A_k}} \qquad (3\text{-}18)$$

where q_i is the net radiation heat transfer for node i. Similar equations can be written for surfaces k and j.

The emissive power of a body, E_b, is given by

$$E_b=\sigma T^4 \qquad (3\text{-}19)$$

where T is the temperature of the body and σ is the Stephan-Boltzman constant that is equal to $5.669*10^{-8}$. Substituting the relationship for emissive power, Equation 3-19, into the radiant heat exchange Equation 3-18 results in a highly nonlinear heat transfer equation with temperature to the fourth power where

$$E_{b,i}-E_{b,j}=\sigma(T_i^4-T_j^4) \qquad (3\text{-}20)$$

To keep the system of attic heat transfer equations linear so that it may be easily solved, Equation 3-20 must be linearized. By rearranging the (T^4_i - T^4_j) term a linearizing approximation may be obtained from Holman (p.394)

$$(T_i^4-T_j^4)=(T_i-T_j)(T_i+T_j)(T_i^2+T_j^2) \qquad (3\text{-}21)$$

For the heat transfer model developed here the linearization term (T_i + T_j)(T^2_i + T^2_j) is calculated from the previous hour's temperatures. Equation 3-18 can then be written in terms of (T_i - T_j) only, thus linearizing the equation. Using the previous hour's temperatures will produce significant errors if the temperatures are changing rapidly. The worst case for attics occurs when temperatures change rapidly after the sun rises in the morning when the sheathing changes temperature the fastest. For a clear spring day that has rapid temperature changes measurements at AHHRF have shown that the North facing sheathing (node 2) changes temperature at approximately 6°C an hour and the South Sheathing (node 4) at 11°C an hour. This rapid change takes place between 10 and 11 a.m. Calculating the linearization term using 10 a.m. temperatures and then using 11 a.m. temperatures will show how much

error is induced by using 10 a.m. temperatures to linearize radiation heat transfer at 11 a.m.

Using 10 a.m. temperatures $(T_2 + T_4)(T^2_2 + T^2_4) = 7.5*10^7$

Using 11 a.m. temperatures $(T_2 + T_4)(T^2_2 + T^2_4) = 8.2*10^7$

Thus this linearization technique can produce errors up to about 9% in this linearization term. This implies the same percentage error in $(T^4_2 - T^4_4)$, $E_{b,2} - E_{b,4}$ and the total radiation heat transfer between these two nodes, q_{2-4}. For less rapid change in temperatures experienced at the other hours of the day the error is much smaller, typically 1% to 2%.

Equation 3-18 can now be written in a linearized form

$$q_i = A_i h_{R,i-j}(T_i - T_j) + A_i h_{R,i-k}(T_i - T_k) \qquad (3\text{-}22)$$

where $h_{R,i-j}$ are radiation heat transfer coefficients from node i to node j that are calculated from

$$h_{R,i-j} = \frac{\sigma(T_i + T_j)(T_i^2 + T_j^2)}{\frac{1-\epsilon_i}{\epsilon_i} + \frac{1}{F_{i-j}} + \frac{(1-\epsilon_j)A_i}{\epsilon_j A_j}} \qquad (3\text{-}23)$$

The emissivity of surfaces found in building construction is given by ASHRAE (1989)(Chapter 37). For the inside sheathing surfaces a typical value for wood is $\epsilon = 0.90$ and for the attic floor that is assumed to be covered with fibreglass insulation the typical emissivity glass (from ASHRAE (1989), Chapter 37) is used, $\epsilon = 0.94$. The emissivity of glass is also typical of diffuse surfaces, and the fibreglass insulation is a diffuse surface due to its roughness. Equation 3-23 is applied to each of the three interior attic radiation heat transfer nodes: the floor and the two pitched roof surfaces. The shape factors, F_{i-j}, are found using Equations 3-9 and 3-10.

3.1.2 Solar Radiation (Nodes 3 and 5)

Solar gain is a significant term in the energy balance because it has large peak values. For the AHHRF attic sheathing area this amounts to a peak of 15kW for 550 W/m^2 in winter when attic moisture problems are most prominent. In the summer the solar gain can be as high as 1050 W/m^2 on a clear day. These large solar gains heat the attic above the ambient temperature and thus have a large effect on moisture transport in the attic by forcing moisture out of the warm sheathing. This dries the sheathing and raises the moisture content of the attic air.

Solar gains are only applied to the external sheathing surfaces. The energy transfer due to solar radiation is

$$q_R = A\alpha G \qquad (3\text{-}24)$$

where q_R is radiation heat transfer rate [W]

A = Surface area [m^2]

α = Surface absorbtivity $\approx$ 0.90 for shingles (ASHRAE (1989) Chapter 37)

G = Total Solar Radiation [W/m^2], both direct and diffuse.

The values of G must be specified as entered data to the model and will generally be different for north and south sheathing surfaces. Values measured for this study at the AHHRF have shown south sheathing solar radiation peaks of about 550 [W/m^2] with north sheathing peaks of only 60 [W/m^2] on a clear winter day. However, on a cloudy winter day both roof surfaces receive a similar quantity of solar radiation, with peaks of about 120 [W/m^2] on both surfaces. The differences between these values show how important it can be to have good estimates of cloud cover when estimating attic temperatures.. Snow on the roof will change the absorbtivity and thus the solar gains. This effect will be examined in the simulations presented in Chapter 7.

3.1.3 Radiant Exchange of Exterior Surfaces with Sky and Ground (Nodes 3 and 5)

In addition to the daytime solar gain the outside of the pitched roof sheathing has low temperature long wave radiant exchange with the sky and the ground. This exchange is responsible for cooling of the sheathing at night as it radiates energy to the cooler sky. This nighttime temperature reduction in the sheathing is also important for moisture transport. Because the sheathing is the coldest attic surface at night it tends to have a lower vapour pressure and thus the water vapour in the attic air is transported to the inner sheathing surfaces. The cooling of the sheathing also leads to an increased quantity of condensed mass at the surface. On a cloudy night the cooling of the sheathing is reduced because the radiation exchange is with clouds that are warmer than the sky temperature. Both the clouds and the ground are assumed to be at the outside air temperature. The view factors that account for the proportion of sky, cloud or ground seen by the pitched roof surface are from Ford (1982).

Exterior Radiation Heat Transfer

The net radiation exchange for exterior pitched roof sheathing surfaces has the same form as Equations 3-22 and 3-23 for the internal radiation because this is a

three body problem involving the roof surface, the sky and the ground and the clouds (which are at the same temperature). The rate of radiation heat exchange, $q_{R,i}$, for an exterior attic surface, i, is

$$q_{R,i}=\frac{E_{b,i}-E_{b,sky}}{\frac{1-e_i}{A_i e_i}+\frac{1}{A_i F_{i-sky}}}+\frac{E_{b,i}-E_{b,g}}{\frac{1-e_i}{A_i e_i}+\frac{1}{A_i F_{i-g}}} \qquad (3\text{-}25)$$

where $E_{b,i}$ = Emissive power of surface i at T_i

$E_{b,sky}$ = Emissive power of sky = σT^4_{sky}

$E_{b,g}$ = Emissive power of ground and clouds (that are assumed to be at T_{out}) = σT^4_{out}

A_i = Area of surface

ϵ = Emissivity of surface. Emissivity of shingles is estimated to be = 0.90 from ASHRAE (1989), Chapter 37.

$F_{i\text{-}sky}$ is the view factor from pitched roof surface i to the clear sky.

$F_{i\text{-}g}$ is the view factor from the pitched roof surface i to the ground and the clouds.

The sky temperature T_{sky} depends on the water vapour pressure in the air and is discussed in the next section. The view factors give the fraction of exposure to the ground (and clouds) and the sky for the pitched roof surfaces. Using the same view factors for both pitched roof surfaces assumes that the cloud cover is uniformly distributed over the sky. The view factors will be discussed in detail in the following sections.

Equation 3-25 is linearized the same way as the interior radiation (see Equation 3-22) so that for exterior surface i (where i = 5 for the outside of the south sheathing and i = 3 for the outside of the north sheathing)

$$q_{R,i}=A_i h_{R,i-g}(T_i-T_{out})+A_i h_{R,i-sky}(T_i-T_{sky}) \qquad (3\text{-}26)$$

where $h_{R,i\text{-}g}$ is the radiation heat transfer coefficient from roof surface i to the ground and clouds and is given by

and $h_{R,i\text{-}sky}$ is the radiation heat transfer coefficient from roof surface to the clear sky and is given by

Effective Sky Temperature for Radiation

The sky temperature, T_{sky}, is the equivalent temperature of an imaginary

$$h_{R,i-g}=\frac{\sigma(T_i+T_{out})(T_i^2+T_{out}^2)}{\frac{1-e_i}{e_i}+\frac{1}{F_{i-g}}} \tag{3-27}$$

$$h_{R,i-sky}=\frac{\sigma(T_i+T_{sky})(T_i^2+T_{sky}^2)}{\frac{1-e_i}{e_i}+\frac{1}{F_{i-sky}}} \tag{3-28}$$

blackbody that radiates energy at the same rate as the sky. The effective sky temperature, T_{sky}, is a function of air temperature, T_{out}, and water vapour pressure P_v. Parmelee and Aubele (1952) developed the following empirical fit to measured data to estimate T_{sky} for horizontal surfaces exposed to a clear sky.

$$T_{sky}=T_{out}\left(0.55+5.68*10^{-3}\sqrt{P_v}\right)^{0.25} \tag{3-29}$$

where P_v is in Pascals and the temperatures are in Kelvin. Sample calculations show how T_{sky} can be very different from T_{out}. For example at T_{out} = 273K and 50%RH (so that P_v = 305 Pa) then T_{sky} = 245K, almost 30K difference. This effect of a reduced sky temperature becomes more pronounced at lower temperatures where even saturated air has a low water vapour pressure. Because Equation 3-29 is for horizontal surfaces fully exposed to a clear sky, Ford (1982) (p.96) developed the view factors $F_{i\text{-}sky}$ and $F_{i\text{-}g}$ to account for the amount of cloud in the sky and the slope of the pitched roof surfaces.

View Factor To Account For Cloud Cover

The view factor from a horizontal surface, $F_{h\text{-}sky}$, to the sky that accounts for cloud cover is given by

$$F_{h-sky}=(1-S_C) \tag{3-30}$$

where S_C is the fraction of sky covered by cloud that must be estimated as an input to the model. S_C = 0 means there is no cloud and S_C = 1 implies complete cloud cover.

View Factor To Account For Inclination

The fraction of the sky seen by a tilted surface, $F_{i\text{-}sky}$, is directly proportional to the angle of inclination from the horizontal, β [degrees], such that

$$F_{i-sky}=\frac{180-\beta}{180} \tag{3-31}$$

Combining Equation 3-31 with 3-30 gives the view factor, $F_{i\text{-}sky}$, from a tilted roof to a cloudy sky at T_{sky}

$$F_{i-sky}=\frac{(1-S_C)(180-\beta)}{180} \tag{3-32}$$

The pitched roof surface sees either the clouds and ground or the sky and so the two view factors must add up to unity. Assuming that the ground, cloud and air temperatures are the same then a view factor to the ground and clouds, $F_{i\text{-}g}$, can be defined as

$$F_{i-g}=1-F_{i-sky} \tag{3-33}$$

3.1.4 Radiant Exchange of the Ceiling (Node 7) with the Room Below

This is modelled as a two body enclosed system where one body is the ceiling and the other body is the interior surfaces. The interior surfaces are assumed to be all at the same temperature as the inside air, T_{in}. The same linearization as for the pitched roof surfaces and the attic floor is applied so that the radiation heat transfer, $q_{R,7}$, is a linear function of temperature. The heat transfer coefficient, $h_{R,7\text{-}in}$, is calculated based on the previous hour's temperatures. The ceiling is node 7 and so the radiation heat transfer at this node can be written as

$$q_{R,7}=A_7 h_{R,7-in}(T_7-T_{in}) \tag{3-34}$$

where the radiation heat transfer coefficient is

$$h_{R,7-in}=\frac{\sigma(T_7+T_{in})(T_7^2+T_{in}^2)}{\frac{1-\epsilon}{\epsilon}+\frac{1}{F_{7-in}}+\frac{(1-\epsilon)A_7}{\epsilon A_{in}}} \tag{3-35}$$

where A_7 = ceiling area

A_{in} = Internal house surface area

ϵ = 0.9 for interior surfaces. This is a typical value for painted surfaces, wood and paper from ASHRAE (1989) Chapter 37.

$F_{7\text{-}in}$ = 1 because all the surfaces are enclosed.

3.2 Convection Heat Transfer

3.2.1 House Internal Free Convection (Node 7)

Due to low air velocities in the house turbulent natural convection is assumed to be dominant because there is no forced convection inside the house. The heat transfer on the ceiling due to free convection is given by

$$q_T = h_T A \Delta T \tag{3-36}$$

where q_T is the free convection heat transfer rate [W]

h_T is the free convection heat transfer coefficient [W/m^{2}K]

A is the surface area

ΔT is the temperature difference

The turbulent free convection heat transfer coefficient, h_T [W/m^{2}K], is given by Holman (1981), p.285, as

$$h_T = Y_T (\Delta T)^{\frac{1}{3}} \tag{3-37}$$

where Y_T depends on surface geometry and orientation and the direction of heat flow and ΔT is the temperature difference between the surface and the surrounding air. Ford (1982) used the free convection heat transfer coefficients of Fuji and Imura(1972) for convection heat transfer (over flat plates) in both the attic and the house. Fuji and Imura found heat transfer coefficients for multiple plate orientations with the plates both heated and cooled. For the model developed here it is assumed that the house ceiling is a cooled horizontal plate facing downwards. This implies that the attic is cooler that the house which is true almost all of the time in temperate climates. Fuji and Imura used data correlations to suggest that the Nusselt number for a horizontal cooled plate facing downwards is given by

$$\frac{h_T L}{k} = 0.13(GrPr)^{\frac{1}{3}} \tag{3-38}$$

where Gr = Grashof Number

Pr = Prandtl number

k = thermal conductivity [W/mK]

L = Length Scale for convection heat transfer [m]

The Grashof number represents the ratio of buoyancy to viscous forces and is given by

$$Gr=\frac{g\beta_T\Delta TL^3}{\nu^2} \tag{3-39}$$

where β_T is the volume coefficient of thermal expansion

ν is the kinematic viscosity of the fluid [m^2/s]

g is gravitational acceleration [m/s^2].

For an ideal gas, $\beta_T = 1/T$, where T is the absolute temperature of the gas. The Prandtl number is given by

$$Pr=\frac{\nu}{\lambda} \tag{3-40}$$

where λ is the thermal diffusion coefficient [m^2/s].

Gr and Pr can be estimated for air given typical values of λ and ν. For air Pr is typically 0.71, k is about 0.02624 [W/mK] and Gr is approximately $2084L^3\Delta T$. The length scale, L, in Gr cancels with the L on the left hand side of Equation 3-38 and does not need to be estimated. Substituting these values into Equation 3-38 yields the following equation for free convection heat transfer coefficient

$$h_T=3.2(\Delta T)^{\frac{1}{3}} \tag{3-41}$$

To keep the heat transfer equations linear, ΔT is evaluated using the previous hours temperatures.

3.2.2 Attic Internal (Nodes 2 and 4) and External Convection (Nodes 3 and 5)

The convection inside the attic has been assumed by previous authors (e.g. Ford (1982) and Burch and Luna (1980)) to be dominated by free convection. For an enclosed space, such as an attic, the ratio of buoyancy forces (due to temperature differences) to inertial forces (due to forced air movement) determines wether the surface heat transfer is due to free or forced convection. In most attics the ventilation rates are high which results in relatively high forced air velocities. In addition, the ventilation flows close to the attic leaks, even at low ventilation rates, will act to disrupt any motion due to free convection. This means that forced

convection due to ventilation will be more important for the convection heat transfer processes on the inside surfaces of the attic. The model developed for this study uses forced convection heat transfer coefficients, h_U, whose magnitudes depend on attic ventilation rates. This is important because it makes the energy balance for the attic more dependent on the ventilation rates. In addition, the mass transfer coefficients used in the moisture model are linearly related to the convection heat transfer coefficients so that the attic ventilation rate will also change the surface mass transfer rates of moisture in the attic.

Both natural convection and forced convection inside of the attic produce heat transfer coefficients that are of the same magnitude so that assuming forced convection is not critical. Using Equation 3-41 to calculate the free convection heat transfer and Equation 3-55 (that will be developed in the following sections) for forced convection, a range of heat transfer coefficients may be estimated. For free convection the range of h_T is about 0.3 to 6 W/m^{2}K, and for forced convection the range of h_U is about 1 to 10 W/m^{2}K, corresponding to the low and high ventilation rates encountered in the attics. The following section shows how the forced convection heat transfer coefficients are calculated and how the assumptions for calculating attic air velocities due to ventilation used in this model effect the dominance of free and forced convection.

For both the internal attic surfaces and the external pitched roof surfaces the forced convection heat transfer is given by

$$q = A h_U \Delta T \tag{3-42}$$

where q_U is the forced convection heat transfer coefficient [W]

A = Surface area [m^2]

h_U [W/m^{2}K] is calculated using Equation 3-52

ΔT = Temperature difference between surface and the surrounding air.

The ratio of buoyancy to inertia forces is used to determine if natural or forced convection is dominant. The buoyancy forces are represented by Gr from Equation 3-39 and the ration of inertial to viscous forces are represented by the Reynolds number, Re

$$Re = \frac{U_U L}{\nu} \tag{3-43}$$

where U_U is the velocity of the forced flow due to attic ventilation. Based on an

order of magnitude analysis of the natural convection boundary layer equations Holman (1982) p.295 suggests the following criterion for the domination of natural convection over forced convection

$$\frac{Gr}{Re^2}>1 \qquad (3\text{-}44)$$

The ratio of buoyancy forces to inertia force in Equation 3-44 is called the Richardson number, Ri. Ri is given by substituting Equations 3-39 and 3-43 into 3-44 such that

$$Ri=\frac{g\beta_T\,\Delta TL}{U_U^2}>1 \qquad (3\text{-}45)$$

In Ri the viscosity, ν, in Gr and Re cancels so that Ri is independent of viscosity as expected for forced turbulent flows.

The dominance of free or forced convection depends on the value chosen for a typical attic forced air velocity, U_U. Previous attic heat transfer studies by Ford (1982) and Burch and Luna (1980) calculated U_U by assuming a plug flow model of air flow through the attic so that

$$U_U=\frac{Q_aL}{3600s} \qquad (3\text{-}46)$$

where Q_a = attic ventilation rate in air changes per hour [ACH] and L [m] was assumed by Ford and Burch and Luna to be the length of attic in flow direction. For typical values measured in this study for Q_a equal to 5 ACH and L equal to 7m then, from Equation 3-46, U_U is approximately $1*10^{-2}$ m/s. Using this estimate of velocity in Equation 3-45 with a typical attic length scale for convection flows of 1m yields

$$Ri=380\Delta T \qquad (3\text{-}47)$$

This ratio of buoyancy to inertial forces implies natural convection is dominant even at very low temperature differences.

The plug flow model for attic ventilation is unrealistic because when air enters or leaves the attic it does so through a combination of small cracks (the distributed leakage) and localized leakage sites. The flow velocity through these leaks is much higher than the plug flow model indicates. To estimate this velocity the ventilation

rate of the attic is divided by the area that it flows through. The flow area is the leakage area of the attic A_{LA} [m^2]. A_{LA} is the area of an orifice that would have the same flow rate as the attic at 4 Pa and is found by equating orifice flow to the general flow Equation 2-1.

$$A_{LA}=C_{d,a}\sqrt{\frac{\rho_a}{2}}\Delta P^{0.5-n_{d,a}} \qquad (3\text{-}48)$$

where $C_{d,a}$ and $n_{d,a}$ are the distributed leakage coefficient and power for the attic, ρ_a is the density of the attic air and ΔP = 4 Pa. The A_{LA} calculated using Equation 3-48 is the total attic leakage area of which about half will have inflow and half will have outflow. The flow area used to estimate velocities will then be half of the total A_{LA}. This would overestimate the flow velocity because further from the leaks the velocity will be lower. This implies that there are different heat transfer coefficients for different parts of the attic depending on the distance from the leakage sites. What is required is a typical advection velocity that can be applied to all interior attic surfaces. As a first approximation U_U is calculated for this study by dividing the velocity by four. This factor could be adjusted to provide better approximations of the heat transfer coefficients but will not be changed here due to lack of measured data for attic heat transfer coefficients and flow velocities. The velocity, U_U, can then be estimated by

$$U_U=\frac{M_a}{\rho_a\frac{A_{LA}}{2}}\frac{1}{4} \qquad (3\text{-}49)$$

where M_a [Kg/s] is the attic ventilation rate and A_{LA} is divided by 2 in Equation 3-49 as an estimate of the inflow area and 1/4 is the velocity reduction factor. An estimate of U_U using Equation 3-49 can be made using the same attic ventilation rate as for the plug flow model of 5 ACH. The volume of the attics used in this study is 61 m^3 and A_{LA} is about 1500 cm^2 (as will be shown later in Chapter 5). Substituting these values into Equation 3-49 gives U_U equal to 0.3 m/s. This is thirty times larger than the results of the plug flow estimate (Equation 3-46) suggesting that the plug flow model may not be a good estimate of attic air velocities for heat transfer calculations.

Using U_U equal to 0.3 m/s the Richardson number (Equation 3-45) is

$$Ri = 0.4\Delta T \qquad (3\text{-}50)$$

At typical attic air to surface temperature differences of 5K or less (from measurements made for this study at AHHRF) this result for Ri implies that neither free or forced convection is dominant inside the attic. Because Ri is inversely proportional to U^2_U small changes in U_U will make Ri much smaller and increase the likelihood of forced convection being dominant. However free convection could still occur for extreme conditions in the middle of clear days with low ventilation rates when U_U is small and ΔT is large. Measurements made for this study at AHHRF (see Chapter 5) have shown that sheathing surfaces can be up to 5K hotter than the attic air under these conditions. Because extreme conditions are required for free convection to occur it is assumed that forced convection should be used for the internal attic surfaces. In addition, the ventilation flows act close to the attic surfaces since all the leaks are in the surfaces and they also act to break up any natural convection cells within the attic space. These factors also suggest that forced convection gives a better estimate of the surface heat transfer.

The most important effect of the forced convection method is that the heat transfer is a function of the ventilation rate. This is important because this effect was not included by the free convection assumed in previous studies. Making the convection heat transfer coefficients functions of ventilation rate also has an effect on the moisture transport model because it uses the convection heat transfer coefficients to calculate mass transfer coefficients for the interior attic surfaces. Another advantage of using forced convection heat transfer coefficients is that they are the same for every surface. For free convection the heat transfer coefficients change depending on surface orientation (horizontal, vertical, at an angle and facing up or down) and direction of heat transfer. Using forced convection coefficients eliminates these complications.

The above analysis showed that neither free or forced convection is always dominant in an attic. A future refinement of this heat transfer model is to use a combination of heat transfer coefficients. When ventilation rates are high the forced convection coefficient would be used and at low ventilation rates with high temperature differences between the wood surfaces and attic air, the free convection coefficient would be used. This combination was not examined here because the method by which the two cases combine for attics requires further experiments that are beyond the scope of this study.

The following section shows how the forced heat transfer coefficients were estimated. For turbulent forced convection over a flat plate Holman (1981), p.202, gives a relationship for the Nusselt number, Nu, (ignoring the initial laminar region)

$$Nu=\frac{h_U L}{k}=0.037 Re^{\frac{4}{5}} Pr^{\frac{1}{3}} \tag{3-51}$$

and substituting for Re and Pr gives

$$\frac{h_U L}{k}=0.037\left(\frac{U_U L}{\nu}\right)^{\frac{4}{5}}\left(\frac{\nu}{\lambda}\right)^{\frac{1}{3}} \tag{3-52}$$

where λ is the thermal diffusion coefficient and ν,λ and k are all functions of temperature. Ford (1982) linearized the temperature dependence of Equation 3-52 over the range of 250K (-23°C) to 300K (27°C) to obtain

$$h_U=(6.940-0.0344T_e)U_U^{\frac{4}{5}}L^{-\frac{1}{5}} \tag{3-53}$$

where T_e = Film Temperature (in degrees Celsius from Ford) at which ν, α_T and k are evaluated, and is the mean temperature of the surface, T_i, and the attic air, T_a:

$$T_e=\frac{(T_i+T_a)}{2} \tag{3-54}$$

T_e is calculated using the previous hour's temperatures so that the overall heat transfer equation remains linear in temperature.

Ford found that h_U calculated from Equation 3-53 matches the measured data of Burch (1980b) and McAdams (1954) with L equal to 0.5m. This is a purely empirical value for L and does not have any physical significance. This value of L only means that convective heat transfer coefficients calculated using Equation 3-53 will match the measured data of Burch and McAdams. Including this length scale and converting from °C to K, Equation 3-53 can be written as

$$h_U=(18.192-0.0378T_e)U_U^{\frac{4}{5}} \tag{3-55}$$

where h_U is the turbulent forced convection heat transfer coefficient [W/m^{2}K], U_U is determined from Equation 3-49 and T_e is found from Equation 3-54. Equation 3-55

is used in Equation 3-42 to calculate the internal attic forced convection heat transfer. Ford (1982) used Equation 3-53 for external surfaces only because the internal surfaces were assumed to have free convection.

For the outside sheathing the flow velocity, U_U is equal to the ambient wind velocity, U. Because U is typically ten times greater than U_U, forced convection is always dominant on the exterior surfaces of the attic. For the exterior pitched roof sheathing surfaces Equation 3-55 is used to find h_U with U_U equal to U, the external wind speed.

The expressions for forced (Equation 3-55) and free (Equation 3-38) heat transfer coefficients can be used to find how the ventilation flow velocity determines which is dominant. The ratio of forced to free convection heat transfer coefficients (ignoring coefficients) is given by

$$\frac{h_U}{h_T} \propto \frac{Re^{\frac{4}{3}} Pr^{\frac{1}{3}}}{(RiRe^2)^{\frac{1}{3}} Pr^{\frac{1}{3}}} \qquad \text{(3-56)}$$

where Gr has been replaced by ($RiRe^2$). Pr cancels in Equation 3-56 which can then be written in terms of Ri and Re only

$$\frac{h_u}{h_T} \propto \frac{Re^{\frac{2}{13}}}{Ri^{\frac{1}{3}}} \qquad \text{(3-57)}$$

To find this ratio in terms of velocity the following substitutions are used : Re is proportional to U and Ri is proportional to U^{-2}. The ratio of forced to free heat transfer coefficients is then given by

$$\frac{h_U}{h_T} \propto U^{\frac{4}{3}} \qquad \text{(3-58)}$$

This means that the forced convection heat transfer coefficient becomes more dominant with increasing velocity.

3.3 Conduction Heat Transfer

Conduction occurs through the ceiling of the house, the pitched slope roof surfaces and the gable ends. The conduction is assumed to be one dimensional

because each surface has only one node. The general equation for one dimensional conduction is given by Holman (1981), p.2., as follows

$$q_K = \frac{A}{R}\Delta T \tag{3-59}$$

where q_K = heat conducted between nodes [W]

A = Surface area over which ΔT acts [m^2]

R = Thermal Resistance between nodes [m^2K/W]

ΔT = Temperature difference between nodes [K].

The thermal resistance depends on the thickness and material properties. The inside and outside of the pitched roof surfaces and (nodes 2,3,4 and 5) and the gable end walls (nodes 9 and 10) are assumed to have the same thickness of wood sheathing. The thermal resistance of the sheathing is given by

$$R = \frac{\Delta X}{k_W} \tag{3-60}$$

where ΔX = sheathing thickness [m]. For the attics tested in this study ΔX = 0.01m.

k_W = thermal conductivity of wood ≈ 0.1 [W/mK], ASHRAE (1989), Chapter 37.

Substituting these values into Equation 3-60 gives the thermal resistance of the sheathing as 0.1 m^2K/W. The sheathing thermal resistance is increased if there is snow on the roof. This effect is considered later in Chapter 7. Heat conduction through the ceiling occurs between the ceiling of the house (node 7) and the attic floor (node 8). The thermal resistance of the ceiling is modelled as the insulation and joist thermal resistances in parallel with the drywall resistance in series with this parallel combination. The total thermal resistance of the ceiling, R_c, is given by

$$R_c = R_A + \frac{1}{\frac{1}{R_X} + \frac{1}{R_W}} \tag{3-61}$$

where R_A = Drywall resistance [m^2K/W]

R_X = Insulation resistance [m^2K/W]

R_W = Joist (Wood) resistance [m^2K/W]

In this study the joist spacing was 61cm (24 inches) with 10cm insulation depth so that R_c = 2.3 m^2K/W. For thicker insulation the resistance increases. For example

with 15cm insulation depth, R_c = 3.4 m^2K/W. R_c is used as R in Equation 3-59 to find the heat conducted through the ceiling.

3.4 Accounting for Thermal Storage

In order to remove the assumption of steady-state, an estimate must be made for the rate of change of thermal energy at each node. A simple method is to use a lumped heat capacity analysis which assumes a uniform temperature for each node. This is only valid if internal conduction is more rapid than the surface heat transfer. Holman (1982), p.113, gives a criteria for the limits of a lumped heat capacity analysis using the Biot number which estimates the ratio of surface heat transfer to internal conduction, such that:

$$Bi = \frac{h_U \left(\frac{V}{A}\right)}{k} < 0.1 \qquad (3\text{-}62)$$

where h_U = surface heat transfer coefficient [W/m^2K]

A = Surface area [m^2]

V = Volume [m^3]

k = thermal conductivity [W/mK]

This is only a rough estimate of the applicability of lumped heat capacity analysis and Holman (p.114) gives examples of lumped heat capacity systems for Bi up to about 3.

For the same h_U and k the node with the largest V/A ratio is least likely to meet the restriction of Equation 3-62. Node 6 representing the joists and trusses in the attic is the most critical. For 5cm x 10cm (2" x 4") construction, then V/A is equal to 0.017m. To estimate h_U, the convection heat transfer coefficient from Equation 3-55 is used with typical values of U_U equal to 0.3 m/s and T_f equal to 273K. This gives a value of h_U equal to 3 W/m^2K. Using k_W equal to 0.1 W/mK then Equation 3-62 gives Bi equal to 0.5. For the sheathing Bi is approximately equal to 0.1. These results show that the lumped heat capacity analysis is applicable to the sheathing but the assumption of a single temperature for the rest of the wood in the attic may be a poor one. Holman (1981), p.122, shows how to estimate the difference between the centreline temperature of a cylinder and the external temperature as a function of Bi, time, thermal conductivity, thermal diffusivity and chacteristic dimensions. Letting V/A be the characteristic radius of a cylinder and using a time period of one hour (as used in this model), Holman shows that the

centerline temperature will only be 10% different from the exterior temperature. The data presented by Holman are responses to step changes in temperature, so the response of attic wood to more slowly changing temperatures will have errors less than 10% on the centreline. In addition, the average temperature difference for the whole of the wood will be even less than the centreline.

Because the sheathing meets the requirements for a lumped heat capacity analysis, the rest of the wood has small errors (less than 10%), and in the interests of simplicity the lumped heat capacity analysis is used for this study. As stated earlier in this chapter, the assumption of a lumped heat capacity would be further improved by dividing the wood into more nodes.

The rate of change of thermal energy at a node for a lumped heat capacity is found using a finite difference approximation to the time derivative of temperature such that (from equations 3-1 and 3-2)

$$\rho V C_{sh} \frac{(T^i - T^{i+1})}{\tau} \qquad (3\text{-}63)$$

where ρ = density of node [Kg/m_3]

V = Volume of node [m_3] so that ρV = Mass of node [Kg]

C_{sh} = Specific Heat [J/KgK]

T^i = temperature of node at time step i

T^{i+1} = temperature of node at time step i+1

τ = Time step. One hour is used in the model as this is the interval between measured data points used for verification.

Equation 3-63 assumes that the temperature changes linearly from timestep to timestep.

3.5 Latent Heat Released by Condensation.

When moisture condenses in the attic latent heat is given off which may increase the temperatures in the attic. If the heat transfer due to condensation is significant in the attic then there needs to be an iterative process between the heat transfer and moisture transport models because the moisture transport will significantly effect the heat transfer and visa-versa. The latent heat only needs to be considered when condensation is occurring. To determine if latent heat effects are significant, typical values of latent heat, radiation, convection and conduction fluxes are compared.

• **Latent Heat**

A typical mass flux from the attic air to the sheathing is 10^{-5} Kg/s calculated by the moisture transport model for the AHHRF attics with a sheathing area of 30.3m^2. The latent heat released in the transformation from vapour to solid is h_{gs} = 2834 KJ/Kg. The heat flux due to latent heat released is then approximately 1 W/m^2.

• **Solar Radiation**

Values measured for this study at AHHRF (in Edmonton, Alberta)have shown that there is a wide range of solar radiation. The range is from approximately 60W/m^2 for a cloudy winter day to 1050 W/m^2 on a clear summer day.

• **Convection**

With a convective heat transfer coefficient of 3 W/m^{2}K (as calculated in section 3.4) and a typical air to wood temperature difference measured at AHHRF of 2K (the range is from approximately zero to about 5K) a typical convective flux is about 6W/m^2.

• **Conduction**

Conduction through the sheathing is given by Equation 3-59. For the sheathing R is equal to 0.2 m^{2}K/W. Using this value of R and estimating the temperature difference between the inside and the outside of the sheathing (ΔT) as 2K, the conductive flux is about 20 W/m^2. The 2K temperature difference across the sheathing is a typical value measured in the test attics for this study as will be shown later in Chapter 6.

• **Internal Radiation**

Consider the radiation exchange between the south facing sheathing and the attic floor during the day. Measurements from AHHRF for this study presented in later (in Chapter 5) give typical daytime temperatures (for a clear spring day) of 303K for the sheathing and 298K for the attic floor. The radiation heat transfer coefficient from Equation 3-23 found using these temperatures is approximately 4.61 W/m^{2}K. Using this result in Equation 3-22 from the heat transfer rate gives a radiative heat flux of about 23 W/m^2.

These example calculations show that the heat flux due to latent heat is less than all the other heat fluxes in the attic for typical conditions. This means that ignoring the latent heat released by condensation will not have a significant effect on the attic heat transfer, and an iterative solution between the heat transfer and moisture transport models is not necessary. The heat flux due to latent heat released by condensation has been included in an attic heat transfer model by Gorman (1987),

p.30. Gorman found that its inclusion did not have a significant effect on wood moisture content predictions.

3.6 Node Heat Transfer Equations

At each of the 10 nodes the rate of change of energy (see Equation 3-1, 3-2 and 3-63) is equated to the net heat flow to the node due to radiation, convection and conduction. This results in 10 heat balance equations that must be solved simultaneously for the 10 unknown temperatures. In each of the following equations the subscript on temperature, T, refers to the node location and the superscript to the timestep.

Node 1. Attic Air

The attic air has convective (the h_U terms) heat transfer from all the interior attic surfaces - nodes 2, 4, 8, 6 and 9 as shown Figure 3-1. Although each convection term uses the same velocity, U_U, the different temperatures will change the film temperature, T_f, and thus the heat transfer coefficient. In addition the convective flows in and out of the attic, M_a, and the flow through the ceiling, M_c, transport heat in and out of the attic air. When ventilation rates are high, M_a is large and this becomes the dominant term so that the attic air has almost the same temperature as the out door air. When M_a is small, M_c and the h_U terms become more important so that solar radiation heating the pitched roof surfaces will heat the attic air. A source or sink term, q_{ss} [W], (e.g. a hot furnace flue) is also included for the heat balance on the attic air, although in the present study this term was zero.

$$\rho_a V_a C_{sh,a}\frac{(T_1^i-T_1^{i-1})}{\tau}=h_{U,8}\,A_8(T_8^i-T_1^i)+h_{U,4}\,A_4(T_4^i-T_1^i)+h_{U,2}\,A_2(T_2^i-T_1^i) \qquad (3\text{-}64)$$
$$+A_9h_{U,9}(T_9^i-T_1^i)+M_cC_{sh,a}(T_{in}^i-T_1^i)+M_aC_{sh,a}(T_{out}^i-T_1^i)+h_{U,6}\,A_6(T_6^i-T_1^i)+q_{ss}$$

where V_a = volume of the attic [m^3] (61m^3 for the AHHRF test houses)

$C_{sh,a}$ = specific heat of air. This assumed to be independent of temperature and is equal to 1000 J/KgK

$h_{U,2}$ = forced convection heat transfer coefficient from Equation 3-55

$h_{U,4}$ = forced convection heat transfer coefficient from Equation 3-55

$h_{U,6}$ = joist and truss forced convection heat transfer coefficient from Equation 3-55

$h_{U,8}$ = forced convection heat transfer coefficient from Equation 3-55

$h_{U,9}$ = end wall forced convection heat transfer coefficient from Equation 3-55

$A_2 = A_4$ = sheathing surface area

A_9 = end wall surface area. Both end walls are assumed to be identical and so this is the area of both endwalls combined

A_6 = area of joists and trusses

M_c = mass flow rate through the ceiling from ventilation model

M_a = mass flow rate through the attic from ventilation model.

Node 2. Inside North Sheathing

The inside of the sheathing exchanges heat with the attic air by convection (h_U) and with the outside of the sheathing by conduction (A/R). In addition there is radiant exchange with the attic floor and the inside of the south sheathing (the h_R terms).

$$\rho_W V_2 C_{sh,W} \frac{(T_2^i - T_2^{i-1})}{\tau} = h_{U,2}\, A_2 (T_1^i - T_2^i) + \frac{A_2}{R_2}(T_3^i - T_2^i) + h_{R,2\text{-}8}\, A_2 (T_8^i - T_2^i) + h_{R,2\text{-}4}\, A_2 (T_4^i - T_2^i) \qquad (3\text{-}65)$$

where ρ_W = density of wood, approximately 400Kg/m^3

V_2 = half of the north sheathing volume

A_2 = surface area of north roof pitched surface

R_2 = thermal resistance of sheathing from Equation 3-60

$h_{R,2\text{-}8}$ = radiation heat transfer coefficient from Equation 3-23

$h_{R,2\text{-}4}$ = radiation heat transfer coefficient from Equation 3-23

Node 3. Outside North Sheathing

The outside pitched roof sheathing surface has radiant exchange with the ground and the clouds, $h_{R,3\text{-}g}$, the sky, $h_{R,3\text{-}sky}$ and daytime solar gain, G_3. The radiant exchange to the sky is important on clear nights because this reduces the sheathing temperature and makes it prone to moisture condensation. There is also convective exchange with the outside air, $h_{U,3}$, and conduction through the sheathing to the inner sheathing (A/R). The separation of sheathing into north and south allows the two pitched roof surfaces to have different solar gains. The test houses used in this study were in an east-west row with one sheathing surface facing south and the other facing north.

$$\rho_W V_3 C_{sh,W} \frac{(T_3^i - T_3^{i-1})}{\tau} = h_{U,3}\, A_3 (T_{out}^i - T_3^i) + \frac{A_3}{R_3}(T_2^i - T_3^i) + A_3 G_3 \lambda_3 + h_{R,3\text{-}sky}\, A_3 (T_{sky}^i - T_3^i) + h_{R,3\text{-}g}\, A_3 (T_{out}^i - T_3^i) \quad (3\text{-}66)$$

where $V_3 = V_2$, $A_3 = A_2$, $R_3 = R_2$,

$h_{U,3}$ = exterior forced convection heat transfer coefficient from Equation 3-55, with the ambient wind speed, U, substituted for the internal attic velocity, U_U.

λ_3 = absorbtivity of shingles which is approximately 0.9 from ASHRAE (1989), Chapter 37

G_3 = solar radiation on north sheathing

$h_{R,3\text{-}sky}$ = radiation heat transfer coefficient from roof to sky from Equation 3-28

$h_{R,3\text{-}g}$ = radiation heat transfer coefficient from roof to ground and clouds from Equation 3-27.

To include the effect of the thermal mass of the shingles outside the sheathing, the thermal mass of this node is doubled by doubling the effective volume. The actual thermal mass of the shingles is much larger (by a factor of 15) but calculations performed later for model verification (in Chapter 6) have shown that the attic temperature predictions are insensitive to changing the effective mass of the sheathing.

Node 4. Inside South Sheathing

The inside of the south sheathing has the same heat transfer contributions as the inside north sheathing.

$$\rho_W V_4 C_{sh,W} \frac{(T_4^i - T_4^{i-1})}{\tau} = h_{U,4}\, A_4 (T_1^i - T_4^i) + \frac{A_4}{R_4}(T_5^i - T_4^i) + h_{R,4\text{-}8}\, A_4 (T_8^i - T_4^i) + h_{R,4\text{-}2}\, A_4 (T_2^i - T_4^i) \quad (3\text{-}67)$$

where $V_4 = V_2$, $A_4 = A_2$, $R_4 = R_2$

$h_{R,4\text{-}8}$ = radiation heat transfer coefficient from Equation 3-23

$h_{R,4\text{-}2}$ = radiation heat transfer coefficient from Equation 3-23

Node 5. Outside South Sheathing

The outside of the south sheathing has the same heat transfer contributions as the outside north sheathing.

$$\rho_W V_5 C_{sh,W} \frac{(T_5^i - T_5^{i-1})}{\tau} = h_{U,5}\, A_5 (T_{out}^i - T_5^i) + \frac{A_5}{R_5}(T_4^i - T_5^i) \qquad (3\text{-}68)$$
$$+ A_5 G_5 \lambda_5 + h_{R,5-sky}\, A_5 (T_{sky}^i - T_5^i) + h_{R,5-g}\, A_5 (T_{out}^i - T_5^i)$$

where $V_5 = V_2$, $A_5 = A_2$, $R_5 = R_2$

$h_{U,5}$ = exterior forced convection heat transfer coefficient from Equation 3-60, with the ambient wind speed, U, substituted for the internal attic velocity, U_U. this is not necessarily equal to $h_{U,3}$ because the sheathing surfaces may be at different temperatures.

G_5 = solar radiation on south sheathing

λ_5 = surface absorbtivity $\approx$ 0.9 for shingles

$h_{R,5\text{-}sky}$ = radiation heat transfer coefficient from roof to sky from Equation 3-28

$h_{R,5\text{-}g}$ = radiation heat transfer coefficient from roof to ground and clouds from Equation 3-27

The increased thermal mass contributed by the sheathing is dealt with in the same way as for the outside of the north sheathing i.e. the thermal mass of this node is doubled by doubling the effective volume.

Node 6. Attic Joists and Trusses

The joists and trusses only exchange heat with the attic air by convection, therefore they act to increase the thermal mass of the attic air.

$$\rho_W V_6 C_{sh,W} \frac{(T_6^i - T_6^{i-1})}{\tau} = h_{U,6}\, A_6 (T_1^i - T_6^i) \qquad (3\text{-}69)$$

where V_6 = Volume of joists and trusses

A_6 = Surface Area of joists and trusses.

Node 7. Underside of House Ceiling

The underside of the ceiling has radiant exchange with the inside surfaces of the house that are assumed to be at T_{in}, i.e. the same temperature as the air in the house. The house is assumed to have internal free convection and so the ceiling exchanges heat with the house air. There is also conduction through the ceiling to

the floor of the attic.

$$\rho_7 V_7 C_{sh,7}\frac{(T_7^i-T_7^{i-1})}{\tau}=h_{U,7}\,A_7(T_{in}^i-T_7^i)+h_{R,7-in}\,A_7(T_{in}^i-T_7^i)+\frac{A_7}{R_7}(T_8^i-T_7^i) \qquad (3\text{-}70)$$

where ρ_7 = Average Density of ceiling drywall, joist and insulation

V_7 = 1/2 volume of ceiling drywall, joist and insulation

$C_{sh,7}$ = specific heat of node 1. For the wood - $C_{sh,W}$ = 1100 J/KgK and for the drywall - $C_{sh,\delta}$ = 1080 J/KgK so use C_{sh7} = 1100 J/KgK

τ = timestep = 3600s for all nodes

$h_{U,7}$ = convective heat transfer coefficient from Equation 3-41

A_7 = ceiling area

$h_{R,7\text{-}in}$ = radiation heat transfer coefficient from Equation 3-35

R_7 = ceiling conduction resistance from Equation 3-61

Node 8. Attic Floor

The attic floor exchanges heat by radiation to the pitched roof surfaces, forced convection with the attic air and by conduction through the ceiling form the house below. The radiation terms are important because during high daytime solar gains the warm sheathing can raise the attic floor temperature above the attic air and reduce heat loss through thc ceiling. Conversely cooler attic sheathing on clear nights will make the attic floor colder.

$$\rho_8 V_8 C_{sh,8}\frac{(T_8^i-T_8^{i-1})}{\tau}=h_{U,8}\,A_8(T_1^i-T_8^i)+\frac{A_8}{R_8}(T_3^i-T_8^i)+h_{R,8-4}\,A_8(T_4^i-T_8^i)+h_{R,8-2}\,A_8(T_2^i-T_8^i) \qquad (3\text{-}71)$$

where $\rho_8 = \rho_7$, $V_8 = V_7$, $A_8 = A_7$, $R_8 = R_7$,

$C_{sh,8} = C_{sh,7}$

$h_{R,8\text{-}4}$ = radiation heat transfer coefficient from Equation 3-23

$h_{R,8\text{-}2}$ = radiation heat transfer coefficient from Equation 3-23

Node 9. Inside both Endwalls

Both the endwalls (east and west) are assumed to be identical and are lumped together. The inside of the endwalls exchanges heat with the attic air by forced convection and with the outside of the endwalls by conduction. The end walls are another path for heat to enter or leave the attic. The effective resistance of this path is governed by the surface forced convection heat transfer coefficients on the inside

and the outside of the endwalls and by their conductive resistance.

$$\rho_W V_9 C_{sh,W}(T_9^i - T_9^{i-1}) = h_{U,9}\, A_9(T_1^i - T_9^i) + \frac{A_9}{R_9}(T_{10}^i - T_9^i) \qquad (3\text{-}72)$$

where V_9 = 1/2 total end wall volume

$R_9 = R_4$ assuming same thickness of wood for endwalls and pitched roof sheathing.

Node 10. Outside both Endwalls

The outside of the endwalls exchanges heat with the outside air by forced convection and with the inside of the endwalls by conduction. The external forced convection heat transfer coefficient, $h_{U,10}$, uses the same outside wind speed as the pitched roof surfaces.

$$\rho_{wood} V_{10} C_{shwood}(T_{10}^i - T_{10}^{i-1}) = h_{conv,10} A_{10}(T_{out}^i - T_{10}^i) + \frac{A_{10}}{R_{10}}(T_9^i - T_{10}^i) \qquad (3\text{-}73)$$

where $V_{10} = V_9$, $R_{10} = R_9$

$h_{U,10}$ = exterior forced convection heat transfer coefficient from Equation 3-55 with U substituted for U_U.

3.7 Solution of the Attic Heat Transfer Equations

At each node Equation 3-63 is equated to the sum of the heat fluxes due to radiation, convection and conduction. This results in the above set of equations that are linear in temperature and must be solved simultaneously. This simultaneous solution is found using gaussian elimination. When the temperatures have been calculated the attic air temperature (Node 1) is returned to the attic ventilation model so that a new attic ventilation rate can be calculated. This new ventilation rate is then used in the thermal model at the attic air node to calculate temperatures. This iterative process is continued until the attic air temperature changes by less than 0.1°C. Because the attic ventilation rates are relatively insensitive to the attic air temperature usually fewer than five iterations between thermal and ventilation models are required.

3.8 Summary of Attic Heat transfer Model

The attic heat transfer model uses a multi-node lumped heat capacity analysis to determine the temperatures at ten attic locations shown in Figure 3-1. The heat transfer between the nodes is by radiation, conduction and convection. These

temperatures are used by the moisture transport model to calculate saturation pressures, vapour pressures and wood moisture contents. The heat transfer model is coupled to the attic ventilation model through the temperature of the attic air. The air temperature is used to calculate air densities in the attic which changes the mass flow rates and the driving pressures for ventilation. In turn the attic ventilation rate has a large effect on the attic air temperature and thus the two models are coupled and require an iterative procedure to solve the combined problem. Because the attic ventilation rate is not a very strong function of attic air temperature the models are only weekly coupled and only a few iterations are required for convergence.

The major assumptions of the heat transfer model are:

- The temperature at each node location is uniform so that the lumped heat capacity analysis can be used.
- The flow velocities inside the attic are uniform and are proportional to the attic ventilation rate so that heat (and mass) transfer coefficients are functions of attic ventilation rate.
- Latent heat released by condensing moisture is not included as it does not have a significant effect. Therefore the heat transfer model is not coupled to the moisture transport model.
- The end walls of the attic do not receive any external solar radiation gains and do not have any internal radiation heat transfer.

The major differences from previous attic heat transfer models (e.g. Ford (1982)) are

- An additional node is used to account for the mass of wood in joists and trusses in the attic. This effectively increases the thermal mass of the attic air.
- Attic ventilation and ceiling flow rates are calculated instead of being a required input. This results in an iterative procedure as the attic ventilation and ceiling flow rates depend on the attic temperature.
- Forced convection heat transfer coefficients are used inside the attic. In this study the ventilation rates are found using ATTICLEAK-1 and thus forced convection heat transfer coefficients may be calculated inside the attic. Previous authors have not had a ventilation model to calculate ventilation rates and so they used natural convection heat transfer coefficients. These heat transfer coefficients are important as they make the heat transfer model more dependent on the ventilation model and because the mass transfer coefficients are linearly dependent on the heat transfer coefficients.

• Radiation heat transfer inside the attic is simplified to three nodes: the attic floor and the two pitched roof surfaces. Ford (1982) also included gable ends and eaves but these components have small view factors and are neglected for simplicity in the present study.

Chapter 4. Moisture Transport in Attics

4.1 Introduction

The moisture transport model is based on a mass balance of water in the attic. The mass of water in the attic is assumed to be located at the seven nodes shown in Figure 4-1. The model makes the mass change rate at each node equal to the sum of the fluxes at that node and solves for the vapour pressures at each node that will give this balance. The fluxes include ventilation flows, wood surface exchange and diffusion within the wood. The mass balance is performed simultaneously for all the nodes. The ceiling is assumed to be impermeable to water vapour as most residential buildings will have a vapour retarder in the ceiling. The flow of vapour through the ceiling is only that due to convective flows through gaps in the vapour barrier. It is also assumed that no water vapour is exchanged with the outside air through the shingles on top of the sheathing or through the endwalls which are usually painted. This is due to the relatively low vapour permeability of these surfaces (see ASHRAE Fundamentals (1989), Chapter 37). Thus the outer surfaces of the sheathing are assumed to be impermeable and have zero mass flux.

Figure 4-2 shows the order of magnitude of moisture fluxes for a typical winter day. This is for the same conditions shown for heat transfer rates in Figure 3-2. These moisture fluxes were taken from the results of simulations discussed later in Chapter 7. There is a large range of moisture fluxes from 10^{-9} Kg/s for diffusion within the wood to 10^{-3} Kg/s for the ventilation flows. The internal wood diffusion has a small effect on the total attic moisture balance compared with the ventilation and wood surface convection moisture fluxes. These results show the importance of using the correct ventilation rate and including the wood surface flux directly in the moisture mass balance for the attic air.

The attic air is assumed to be well mixed so that the air vapour pressure is the same at all attic locations. This is the same assumption as used in the thermal and ventilation models where the attic air is treated as a single node. The water vapour in the wood and the mixture of water vapour and attic air are assumed to act as ideal gasses. This is a standard assumption for psychometric calculations. Moisture flow through the ceiling is assumed to mix completely with the attic air. This assumption neglects the possible deposition of moisture in the insulation above holes in the ceiling. The interaction of thermal and moisture models due to heat transport by water vapour and latent heat released by condensation is neglected. The effect of latent heat was discussed in Chapter three and shown to be insignificant. Because

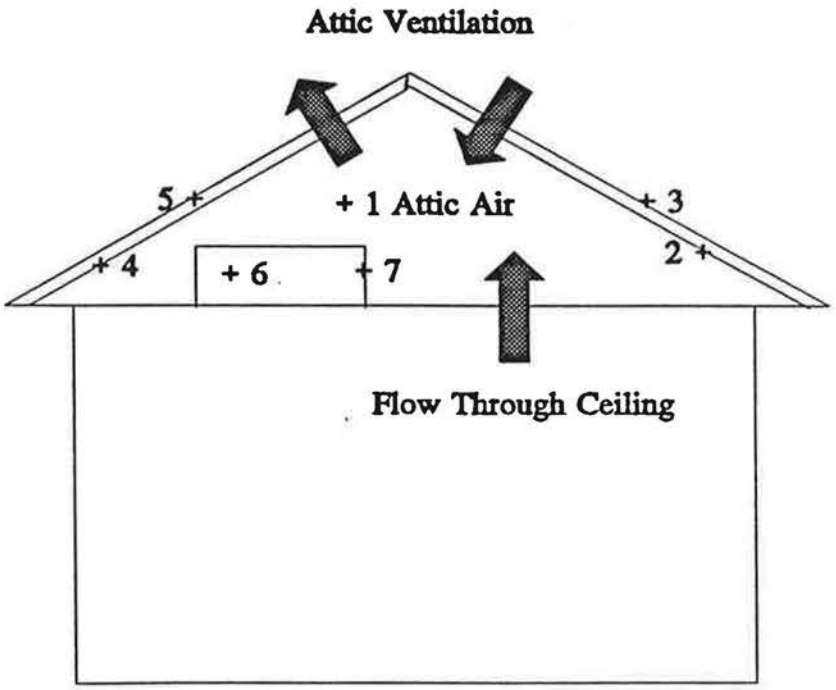

Figure 4-1. Node locations for moisture transport mass balance.

1. Attic air
2. North sheathing surface
3. North sheathing interior
4. South sheathing surface
5. South sheathing interior
6. Truss and joist surface
7. Truss and joist interior

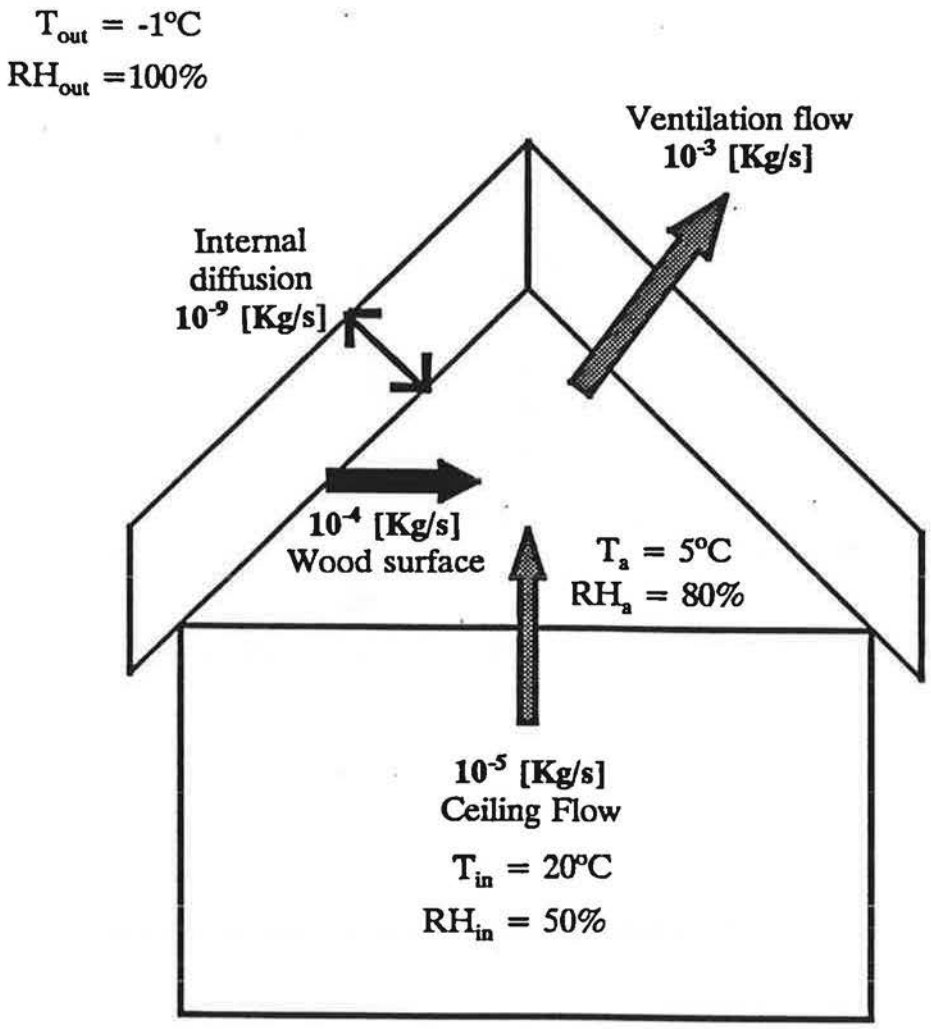

Figure 4-2. Typical attic moisture fluxes [Kg/s] in a maritime climate, with a clear sky and an attic ventilation rate of 7 ACH.

the mass fraction of water vapour in the attic air and the air flowing through the attic is small (always less than half a percent) the contribution of the water vapour to heat transfer is neglected.

The deposition of moisture in the insulation above holes in the ceiling was neglected because the deposition is limited to a small volume above each hole. Although the local moisture content of the insulation is high, the total volume is small and so the contribution of this moisture to the total attic balance is ignored. However, localised deposition of this nature may lead to localised moisture problems in the ceiling of the house. This important study of the three dimensional combined heat, air and moisture transport through these leaks is a topic for future research. The solution to this complex problem is beyond the scope of this study. One dimensional studies of this problem have been carried out by Tao, Besant and Rezkallah (1990) and Ogniewicz and Tien (1981).

The porous insulation on the attic floor can exchange moisture with the attic air. The total mass of insulation in the attic is significant (about 250 Kg in the attics used for this study with a 10cm layer of insulation), however, the moisture concentration is low if condensation is not included. A typical moisture concentration (corresponding to the plateau value of the sorption isotherm) is about 0.2% (Besant (1993), private communication) resulting in a total mass of about 0.5 Kg in the insulation. The surface wood nodes described later in this chapter have a total mass of about 50 Kg, and at 20% moisture content they contain 10 Kg of moisture. These simple calculations show that the wood has more moisture capacity than the insulation so that ignoring the moisture content of the insulation will not introduce large errors into the attic moisture balance. It would be possible to include the insulation in future developments of this model by treating the insulation the same way as the attic wood, i.e. dividing the insulation into an active surface layer that exchanges moisture by convection with the attic air, and an inner insulation layer. Dividing the insulation in this way would make the total mass in the active surface layer of insulation even less, and thus reduce its effect on the attic moisture balance. Another reason why it is not critical to include the insulation in the moisture balance is that it remains at a relatively constant temperature because the house below the ceiling remains at a constant temperature compared to the sheathing and the attic air. Because the insulation is warmer than the wood and attic air in winter (when moisture problems occur) than the insulation the equilibrium moisture content of the insulation will be lower than the wood and attic air.

The moisture transport model developed for this study uses the ventilation and heat transfer models developed in previous chapters to calculate input parameters. These input parameters are the air flow rates through the attic and the ceiling and the temperatures at each node. The air flow rates are used directly to calculate the mass balance of moisture for the attic air. The temperatures are used to calculate saturation pressures for all nodes and vapour pressures for the wood nodes. An important element in the attic moisture transport model is that the wood transfers moisture through its surface and can also store moisture internally. Choong and Skaar (1969 and 1972) and Siau (1984) have shown that the rate of moisture transfer in wood depends on the surface mass transfer and internal diffusion. Gorman (1987) accounted for these two processes by creating two nodes for each sheathing section. The sheathing was separated into a thin (3 mm) surface layer and a thicker (7 mm) inner layer. The surface layer exchanges moisture with the attic air and the inner and outer layer exchange moisture by diffusion of water vapour. This idea is used here with the inclusion of another two nodes to include the rest of the wood in the attic. The sheathing (nodes 2, 3, for north sheathing and 4 and 5 for south sheathing) and the rest of the wood in the attic (joists and trusses, nodes 6 and 7) are split into surface nodes (2, 4 and 7) and interior nodes (3, 5 and 6). Figure 4-3 illustrates the surface and inner wood layers for the sheathing. The distance between nodes used for diffusion, ΔX, is one half of the total sheathing thickness, ΔX_W. ΔX is always one half of ΔX_W independent of the surface thickness, ΔX_S, and the inner thickness, ΔX_I. This is because ΔX_S and ΔX_I must always add up to ΔX_W and ΔX is the sum of one half of ΔX_S and ΔX_I.

The mass transfer equations are written in terms of vapour pressure. Vapour pressure, P_v, is used rather than relative humidity (RH) or humidity ratio (ω) because it is easier to use in the ideal gas law that is applied in many situations in this model. The vapour pressure of wood is defined as the vapour pressure of air that would be in equilibrium with the wood at uniform temperature.

To remove the assumption of steady state it is necessary to write the rate of change of wood moisture content (W_{MC}) with time for the wood nodes in terms of vapour pressure. In this study the relationship developed by Cleary (1985) that relates wood moisture content to temperature and humidity ratio is used (as shown later in section 4.3). Cleary (1985) and Gorman (1987) have used this relationship to find water vapour pressure and humidity ratio so that mass transfer rates between attic air and the wood and within the wood could be calculated. Wood moisture

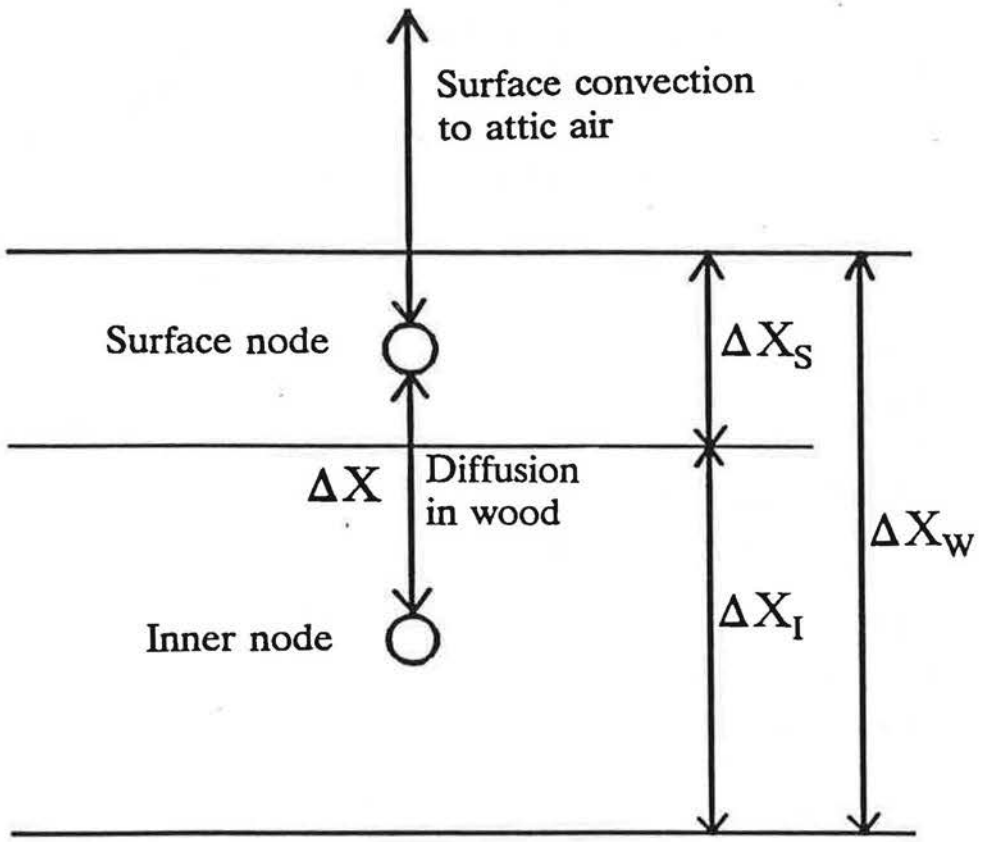

Figure 4-3. Sketch of surface and inner wood layers

contents are expressed as the mass of water as a fraction of the mass of dry wood. This water is considered to be within the cell walls. Defining wood moisture content to be the moisture in cell walls only is important because when the cell walls becomes saturated moisture transported to the wood exists as free water within the cell. In this study this free water is considered to be a condensed mass and is not included in the wood moisture content.

In the model developed for this study condensation is assumed to occur when mass is transferred to a node that is at its saturation pressure, P_{vs}. Therefore the vapour pressure at a node is always less than or equal to the saturation pressure. This condensed mass is not included as moisture in the wood but is kept track of separately. If there is condensed mass at a node then the node remains at saturation pressure until all the condensed mass is removed from the node.

In this study the diffusion of water vapour through the ceiling and to the outside air through the rest of the attic envelope is neglected. This is because the building materials have high resistance to vapour transmission. For the same surface area and vapour pressure difference the rate of vapour transfer to the wood surface is about seven orders of magnitude greater than the rate of vapour diffusion through wood as will be discussed later (see sections 4.4.2 and 4.4.3). The convective moisture flows due to attic ventilation are even larger than the rate of vapour exchange with the wood surfaces and thus the diffusive component of moisture transport is included only to find inner wood moisture contents.

4.2 Major differences from previous attic moisture transport models

Previous attic moisture transport models have been developed by Ford (1982), Cleary (1985) and Gorman (1987). Ford's model is the simplest because wood moisture contents are not calculated. The sheathing surfaces are assumed to have ice or liquid water on them at all times (i.e. they are at saturation). This means that all moisture transported to the sheathing condenses and does not change the wood moisture content. The mass balance for water used by Ford is a single equation for the attic air only. This equation includes the rate of change of mass of water in the attic air and the ventilation flows through the attic but does not include the exchange with the wood surfaces. The amount of moisture transferred from the air to the wood surfaces is calculated from the vapour pressure of the attic air and the saturation pressure of the wood surface (that is a function of its temperature only). The temperatures for Ford's model were calculated using an attic heat balance similar to that used in this study and given in Chapter 3. The ventilation rates for the

attic and the flow rate through the ceiling were not calculated by Ford and had to be supplied by the user.

Cleary's model assumes a steady-state solution to the mass balance of moisture between inside air, attic air and the wood surface. The wood moisture content from the previous hour is used to find the humidity ratio of the wood surface using a relationship developed by Cleary (see section 4.3). Knowing the humidity ratio of the outside air and the attic ventilation rate the humidity ratio of the attic air can be found. The change in moisture content of the attic wood is then found by calculating the mass of moisture transferred to the wood surface based on the new attic humidity ratio and the wood humidity ratio from the previous hour. This new moisture content is used to find the wood humidity ratio for use in the next hour's mass balance. Cleary's model does not include moisture transferred through the ceiling which can be a significant moisture load on the attic. The temperature of the attic wood and the attic ventilation rate are both user inputs to Cleary's model. Cleary's model does not differentiate between water bound within the wood and condensed surface moisture.

Gorman's model is based on Cleary's model but includes additional nodes to account for two attic sheathing surfaces that may be at different temperatures. In addition the flow of moisture into the attic through the ceiling is included in the attic air moisture balance. Gorman made Cleary's model more sophisticated by separating the wood into a surface node that exchanges moisture with the attic air and an inner node that exchanges moisture by diffusion with the surface node. This allows rapid change of surface wood moisture content rather than distributing the moisture throughout the wood. This is important for moisture exchange with the wood because the wood surface will come to equilibrium faster than if the moisture is distributed to the bulk of the wood. The wood surface will then exchange less moisture with the attic air. Gorman also separated condensed mass from water bound within the wood. In Gorman's model a wood surface that is above it's fibre saturation point (Gorman assumed this was 28%) will experience condensation rather than a change in moisture content. The fibre saturation point is the moisture content at which the cell walls of the wood have absorbed all of the water they can hold. Any further moisture accumulation appears as free water within the cells. The temperatures for the wood and the attic air are calculated by Gorman using an attic heat balance similar to that in Chapter 3. The attic ventilation flows were a required user input to Gorman's model.

The following are the major differences between the moisture transport model developed for this study and those discussed above.

• For the mass balance, the model developed for this study solves for all the nodes shown in Figure 4-1 simultaneously. Previous models by Ford (1982), Cleary (1985), and Gorman (1987) balance the air flow mass transfers to find the attic air mass content which is used separately to calculate mass transferred to and from the wood surfaces.

• The model developed here does not assume steady state. Gorman and Cleary assume a steady state solution for all the nodes. Ford did not assume a steady-state solution for the attic air but did not calculate wood moisture contents. The model used in this study uses the same ideal gas relationship as Ford for the rate of change of attic air moisture with time. A relationship for the rate of change of wood moisture content with time has been developed for this model so that the wood nodes are not assumed to be at steady state. This is very important if the moisture content of interior attic surfaces is to be calculated each hour because this moisture content can change rapidly. This, in turn, effects the amount of mass that is condensed.

• The air flow through the attic to and from outside and the flow through the ceiling are different for each hour and are calculated using the attic ventilation model shown in Chapter 2. Previous models have either assumed a constant ventilation and ceiling flow rate or required them to be measured inputs. Using the correct ventilation rate is important not only for the mass balance of water vapour, but also because the attic temperatures and surface heat and mass transfer coefficients are functions of the ventilation rate as will be shown later (see section 4.6).

• Mass condenses at the wood surfaces and appears as free water as well as being absorbed by the wood. Previous attempts to calculate the condensed mass have been based on simple assumptions. Ford (1982) assumed that the wood was always saturated so that any mass flow to the wood appeared as condensation, and wood moisture contents were not calculated. Gorman (1987) assumed that there was no condensation until the wood reached fibre saturation. A more sophisticated approach is assumed in this model that uses the wood moisture content, temperature and vapour pressure relationship developed by Cleary (1985). This relationship is used to estimate an equivalent wood vapour pressure (including the saturation pressure) from wood moisture content and temperature. Condensation is assumed to occur when mass is transferred to a node that is at saturation pressure. This condensed mass is not included as moisture in the wood but is kept track of separately. If there

is condensed mass at a node then the node remains at saturation pressure until all the condensed mass is removed from the node. This process assumes that Cleary's relationship gives the correct vapour pressure over the full range of temperatures experienced in attics. Often the attic is below the temperature range that Cleary's relationship was developed for and the relationship is extrapolated to these lower temperatures. The uncertainty in this extrapolation has not been determined due to lack of measured data. The next section discusses this relationship in greater detail.

4.3 Relating vapour pressure to wood moisture content and temperature

Cleary (1985) took data from the Wood Handbook (1982) to develop a relationship between humidity ratio, ω, temperature, T, and wood moisture content, W_{MC}, as follows

$$\omega = \exp\left(\frac{T}{B_3}\right)(B_4 + B_5 W_{MC} + B_6 W_{MC}^2 + B_7 W_{MC}^3) \qquad (4\text{-}1)$$

where B_3 through B_7 were found by fitting to measured data. Cleary determined the following values for these constants:

B_3 = 15.8°C, B_4 = -0.0015, B_5 = 0.053, B_6 = -0.184 and B_7 = 0.233.

Humidity ratio is defined as the ratio of the mass of water vapour to the mass of dry air in a given volume. Wood moisture content is defined as the ratio of the mass of water to the mass of dry wood in a given sample. The data used by Cleary was found by determining the equilibrium humidity ratio for a measured wood moisture content at several different temperatures. This means that Equation 4-1 should be applied to equilibrium conditions. It is assumed here that the air layer nearest the wood surface is in equilibrium with the surface so that this equation may be applied. Without more data it is difficult to estimate the effect on Equation 4-1 for non-equilibrium conditions. The lowest temperature used to find the coefficients in Equation 4-1 was about -1°C (30 °F). Below this temperature there may be some uncertainty in using this equation. This is important because attic temperatures in winter can be as low as -40°C and Equation 4-1 leads to predictions of low wood moisture contents of about 5% (even at saturation pressure) for these conditions. More detailed measurements at lower temperatures are required to validate Equation 4-1.

Equation 4-1 has some important effects for moisture transport in attics. Figure 4-4 shows how Equation 4-1 gives the relationship between equilibrium wood

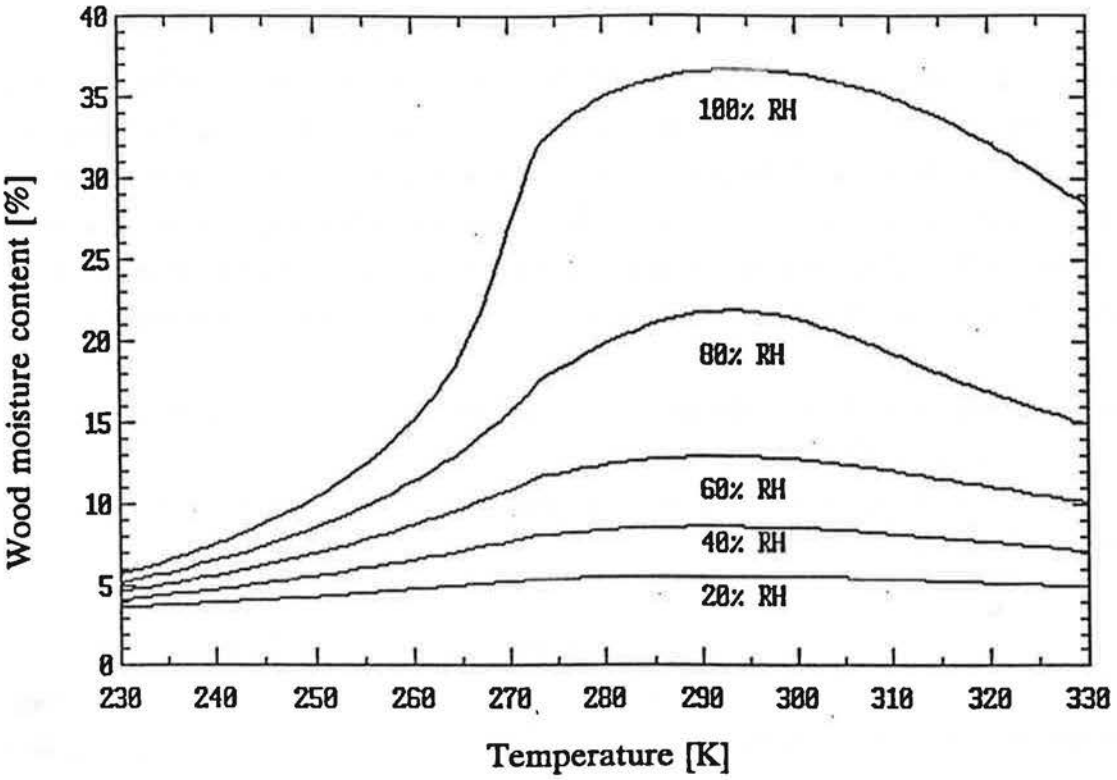

Figure 4-4. Equilibrium wood moisture content (relationship from Cleary(1985)) for a range of relative humidities (RH).

moisture content, temperature and humidity ratio, which is expressed in Figure 4-4 as relative humidity (RH). This figure shows that when the water vapour pressure in the wood is close to saturation (about 98% RH) the wood moisture content is a strong function of temperature. From Siau (1984), p.124, the fibre saturation point is reached when the relative humidity of the air above the surface of the wood (that the wood is in equilibrium with) is about 98%. Above this relative humidity the wood becomes saturated and the cells within the wood fill with free water. If this free water is included in the calculation of wood moisture contents then wood moisture contents of up to about 180% can be found using the equation given by Siau (1984)(p.29, Equation 1-20).

For simplicity the model developed here assumes that no moisture condenses until the wood reaches saturation (100% RH). At typical Canadian winter temperatures of -20°C (253 K) the maximum wood moisture content given by Equation 4-1 is only about 10%. If moisture is transferred to a wood surface at saturation it will not increase the wood moisture content but is assumed for this model to appear as free surface moisture that is condensed. If a wood surface at 0°C (273 K) and 15% wood moisture content is cooled, as happens for winter nights, the vapour pressure in the wood reaches saturation at about -13°C (260 K). Further cooling will force moisture to be condensed out of the wood as the vapour pressure cannot go above saturation. This production of condensed mass by cooling of the wood is an important factor in calculating mass condensation on attic surfaces for the moisture transport model developed here, but is only true if the assumption that Equation 4-1 can be extrapolated to lower temperatures is valid.

The maximum moisture content calculated using Equation 4-1 is about 35% at 22°C (295 K). This is at the high end of estimated values for fibre saturation limit. Typical estimates of fibre saturation point for wood in Siau (p.20, 124 and 125) are about 30% but higher values have been measured depending on the measurement method used. Due to this uncertainty in estimating fibre saturation for wood no upper limit will be placed on wood moisture content as used by other authors and wood moisture contents will be calculated using Equation 4-1, with no other limits. The highly non-linear nature of Equation 4-1 is illustrated in Figure 4-5 which shows equilibrium vapour pressure as a function of wood moisture content and temperature. At high wood moisture contents (above 15%) at a constant temperature the wood moisture content changes very rapidly with vapour pressure. At low wood moisture content the wood moisture content changes very little with vapour pressure, and

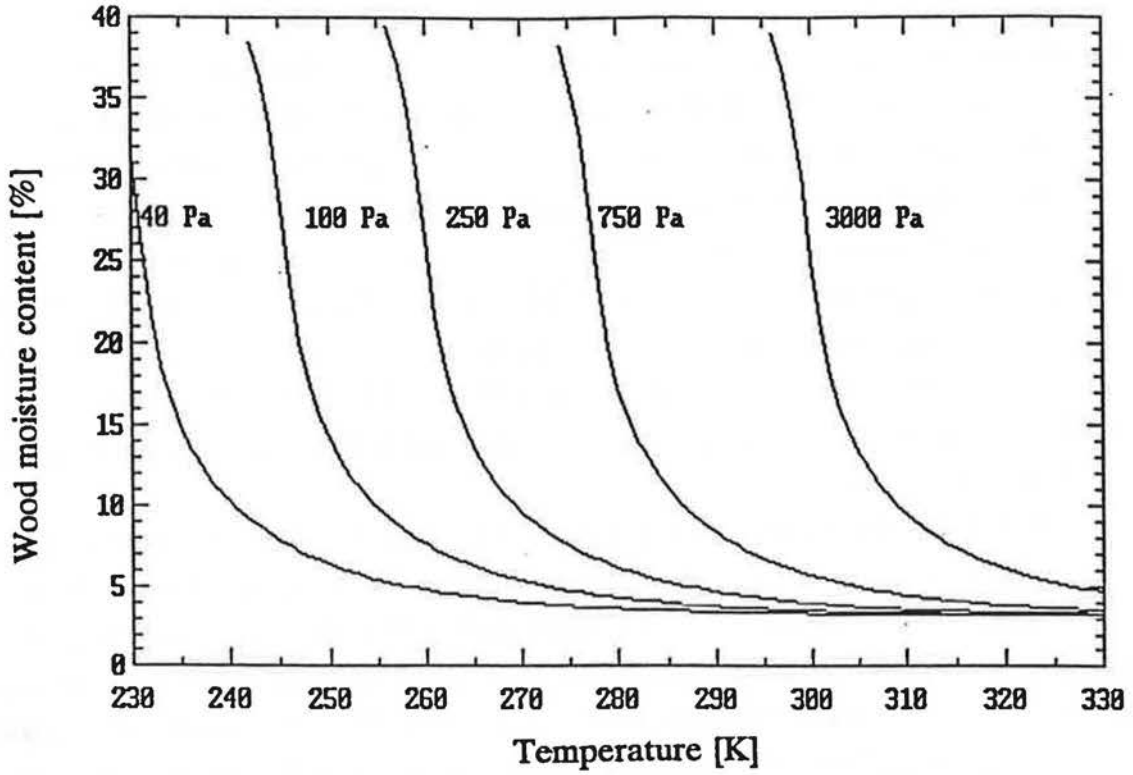

Figure 4-5. Equilibrium Wood Moisture Content (relationship from Cleary (1985)) for a range of Vapour Pressures.

equilibrium vapour pressure for the wood is almost temperature independent. A lower limit of wood moisture content of 3.2% is determined by the values of the fitted coefficients in Equation 4-1 when vapour pressure and humidity ratio are zero. This artificial lower limit is set so that vapour pressure and humidity ratio are not calculated to be negative.

4.4 Development of nodal equations

For each of the nodes shown in Figure 4-1 the rate of change of mass of moisture at the node with time is set equal to the sum of the fluxes at each node. The equations are written in terms of vapour pressure with the direction of moisture transport from high to low pressure. For the attic air the rate of change of mass is expressed in terms of vapour pressure using the ideal gas law. For the wood nodes the procedure is more complex because the vapour pressure is based on the wood moisture content and the temperature as shown in the next section, 4.4.1. The fluxes of vapour transport within the wood are by diffusion as shown in section 4.4.2. At the wood surfaces a heat transfer-mass transfer analogy is used to estimate the rate of mass transport as will be shown later in section 4.4.3. All of these terms are combined for each node in the mass balances for each node outlined in section 4.4.4.

4.4.1 Estimating the rate of change of mass of water at a wood node with time

The rate of change of mass of water at a node is given by

$$\frac{dm_v}{dt} = \frac{d(m_W W_{MC})}{dt} = m_W \frac{dW_{MC}}{dt} \qquad (4\text{-}2)$$

where m_v is the mass of water at the node, m_W is the mass of dry wood at the node and W_{MC} is the moisture content of the node. The mass of wood is a known input and does not change with time. The rate of change of mass of water at the node is then only a function of wood moisture content. To estimate the rate of change of wood moisture content Equation 4-1 is used to convert wood moisture content to vapour pressure and temperature. This must be done because the mass transport equations are functions of vapour pressure and not wood moisture content.

Because Equation 4-1 is in terms of humidity ratio, ω, the following relationships are used to convert ω to vapour pressure. Assuming an ideal gas mixture ASHRAE (1989), p.6.4, gives

where P_a is atmospheric pressure. Because atmospheric pressure is about 100kPa and vapour pressure is typically 2 to 3 orders of magnitude below this, Equation 4-3

$$\omega = 0.622 \frac{P_v}{P_\infty - P_v} \tag{4-3}$$

may be approximated as

$$\omega = 0.622 \frac{P_v}{P_\infty} \tag{4-4}$$

Substituting Equation 4-4 into 4-1 gives

$$P_v = \frac{P_\infty}{0.622} \exp\left(\frac{T}{B_3}\right)(B_4 + B_5 W_{MC} + B_6 W_{MC}^2 + B_7 W_{MC}^3) \tag{4-5}$$

now the time rate of change of wood moisture content in Equation 4-2 can be expressed as

$$\frac{dW_{MC}}{dt} = \frac{\partial W_{MC}}{\partial P_v}\frac{dP_v}{dt} + \frac{\partial W_{MC}}{\partial T}\frac{dT}{dt} \tag{4-6}$$

The dP_v/dt and dT/dt terms will be determined later using a finite difference approximation. $\partial(W_{MC})/\partial P_v$ and $\partial(W_{MC})/\partial T$ are found from Equation 4-5 as follows. $\partial(W_{MC})/\partial P_v$ is found by differentiating Equation 4-5 with respect to wood moisture content to give

$$\frac{\partial P_v}{\partial W_{MC}} = \frac{P_\infty}{0.622} \exp\left(\frac{T}{B_3}\right)(B_5 + 2B_6 W_{MC} + 3B_7 W_{MC}^2) \tag{4-7}$$

The inverse of Equation 4-7 can be used in Equation 4-5. To find $\partial(W_{MC})/\partial T$ Equation 4-5 is rearranged to express temperature in terms of wood moisture content and the following substitution used to keep the equations compact

$$fn(W_{MC}) = (B_4 + B_5 W_{MC} + B_6 W_{MC}^2 + B_7 W_{MC}^3) \tag{4-8}$$

then

$$T = B_3 \ln\left(\frac{P_v}{0.622\, P_\infty\, fn(W_{MC})}\right) \tag{4-9}$$

The partial derivative of Equation 4-9 with respect to wood moisture content is

$$\frac{\partial T}{\partial W_{MC}} = B_3 \left(\frac{0.622\, P_- fn(W_{MC})}{P_v} \left(- \frac{P_v}{0.622\, P_- (fn(W_{MC}))^2} \frac{d\, fn(W_{MC})}{dW_{MC}} \right) \right) \quad (4\text{-}10)$$

Inverting this relationship and substituting the derivative of Equation 4-8 gives

$$\frac{\partial W_{MC}}{\partial T} = \left(- \frac{B_3}{fn(W_{MC})} (B_5 + 2B_6 W_{MC} + 3B_7 W_{MC}^2) \right)^{-1} \quad (4\text{-}11)$$

Equations 4-7 and 4-11 are now substituted in Equation 4-6 so that the rate of change of moisture content with time is given by

$$\begin{aligned} \frac{dW_{MC}}{dt} = & \left(\frac{P_-}{0.622} \exp\left(\frac{T}{B_3} \right) (B_5 + 2B_6 W_{MC} + 3B_7 W_{MC}^2) \right)^{-1} \frac{dP_v}{dt} \\ & + \left(\frac{-B_3 (B_5 + 2B_6 W_{MC} + 3B_7 W_{MC}^2)}{(B_4 + B_5 W_{MC} + B_6 W_{MC}^2 + B_7 W_{MC}^3)} \right)^{-1} \frac{dT}{dt} \end{aligned} \quad (4\text{-}12)$$

As in the thermal model in Chapter 3 the time derivatives are found using a finite difference approximation so that at the i^{th} hour

$$\frac{dT^i}{dt} = \frac{T^i - T^{i-1}}{\tau} \quad (4\text{-}13)$$

$$\frac{dP_v^i}{dt} = \frac{P_v^i - P_v^{i-1}}{\tau} \quad (4\text{-}14)$$

where the temperatures are found from the heat transfer model and P_v^i is the unknown to be found from the mass balance equation. The time step, τ, is one hour, the same as for the heat transfer model.

The partial derivatives of wood moisture content with respect to vapour pressure and temperature must be evaluated at each hour for the finite difference scheme. Because wood moisture content is not known for the current hour (i) the moisture content from the previous hour (i-1) and the temperatures for the previous hour are used in Equations 4-11 and 4-7. For node j at hour i the partial derivatives are approximated by

$$\frac{\partial W^{i}_{MC,j}}{\partial P^{i}_{v,j}} = \left(\frac{P_{\infty}}{0.622} \exp\left(\frac{T_j^{i-1}}{B_3} \right) (B_5 + 2B_6 W^{i-1}_{MC,j} + 3B_7 (W^{i-1}_{MC,j})^2) \right)^{-1} \qquad (4\text{-}15)$$

$$\frac{\partial W^{i}_{MC,j}}{\partial T^{i}_{j}} = \left(\frac{-B_3 (B_5 + 2B_6 W^{i-1}_{MC,j} + 3B_7 (W^{i-1}_{MC,j})^2)}{B_4 + B_5 W^{i-1}_{MC,j} + B_6 (W^{i-1}_{MC,j})^2 + B_7 (W^{i-1}_{MC,j})^3} \right)^{-1} \qquad (4\text{-}16)$$

These partial derivatives are substituted into Equation 4-2 together with the finite difference approximations for change of temperature and vapour pressure (Equations 4-13 and 4-14). This gives the finite difference approximation for the rate of change of mass of water at node j.

$$m_W \frac{dW^{i}_{MC,j}}{dt} = m_W \left(\frac{\partial W^{i}_{MC,j}}{\partial P^{i}_{v,j}} \left(\frac{P^{i}_{v,j} - P^{i-1}_{v,j}}{\tau} \right) + \frac{\partial W^{i}_{MC,j}}{\partial T^{i}_{j}} \left(\frac{T^{i}_{j} - T^{i-1}_{j}}{\tau} \right) \right) \qquad (4\text{-}17)$$

4.4.2 Diffusion Coefficient for Moisture in Wood

The diffusion coefficient for moisture in wood relates the flux and concentration gradient of wood moisture. The diffusion coefficient is defined under steady-state and isothermal conditions by Siau (1984), p.151, as

$$D_W = \frac{M_v}{A} \frac{\Delta X}{\Delta \Omega_{H2O}} \qquad (4\text{-}18)$$

where D_W is the diffusion coefficient for moisture in wood [m^2/s], M_v is the mass flow rate of water [Kg/s], ΔX is the distance in the flow direction [m], and $\Delta \Omega_{H2O}$ [Kg/m^3] is the concentration difference across distance ΔX.

Siau (1984), Chapter 6, has shown that the diffusion coefficient depends on temperature, moisture content, wood type and directional properties (where diffusion is parallel or perpendicular to the wood grain). For simplicity and because there is only a single node for each wood section, a constant diffusion coefficient is used in this study. The variation in diffusion coefficient with temperature and wood moisture content is about one order of magnitude (Siau (1984), p.158). Neglecting this effect

in the present study does not introduce large errors in the attic moisture balance calculations because the amount of water vapour transported by diffusion is several orders of magnitude less than the other transport terms. Experiments by Choong and Skaar (1969 and 1972) to separate surface resistance from internal resistance for moisture transfer through wood showed differences of approximately a factor of 2 in diffusion coefficient for flows parallel or perpendicular to the wood grain. The separation of surface and internal diffusion resistance is important since most experiments to determine permeability include both effects. As the samples become thicker the internal diffusion term becomes more dominant. Choong and Skaar tested two samples of different thicknesses dried under identical conditions and used theoretical relationships from Newman (1931) to isolate the diffusion term. This yielded diffusion coefficients on the order of 10^{-9} to 10^{-8} m^2/s for the woods they tested which were yellow poplar and sweetgum. More recent work by Cunningham (1990) gives an estimate of $D_W = 3*10^{-10}$ m^2/s for pine. This value by Cunningham is used in this moisture transport model as pine is more typical of wood used in attic construction. Fir and spruce are used in the plywood and trusses respectively in the attics used in this study. All of these values of diffusion coefficient are small so the exact value used is not critical for the moisture model developed in this study.

Assuming that water vapour acts as an ideal gas within the wood allows the concentration difference $\Delta\Omega_{H2O}$ to be written in terms of a vapour pressure difference, ΔP_v as follows

$$D_W = \frac{M_v}{A}\frac{\Delta X R_{H2O} T}{\Delta P_v} \qquad \textbf{(4-19)}$$

where R_{H2O} is the gas constant for water vapour (462 J/KgK), T is the temperature [K] and ΔP_v is the vapour pressure difference [Pa]. The water vapour mass flow due to diffusion within the wood from node j to node i is then given by

$$M_{v,i} = \frac{DA}{\Delta X R_{H2O} T_i}\left(\frac{T_i}{T_j}P_{v,j} - P_{v,i}\right) \qquad \textbf{(4-20)}$$

Equation 4-20 is the relationship used to determine water vapour mass flows due to internal diffusion for each wood node.

4.4.3 Mass Transfer Coefficient at Wood Surface

The rate of water vapour transfer at the wood surface is determined using a heat transfer to mass transfer analogy as shown by Holman (1981), p.492-494. Because phenomenological laws governing heat and mass transfer are similar, a relationship can be developed between heat and mass transfer at a surface. Holman (1981), p.494, shows that by equating friction factors based on heat and mass transfer coefficients for flow through pipes

$$h_v = \frac{h_U}{C_{sh,a}(Le)^{\frac{2}{3}}} \qquad (4\text{-}21)$$

where h_v = mass transfer coefficient for water vapour, m/s

h_U = heat transfer coefficient from heat transfer model, J/sm^{2}K

$C_{sh,a}$ = Specific heat of air ≈ 1000 J/KgK

Le = Lewis number

In the model developed for this study Equation 4-21 is assumed to apply to flow over the wood surfaces in the attic. A similar relationship has been used in a previous attic moisture model by Gorman (1987) to relate heat and mass transfer at the wood surface. Using a typical heat transfer coefficient of about 5 W/m^{2}K the corresponding mass transfer coefficient calculated using Equation 3-21 is about 5.3 * 10^{-3}m/s.

The Lewis number, Le, is given by the ratio of thermal diffusivity to water vapour diffusion coefficient. The ASHRAE fundamentals handbook (1989), p.5-9, gives a typical value of Lewis number for air and water vapour of 0.919. As with the internal diffusion the concentration of water vapour can be expressed assuming an ideal gas relationship such that the rate of mass transfer at the wood surface is given by

$$M_v = \frac{h_v A}{R_{H2O} T} \Delta P_v \qquad (4\text{-}22)$$

where ΔP_v is the difference in vapour pressure between the wood surface and the air flowing over it. Equation 4-22 is used for all the wood surface nodes to determine the amount of mass transferred between the surface and the attic air.

4.4.4 Mass transfer Biot number

The biot number for mass transfer is determined by the ratio of the rate of mass transfer at the surface to the internal mass transfer. For the lumped heat capacity approximation to be valid the value of Biot number must be low (<0.1). In this case the ratio is of the surface convection coefficient to the internal diffusion coefficient.

$$Bi_{H2O} = \frac{h_v\left(\frac{V}{A}\right)}{D_w}$$

where Bi_{H2O} is the mass transfer Biot number, h_v is the surface convection mass transfer coefficient, V/A is the volume to area ratio (or characteristic length) and D_W is the diffusion coefficient for moisture in wood. Using the typical value of h_v = $5.3*10^{-3}$ (as shown in the previous section), V/A is the sheathing thickness of 0.01m and a diffusion coefficient of $3*10^{-10}$ gives Bi_{H2O} of approximately $2*10_5$. This value of Bi_{H2O} shows that using a single moisture content for each wood location in the attic is a poor approximation. Even using one of the lower estimates of diffusion coefficient and making the surface layer only 1% of the total wood thickness would not produce a low enough Bi_{H2O}. This is because the rate of diffusion transport of moisture in wood is very slow and considerable moisture gradients exist in the attic wood. One method of reducing the errors from the lumped heat capacity analysis would be to further divide the wood into thinner layers. This is a possible future development for attic moisture models. The rate of moisture transport in the wood is complicated by temperature and moisture content effects, and free water above freezing may move by capillary action. In order to also include these effects, another solution to this problem is to find an appropriate surface layer thickness that provides realistic predictions of surface moisture content and condensed mass. The effect of changing the effective surface layer thickness will be examined later in the simulations in Chapter 7.

4.4.5 Mass transfer equations for moisture in attics

The mass transfer at each node is found in terms of its vapour pressure. For the wood nodes the transfer depends on diffusion within the wood and convection transfer at the surface. The attic air includes the convective mass transfer with the wood surfaces and the convective flows of outdoor and house air through the attic.

The rate of mass accumulation at a node is equated to the net flux to the node using finite difference approximation for time derivatives. All the following equations are written for the i^{th} hour and all the time derivatives are calculated using the values of vapour pressure and temperature from the previous hour. This results in a system of equations describing the mass transfer in the attic that is linear in vapour pressure. The solution of this set of linear equations with the same number of equations as unknowns is described in section 4.6. The complications arising from condensed masses where the vapour pressure at a node is limited to its saturation pressure are discussed in section 4.5. For each wood node the partial derivatives of wood moisture content, W_{MC}, are calculated using Equations 4-15 and 4-16.

Node 1. Attic air

The rate of change of moisture in the attic air, given by the left hand side of Equation 4-24, is calculated using the ideal gas law. This rate of change depends on the transfer to and from the wood surfaces, the convective flows of air through the attic and any condensed mass. An additional term, M_{ss}, is used for the attic air to account for any source or sink terms (e.g. humidifiers), although in this study this term is zero. The mass balance yields:

$$\frac{V_a(P^i_{v,1}-P^{i-1}_{v,1})}{R_{H2O}T^i_1\tau}=\frac{h^i_{v,4}A_4}{R_{H2O}T^i_4}\left(P^i_{v,4}-\frac{T^i_4}{T^i_1}P^i_{v,1}\right)+\frac{h^i_{v,2}A_2}{R_{H2O}T^i_2}\left(P^i_{v,2}-\frac{T^i_2}{T^i_1}P^i_{v,1}\right)$$
$$+\frac{h^i_{v,7}A_7}{R_{H2O}T^i_7}\left(P^i_{v,7}-\frac{T^i_7}{T^i_1}P^i_{v,1}\right)+\frac{M^i_cP^i_{v,in}}{\rho^i_{in}R_{H2O}T^i_{in}} \qquad (4\text{-}24)$$
$$+\frac{M^i_{in,a}P^i_{v,out}}{\rho^i_{out}R_{H2O}T^i_{out}}-\frac{M^i_{out,a}P^i_{v,1}}{\rho^i_aR_{H2O}T^i_1}-M^i_{\tau,1}+M_{ss}$$

Term 1 is the mass change rate of the attic air assuming an ideal gas and V_a is the attic volume and R_{H2O} is the gas constant for water vapour = 462 J/KgK

Terms 2, 3 and 4 correspond to the mass fluxes from the wood surfaces.

Term 5 accounts for mass of moisture flowing through the ceiling assuming that the flow is from the house to the attic. M_c is the mass flow rate through the ceiling calculated by the ventilation model. For reversed flow from attic to house this term becomes

$$\frac{-M_c^i P_{v,1}^i}{\rho_a^i R_{H2O} T_1^i} \qquad (4\text{-}25)$$

Term 6 is the mass flow into the attic from outside. If M_c is into the attic and M_a is the total attic ventilation rate then $M_{in,a} = M_a - M_c$, but if M_c is out of the attic then $M_{in,a} = M_a$.

Term 7 is the mass flow to outside from the attic. If M_c is into the attic then $M_{out,a} = M_a$, but if M_c is out of the attic then $M_{out,a} = M_a - M_c$.

Term 8, M_τ, is the rate of mass condensation for the attic air which is distributed to the wood surfaces and to the air leaving the attic.

The mass fluxes in terms 2, 3 and 4 contain the following variables, where

A_2 = sheathing surface area

$h_{v,2}$ = surface mass transfer coefficient from Equation 4-21.

A_4 = sheathing surface area = A_4.

$h_{v,4}$ = surface mass transfer coefficient from Equation 4-21.

A_7 = truss and joist surface area

$h_{v,7}$ = surface mass transfer coefficient from Equation 4-21.

Node 2. North sheathing surface

Node 2 exchanges moisture by diffusion with the inner node 3 and with the attic air by convection. The rate of change of mass of water at the wood nodes is given by Equation 4-17.

$$m_{W,2}\left(\frac{\partial W_{MC,2}^i}{\partial P_{v,2}^i}\frac{(P_{v,2}^i - P_{v,2}^{i-1})}{\tau} + \frac{\partial W_{MC,2}^i}{\partial T_2^i}\frac{(T_2^i - T_2^{i-1})}{\tau}\right) + M_{\tau,2}^i$$
$$= \frac{h_{v,2}^i A_2}{R_{H2O} T_2^i}\left(\frac{T_2^i}{T_1^i}P_{v,1}^i - P_{v,2}^i\right) + \frac{D_w A_2}{R_{H2O} T_2^i \Delta X_2}\left(\frac{T_2^i}{T_3^i}P_{v,3}^i - P_{v,2}^i\right) \qquad (4\text{-}26)$$

where

$m_{W,2}$ is the mass of wood at node 2, Kg

ΔX_2 = distance between sheathing nodes for diffusion of water vapour = 1/2 sheathing thickness

$M_{\tau,2}^i$ = rate of mass condensed or evaporated/sublimed during hour i. When $P_{v,2} < P_{vs,2}$ then this term is zero.

Node 3. North sheathing inner layer

The inner wood only exchanges moisture by diffusion with the surface layer because it is assumed that the outer sheathing surface is covered by impermeable shingles. As for node 2, the rate of change of mass of water at the wood nodes is given by Equation 4-17.

$$m_{W,3}\left(\frac{\partial W^i_{MC,3}}{\partial P^i_{v,3}}\frac{(P^i_{v,3}-P^{i-1}_{v,3})}{\tau}+\frac{\partial W^i_{MC,3}}{\partial T^i_3}\frac{(T^i_3-T^{i-1}_3)}{\tau}\right)+M^i_{\tau,3} = \frac{D_w A_2}{R_{H2O}T^i_3\Delta X_2}\left(\frac{T^i_3}{T^i_2}P^i_{v,2}-P^i_{v,3}\right) \quad (4\text{-}27)$$

where

$m_{W,3}$ is the mass of wood at node 3, Kg.

$M_{\tau,3}^{\ i}$ = Mass condensed or evaporated/sublimed during hour i. When $P_{v,3}<P_{vs,3}$ then this term is zero.

Node 4. South sheathing surface

The south sheathing surface has the same moisture exchange mechanisms as the north sheathing surface, node 2. It exchanges moisture by diffusion with the inner node 5 and with the attic air by convection. The rate of change of mass of water at the wood nodes is given by Equation 4-17.

$$m_{W,4}\left(\frac{\partial W^i_{MC,4}}{\partial P^i_{v,4}}\frac{(P^i_{v,4}-P^{i-1}_{v,4})}{\tau}+\frac{\partial W^i_{MC,4}}{\partial T^i_4}\frac{(T^i_4-T^{i-1}_4)}{\tau}\right)+M^i_{\tau,4} = \frac{h^i_{v,4}A_4}{R_{H2O}T^i_4}\left(\frac{T^i_4}{T^i_1}P^i_{v,1}-P^i_{v,4}\right)+\frac{D_w A_4}{R_{H2O}T^i_4\Delta X_4}\left(\frac{T^i_4}{T^i_5}P^i_{v,5}-P^i_{v,4}\right) \quad (4\text{-}28)$$

where

$m_{W,4}$ is the mass of wood at node 4, Kg

ΔX_4 = distance between sheathing nodes for diffusion of water vapour = 1/2 sheathing thickness

$M_{\tau,4}^{\ i}$ = rate of mass condensed or evaporated/sublimed during hour i. When $P_{v4}<P_{vs,4}$ then this term is zero.

Node 5. South sheathing inner layer

The south sheathing inner layer only exchanges moisture with the south sheathing surface layer because it is assumed that the outer surface is covered by impermeable shingles.

$$m_{W,5}\left(\frac{\partial W^i_{MC,5}}{\partial P^i_{v,5}}\frac{(P^i_{v,5}-P^{i-1}_{v,5})}{\tau}+\frac{\partial W^i_{MC,5}}{\partial T^i_5}\frac{(T^i_5-T^{i-1}_5)}{\tau}\right)+M^i_{\tau,5} = \frac{D_w A_4}{R_{H2O}T^i_5\Delta X_4}\left(\frac{T^i_5}{T^i_4}P^i_{v,A}-P^i_{v,5}\right) \quad (4\text{-}29)$$

where

$m_{W,5}$ is the mass of wood at node 5, Kg.

$M_{\tau,5}^{\ i}$ = rate of mass condensed or evaporated/sublimed during hour i. When $P_{v,5}<P_{vs,5}$ then this term is zero.

Node 6. Inside trusses and joists

The inside of the trusses and joists only have a single path for moisture movement. This node is connected to the surface node for the joists and trusses (node 7) by diffusion.

$$m_{W,6}\left(\frac{\partial W^i_{MC,6}}{\partial P^i_{v,6}}\frac{(P^i_{w6}-P^{i-1}_{w6})}{\tau}+\frac{\partial W^i_{MC,6}}{\partial T^i_6}\frac{(T^i_6-T^{i-1}_6)}{\tau}\right) +M^i_{\tau,6}=\frac{D_w A_6}{R_{H2O}T^i_6\Delta X_6}\left(\frac{T^i_6}{T^i_7}P^i_{v,7}-P^i_{v,6}\right) \quad (4\text{-}30)$$

where

$m_{W,6}$ is the mass of wood at node 6, Kg.

$M_{\tau,6}^{\ i}$ = rate of mass condensed or evaporated/sublimed during hour i. When $P_{v,6}<P_{vs,6}$ then this term is zero.

ΔX_6 = Distance between sheathing nodes for diffusion of water vapour = 1/2 mean wood thickness. e.g. for a 50mm by 100mm cross section ΔX_6 = 37.5mm.

Node 7. Surface of trusses and joists

The surface of the trusses and joists exchange moisture with the attic air by convection and with node 6 by diffusion.

$$m_{W,7}\left(\frac{\partial(W^i_{MC,7})}{\partial P^i_{v,7}}\frac{(P^i_{v,7}-P^{-1}_{v,7})}{\tau}+\frac{\partial(W^i_{MC,7})}{\partial T^i_7}\frac{(T^i_7-T^{i-1}_7)}{\tau}\right)+M^i_{\tau,7}$$
$$=\frac{h^i_{v,7}A_7}{R_{H2O}T^i_7}\left(\frac{T^i_7}{T^i_1}P^i_{v,1}-P^i_{v,7}\right)+\frac{D_w A_7}{R_{H2O}T^i_7\Delta X_6}\left(\frac{T^i_7}{T^i_6}P^i_{v,6}-P^i_{v,7}\right) \qquad (4\text{-}31)$$

where

$m_{W,7}$ is the mass of wood at node 3, Kg. For joists and trusses this is assumed to be the mass corresponding to a 1mm thick layer.

$M_{\tau,7}^{i}$ = rate of mass condensed or evaporated/sublimed during hour i. When $P_{v,7}<P_{vs,7}$ then this term is zero.

The mass of wood at each node used for the model verification and for the simulations is given by Table 4-1. These masses are different from the heat transfer model because the wood is divided into a thin surface layer and a thicker inner layer. For the heat transfer model the sheathing is divided into inner and outer surfaces that both have the same mass of 25.7 Kg and the inner and outer truss and joist masses are combined. This gives the same total masses for the moisture transport and heat transfer models.

Table 4-1. Distribution of mass of wood in the attic for model verification and attic simulations

Location	Node	Mass of Wood [Kg]
North Sheathing Surface	2	17.2
North Sheathing Inner	3	34.2
South Sheathing Surface	4	17.2
South Sheathing Inner	5	34.2
Truss and Joist Inner	6	188
Truss and Joist Surface	7	12

4.5 Calculating Condensed Mass.

4.5.1 Wood Surface Nodes.

Previous models have either assumed that all mass transferred to a wood surface condenses (Ford (1982)) or that no mass condenses unless the wood is at fibre saturation point (Gorman (1987)). The model developed for this study is more sophisticated than these previous methods because it uses Equation 4-5 to determine the water vapour pressure at the wood surface. A limiting value of $P_v = P_{vs}$ (100% RH in Figure 4-4) is applied so that water vapour pressures in the wood are never above the saturation pressure, P_{vs}, determined by the temperature of the node. As shown in Figure 4-4, Equation 4-5 limits the wood moisture content at the saturation vapour pressure at low temperatures. This is a characteristic of Equation 4-5 that was not fitted to low temperature wood moisture content data and is being extrapolated here beyond its limits. Therefore there is some uncertainty in the wood moisture content at the saturation vapour pressure. Equation 4-5 is used in the present study because there is insufficient data on low temperature wood moisture contents to develop other relationships.

If the vapour pressure from simultaneous solution of the mass transfer equations is calculated to be greater than the saturation vapour pressure for a node, then the vapour pressure is set equal to the saturation vapour pressure. A new mass balance is performed with the vapour pressure held at the saturation vapour pressure for that node. Once all the other vapour pressures are found (other nodes may also be at saturation) the rate of mass condensation, M_τ, is calculated from the mass balance equation that includes the fluxes to and from other nodes as well as mass changes due to temperature effects when the node is saturated. The effects of temperature are very important because a decrease in temperature for a node at saturation in cold winter weather implies a decrease in wood moisture content as can be seen in Figure 4-4 and as described in section 4.2.4. The mass that was included as wood moisture content now appears as condensed mass at this wood surface. Thus the temperature change at a wood node can change its wood moisture content and condensed mass even if there is no net flux to the node. If the rate of condensed mass change at a node (M_τ)is positive then mass accumulates at the node. This mass is not included in the wood moisture content (and therefore in finding the vapour pressure for the next hour) but is monitored using a separate term, m_τ, that is the total mass accumulated at the surface. If the net mass change is negative then m_τ is reduced. If this reduction makes the total accumulated mass negative then the

difference between the net mass change and the accumulated mass from the previous hour is used to reduce the wood moisture content (and the vapour pressure) of the node. Thus when all the condensed mass has been sublimed, evaporated or reabsorbed by the wood then $m_r = 0$, the vapour pressure is below saturation, and the mass balance for the attic must be repeated as this node is now an unknown.

4.5.2 Attic Air Node.

As with the wood surface nodes the vapour pressure is limited to the saturation vapour pressure (for this node this is determined by the attic air temperature). If there is a net mass flux to the attic air when it is saturated from the combination of attic wood surfaces and air flows then this net mass must result in condensed mass in the saturated attic air. Unlike the wood there is no surface for this mass to accumulate on. The condensed mass is assumed to be distributed to the wood surfaces and the air leaving the attic in proportion to their mass flux exchange with the attic air. Condensed attic moisture is only transferred to wood surfaces for which there is a positive flux from the attic air (at its saturation vapour pressure) to that node. This usually means positive fluxes from the attic air to colder sheathing surfaces (which are at a lower vapour pressure) which agrees with observations of frost buildup on the interior of attic sheathing. The rest of the condensed attic air moisture is advected out with the attic air ventilation flows.

At the wood nodes the additional condensed mass from the attic air is used to calculate a new wood moisture content and vapour pressure, and the mass balance for the attic is repeated with the vapour pressure for the attic air held at the saturation vapour pressure. If the mass transfer with the attic air at saturation makes the wood vapour pressure greater than its saturation vapour pressure then the procedure for considering condensed mass for the wood must also be performed (section 4.5.1). This process of finding which nodes are at saturation (then holding them at their saturation vapour pressure and recalculating the mass balance) is continued until no more nodes reach saturation.

4.6 Solution Methods

If the vapour pressure is less than saturation at all nodes then the moisture model is a system of seven mass balance equations (4-23 through 4-30) in terms of seven unknown vapour pressures. Gaussian elimination (see, for example, James, Smith and Wolford (1977), p.169-182) is used to simultaneously solve these seven equations. Problems occur because the vapour pressure has an upper limit of the

saturation pressure. If a node is at saturation then its vapour pressure is known and is determined by the node temperature. This known vapour pressure must be substituted into the remaining equations for the other nodes and one less equation has to solved. This requires changing the number of equations in the gaussian elimination scheme and becomes even more complex if more than one node is at saturation pressure.

A solution to this problem is to use an iterative technique rather than gaussian elimination to solve the equations. Gaussian elimination is still used to provide initial estimates of vapour pressure which speeds up the iterative process. With the iterative technique each node can be checked for saturation after every iteration and the appropriate vapour pressures held constant in the next iteration. The iterative technique used here makes estimates of the vapour pressure at a node by substituting the vapour pressures from the previous iteration for the other nodes. Each of the seven equations is solved consecutively. The process is speeded up by using the updated vapour pressures within each iteration as they become available. For example, after equation 1 is solved then $P_{v,1}$ is known. This vapour pressure is now substituted wherever it appears in the other six equations rather than waiting for the next iteration. Repeated estimates of vapour pressure are made by cycling through the seven equations until all the vapour pressures change by less than 0.1 Pa. Each node at each iteration is checked to see if the calculated vapour pressure is greater than saturation. If it is then this vapour pressure is set equal to the saturation vapour pressure corresponding to the temperature at that node. The mass balance is then performed with this fixed vapour pressure to find the condensed mass as outlined in sections 4.5.1 and 4.5.2. If no saturation occurs only one iteration is required since the initial estimates from the gaussian elimination method are already the solution to the set of non-saturated equations.

Once the vapour pressure is found for each node the wood moisture content is calculated for the wood nodes using Equation 4-5. To find wood moisture content from the cubic Equation 4-5, the cube root is found analytically using standard mathematical methods from Spiegel (1968).

4.7 Summary

In this chapter a moisture transport model for the attic has been developed. The model includes convective ventilation flows through the attic, the exchange of moisture at wood surfaces and the storage of moisture in the wood. The model uses

ventilation rates and temperatures calculated by the models in Chapters 1 and 2 as inputs. Surface mass transfer coefficients are calculated from the convective surface heat transfer coefficients found in the heat transfer model. Moisture movement within the wood is assumed to be by diffusion. Estimates of diffusion coefficient from other authors indicate that the diffusion process is several orders of magnitude slower than the surface moisture transport. This is important because it means that the wood nodes should be treated as if they are at a single moisture content. To examine this effect different surface layer thicknesses will be examined in the simulations in Chapter 7. The rate of change of moisture content of each node of the model is approximated using a finite difference technique with a timestep of one hour. This length of timestep was chosen because the measured data used for validation are hourly averaged values. A system of seven equations has been developed for the seven nodes shown in Figure 4-1. At each node the rate of change of moisture at the node is set equal to the sum of the fluxes at the node as shown in Equations 4-23 to 4-30. This set of linear equations is solved using an iterative scheme to find the vapour pressures, and hence wood moisture contents and attic air relative humidity. The complication of nodes at saturation where mass is condensing is dealt with by fixing the vapour pressure at these nodes at their saturation pressure. This known value of vapour pressure is then substituted into the remaining equations to be solved.

An important aspect of this model is the use of a relationship developed by Cleary (1985) between wood moisture content, temperature and vapour pressure. This relationship allows the rate of change of moisture content with time to be estimated so that the wood nodes and the attic air vapour pressures may be solved for simultaneously. This relationship is also vital in determining the amount of condensation on a wood surface. The extrapolation of this relationship to low temperatures results in wood surface nodes reaching saturation vapour pressure well below the fibre saturation point of wood (approximately 30%). This has a significant effect on the drying of wood (reduction of moisture content) in cold winter months. To improve the low temperature extrapolation of Cleary's equation more experiments need to be performed to determine the moisture content of wood at low temperatures.

Chapter 5. Measurements for model validation

To validate the attic ventilation, thermal, and moisture models described in the previous chapters field data was taken over the course of two heating seasons, 1990-91 and 1991-92 at The Alberta Home Heating Research Facility (AHHRF). This chapter describes the construction details and configurations of the two attics that were monitored. This includes the background leakage area and vent configuration of the attics and the distribution of the ceiling leakage. The instrumentation and measurement procedures are presented for attic ventilation rates and fan pressurization tests to determine leakage areas. This chapter also includes presentation of some typical results for ventilation rates, attic temperatures and wood moisture content.

There have been several previous studies monitoring ventilation, heat transfer and moisture in attics. Some studies, e.g. Wilkes (1983) and Burch, Lemay, Rian and Parker (1984), have used scale models of attic spaces inside environmental chambers. This allows direct control over the ambient conditions for the attic. However, this does not provide data on real attics exposed to the dynamics of real weather. In addition, the attic in both the above studies had forced fan ventilation with no natural wind. This provides a constant ventilation rate that does not occur in real attics. Limited full scale field testing has been carried out by previous authors. Fairey (1983) performed tests over three days on a fan ventilated attic. Fairey was only interested in heat transfer and concentrated on heat flux measurements with no ventilation, relative humidity of moisture content measurements.

For testing more specifically directed at moisture in attics the following four studies have appeared in the literature. Gorman (1987) did not measure ventilation rates but did measure relative humidity in the attic using a strip chart recorder. Gorman also took limited manual readings of sheathing moisture content and temperatures. Ford (1982) took a total of 350 hours of temperature data at multiple attic locations. In addition Ford measured relative humidities with an aspirated psychrometer (above freezing only) but took no wood moisture content or ventilation measurements. Some of the most thorough attic measurements to date have been provided by Cleary (1985). Cleary measured, temperatures, wind speed, wind direction, solar radiation, wood moisture content and air relative humidity over a six month heating season. Cleary made 24 periodic measurements of ventilation using a tracer gas decay technique and on one occasion measured the house to attic

exchange rate.

The measurements performed for this study provide significantly more information for the evaluation of attic moisture phenomena and validation of attic ventilation, heat transfer and moisture transport models. Data has been taken continuously for over two years, providing a data base of over 5000 hours. This data covers a wide range of weather conditions with outside temperatures ranging from +30°C to -40°C, wind speeds of up to 10 m/s and covering all wind directions. The complete set of wind directions is important (as will be shown later in this chapter and in the following chapter on model verification) because both wind pressure coefficients and wind shelter are highly dependent on wind direction. This study has continuously monitored ventilation rates and house to attic exchange rates that have not been systematically measured before. Ambient conditions of relative humidity, temperature, solar radiation on both pitched roof surfaces, wind speed and wind direction have been measured for use as inputs to the models developed for this study. The relative humidity and temperatures of the house and attic air have been measured and additional measurements of wood moisture content and wood temperature were performed in the attic.

5.1 Attic test facility

The field monitoring program was carried out over a period covering two heating seasons in 1990-91 and 1991-92 at The Alberta Home Heating Research Facility (AHHRF), located south of Edmonton, Alberta. The facility consists of six houses situated in an east-west row as shown in Figure 5-1. Each house has a full basement with a single storey and gable-end attic. The houses are spaced approximately 2.6 m apart. At each end of the row, false end walls were constructed about 3.7 m high but without roof gable peaks, to provide wind shelter and solar shading similar to that experienced by interior houses in the row. The attic ventilation tests were carried out in houses 5 and 6 which are the last two houses at the east end of the row. Both houses are essentially identical in construction and insulation levels and the details of the house construction are given in Table 5-1. All houses at the test site are heated electrically with a centrifugal fan which operates continuously, recirculating 4.5 house interior volumes per hour. The continuous fan operation ensures that the air inside the house is well mixed with the sulphur hexafluoride (SF_6) tracer gas used to monitor house ventilation rates. Both houses have a 6m long 15.2 cm ID flue pipe that extends through the ceiling and roof to terminate in a rain cap level with the roof ridge. This places the flue cap a little below the required height

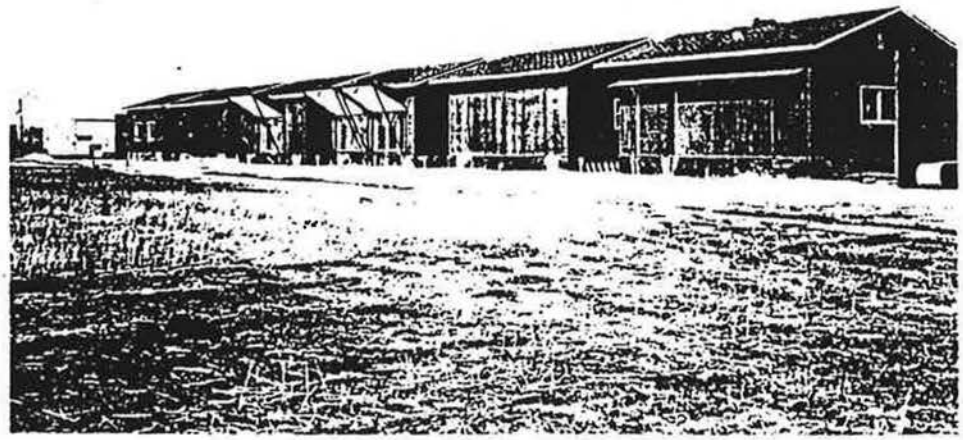

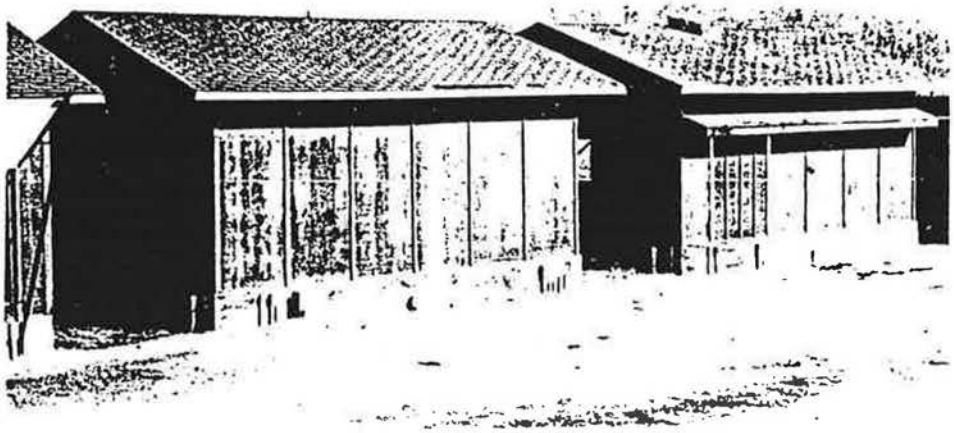

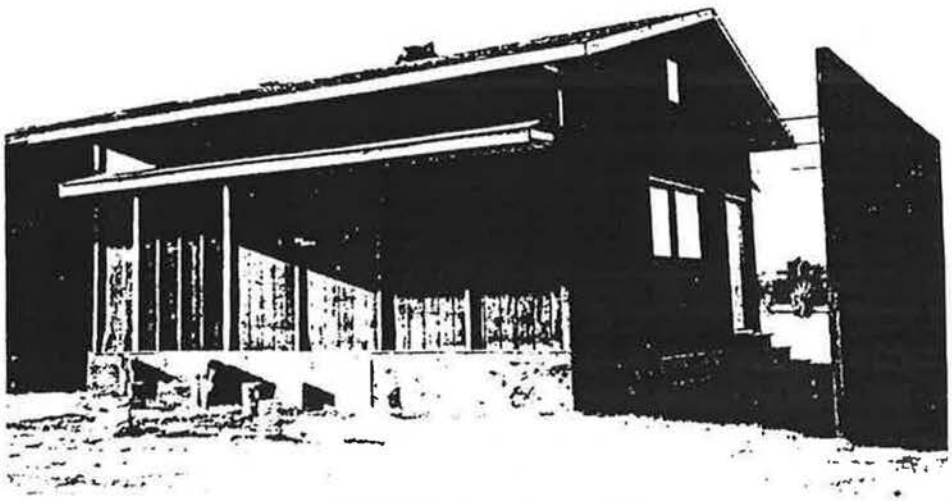

Figure 5-1. Houses 5 and 6 at AHHRF showing building orientation and false end wall.

to meet the building code (NBCC (1990)), however, because the flues are passive (i.e. not connected to a furnace) this does not present a problem. The present tests were carried out with the flue blocked to increase air exfiltration through the ceiling to provide a moisture load for the attic.

Table 5-1
Construction details of houses 5 and 6

Floor Area	6.7 m x 7.3 m (22′ x 24′)
Wall Height	2.4 m (8′)
Basement Height	2.4 m, 1.8 m below grade (8',6′ below grade) Exterior insulation RSI 1.76 (R10) to 0.61 m (2′) below grade
Walls	9.5 mm (3/8") Prestained Plywood 64 mm (2-1/2") Glass fiber batts 51 mm x 102 mm (2" x 4") studs, 40 cm (16") o/c 4 mil poly vapour retarder 12.7 mm (1/2") drywall, painted
Wall Area/Floor Area	1.39/1
Windows	North: 99 cm x 193 cm (39" x 76") double glazed sealed South: none East : 101 cm x 193 cm (40" x 76") double glazed sealed West : same as E
Window Area/Floor Area	11.9%
Ceiling	152 mm (6") Glass fiber batts 4 mil poly vapour retarder 12.7 mm (1/2") drywall, painted
Roof	CMHC approved trusses with 76 cm (2-1/2") stub asphalt shingles 9.5 mm (3/8") plywood sheathing roof pitch 3.0:1 61 m^3 attic volume
Basement	20 cm (8") concrete wall 10 cm (4") concrete slab on 6 mil poly
Electric Furnace Capacity	12 kW

As will be shown later in this chapter, and also in the following chapter discussing model validation, wind shelter is an important factor in determining attic (and house) ventilation rates. In Chapter 2 it was shown that the closest obstacle dominates the wind shelter effect for a building. For the test houses at AHHRF their shelter is dominated by the other houses in the row and the false end walls. Other obstacles that may provide significant shelter are a storage shed and machinery building, both two storeys high, that are about 50m to the northwest of the row of test houses. For more details of the surroundings see Forest and Walker (1993).

The attics in houses 5 and 6 have the same construction. Each attic has plan dimensions of 6.7 m by 7.3 m (including the eaves makes it 7.8 m by 7.3 m) with gable end walls and a full length ridge oriented along the east-west direction. The sloped roof sections face north and south while the gable ends of the attic are vertical extensions of the east and west walls. The roof trusses are constructed of 38 mm by 89 mm spruce joists and are spaced at 61 cm intervals as shown in Figure 5-2. The sloped roof section (with a pitch of 3:1) is raised 0.67 m above the attic floor to accommodate various levels of ceiling insulation for other tests that have been conducted at AHHRF. The sloped roof was covered with 95 mm exterior plywood sheathing and brown asphalt shingles. The ceiling consisted of 12.7 mm painted drywall, 4 mil polyethylene vapour barrier, and 89 mm glass fibre batts between the trusses. The total enclosed attic volume was estimated to be 61 m^3.

The main difference between the two attics used in this study is their air tightness. Attic 5 was a "tight" attic where there were no intentional openings such as roof or soffit vents in the exterior portion on the attic envelope. The only leakage area in attic 5 was the background leakage associated with construction of the attic envelope. Attic 6 was fitted with continuous soffit vents (shown in Figure 5-3) along the north and south eaves and two flush-mounted attic vents (shown in Figure 5-4). The soffit vents were mounted on false eaves that were aligned with the floor of the attic. This was done to have the soffit leakage area in a location that was representative of conventional residential construction. The soffits on attic 6 had a gross open area of 403 cm^2 on each side of the house. The flush-mounted roof vents were commercial vents and had a gross opening area of 384 cm^2. The net area of the roof vents was reduced by a screen which was used to prevent the entry of insects.

During the second heating season, attic 6 was retro-fitted with a roof-mounted fan (Broan Model 334) as shown in Figure 5-5. The fan was designed to exhaust attic air to outdoors (depressurizing the attic). The fan was also operated in the opposite

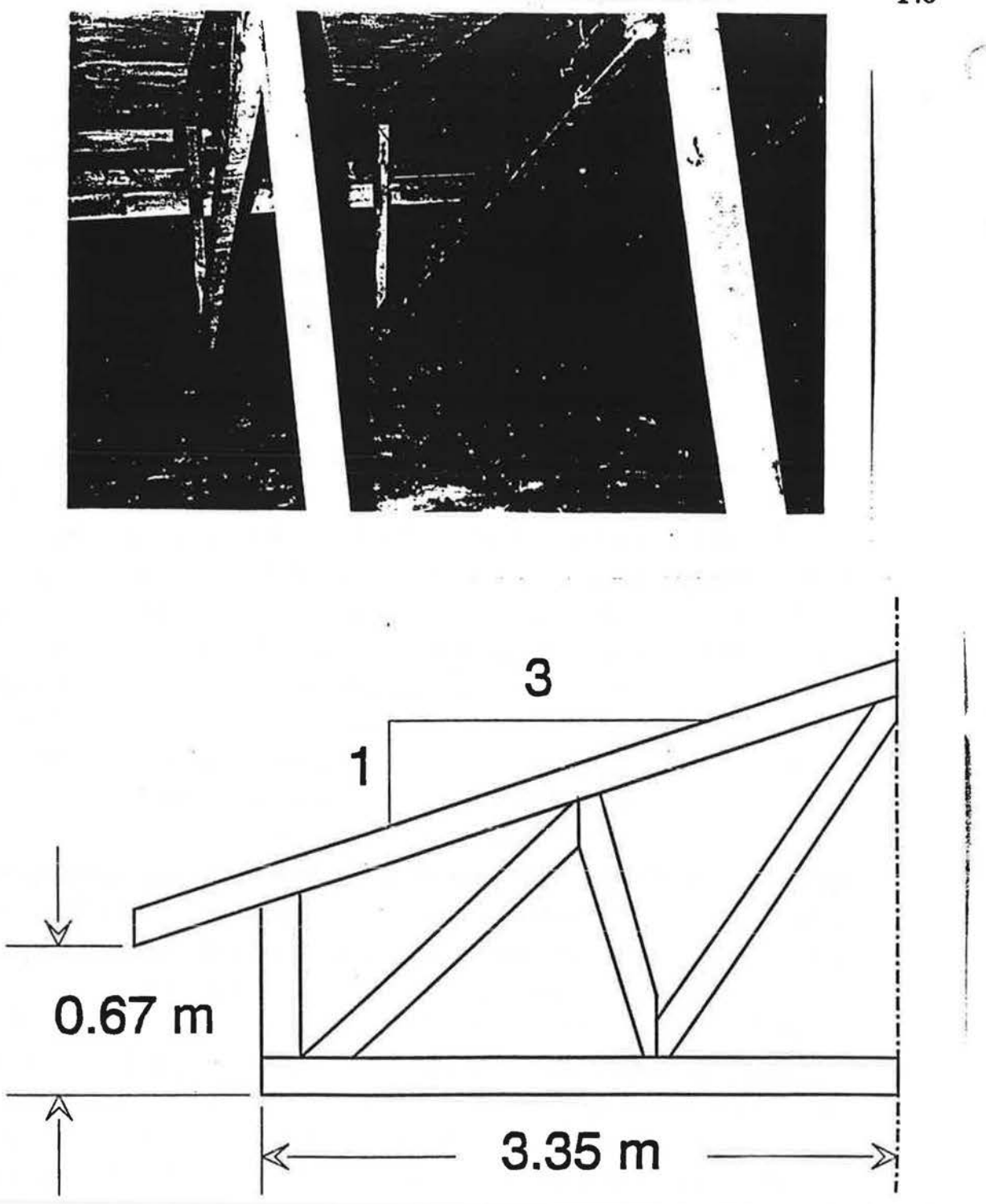

Figure 5-2. Attic interior showing detail of trusses.

Figure 5-3. False eaves on house 6.

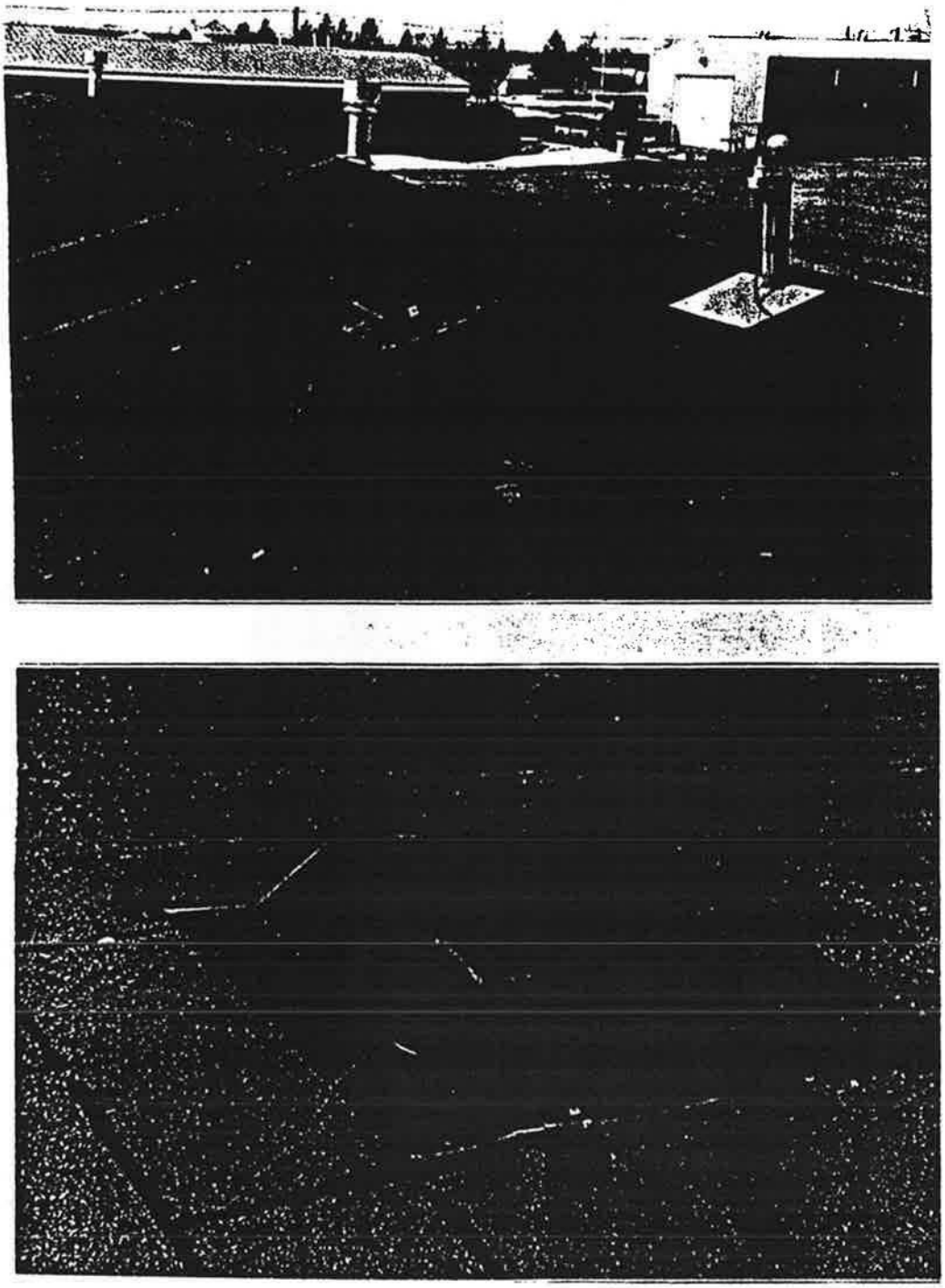

Figure 5-4. Location and installation of roof vents for attic 6.

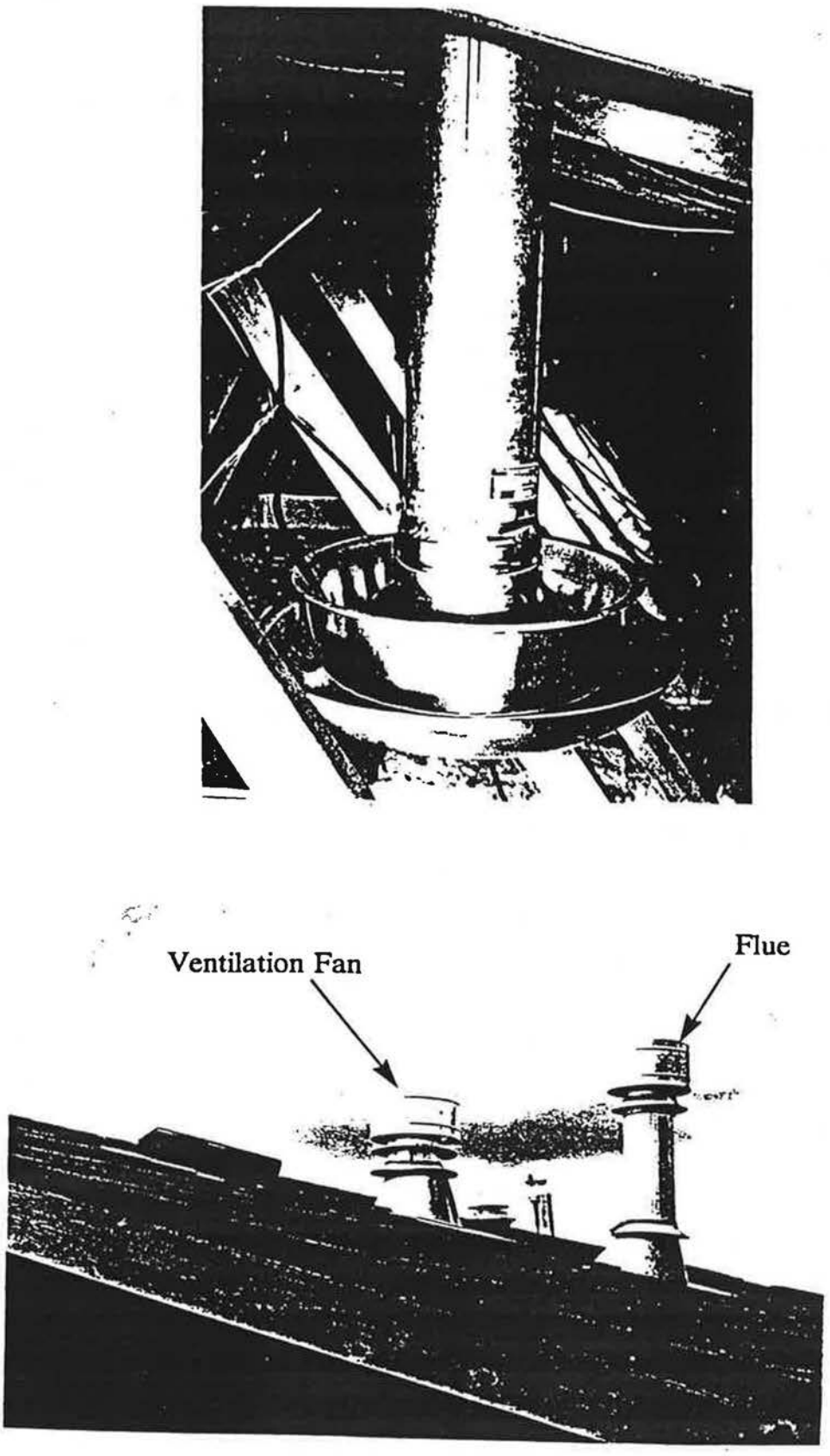

Figure 5-5. Ventilation fan in attic 6 in supply orientation showing interior view and exterior protective rain cap (same as the flue beside it).

mode with the fan blowing outdoor air into the attic (pressurizing the attic). This required that the fan be physically turned upside down in order to reverse the flow direction. This would expose the fan inlet to the outdoor environment. In order to protect the fan, a short length (1 m long) of 15 cm diameter pipe was attached to the inlet of the fan with a rain cap at the open end (the discharge side of the fan was protected by its own rain cap). It was necessary to use the fan with this inlet duct arrangement in both pressurization and depressurization modes so as to maintain the same flow characteristics of the fan in both orientations. This fan-inlet duct system was initially installed on the roof of attic 6 on November 4, 1991 and tested in the exhaust mode between November 4, 1991 and January 30, 1992. The fan was operated on a timed cycle where the fan was on between 10:00 am and 4:00 pm and off for the rest of the day. On February 1, 1992 the fan orientation was reversed and ventilation rate measurements made with the attic pressurized. Prior to installation, the fan-duct system was tested in a calibrated flow apparatus where the fan performance characteristics were measured. These measurements showed that the maximum flowrate for the fan was 0.164 m^3/s (which corresponds to an attic ventilation rate of 9.6 air changes per hour (ACH) based on an attic volume of 61 m^3) and the maximum pressure difference that the fan can generate is 175 Pa. When the fan was installed in the attic the additional flow resistances through the vents and soffits would act to decrease the flow delivered by the fan.

The leakage area in the ceiling interface between the heated interior space of the house and the attic allows air exchange between the two zones. During cold weather, indoor air exfiltrating into the attic may impose a significant moisture load on the attic. One of the main objectives of the tests performed for this study was to measure the indoor-attic exchange rate. The ceilings in houses 5 and 6 were essentially identical in construction and insulation levels. There was some unintentional leakage area, particularly around the electrical junction boxes for the two fluorescent light fixtures in each house. In addition, a 0.5 m by 0.89 m ceiling panel, shown in Figure 5-6, was placed approximately in the centre of the ceiling in both houses. A 7.6 cm diameter hole was placed in the centre of the panel to provide a large leakage site. This intentional leakage site was part of an orifice flow meter which was used to monitor the flow through this leakage area. The ceiling in house 5 had an additional ceiling panel that had three separate leakage sites, 7.6 cm, 2.5 cm, and 0.64 cm diameter respectively, which was used for a separate study on moisture accumulation in the ceiling insulation.

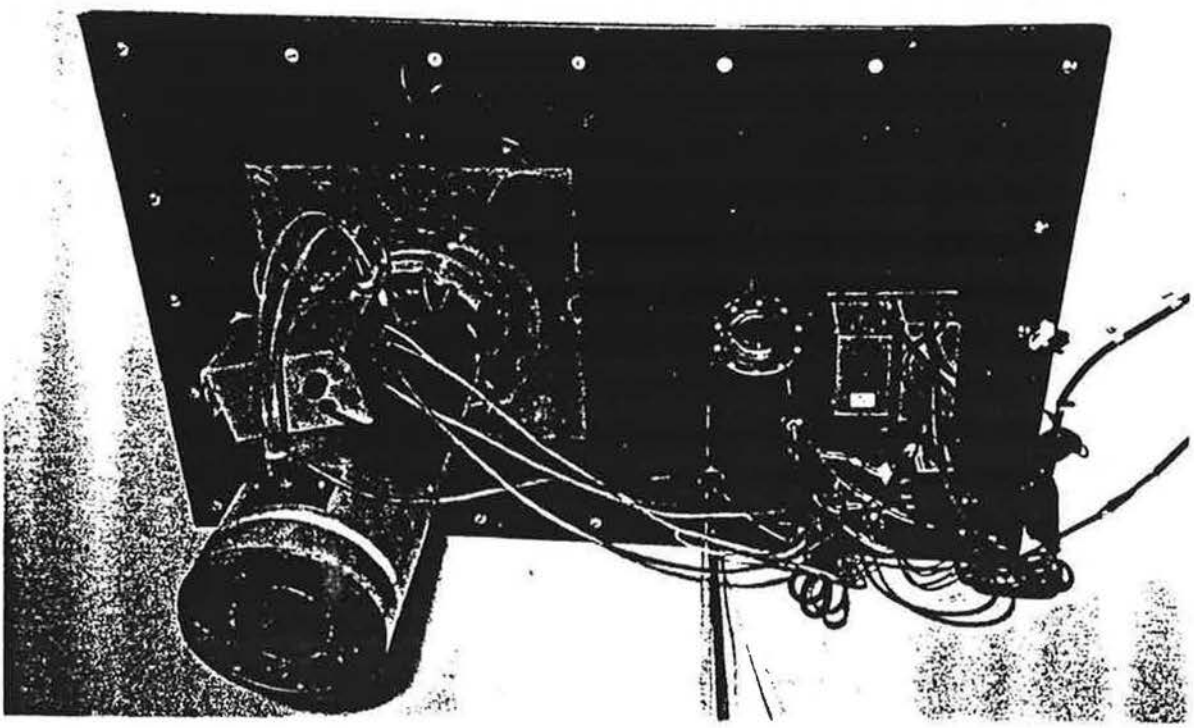

Figure 5-6. Ceiling Panel and Orifice Flow meter.

In order to provide a moisture load on the attic, the indoor air in both houses was humidified throughout the heating season. The humidification was provided by rotating-drum type humidifiers. During the first heating season (1990-91), the indoor relative humidity was maintained at approximately 40% with a variation of ±5%; during the 1991-92 heating season this level was increased to 50% in order to provide a larger moisture load on the attic. The humidifier water consumption rate was measured in the following way. Water for the humidifiers was supplied to an intermediate tank which was a 15 cm ID by 122 cm tall PVC pipe and the water from this tank was fed to the float valve on the humidifier. A pressure transducer near the bottom of the intermediate tank sensed the change in pressure caused by the change in water level as water was consumed by the humidifier. The pressure in the tank was measured by the data acquisition system at the end of each hour and the change in pressure from the previous hour was converted to the hourly water consumption rate. At the end of each 24 hour period, a pump refilled the intermediate tank up to its capacity. It was found that water consumption was highest during very cold periods because the outdoor air which infiltrates into the house contained very little moisture.

5.2 Measurement Procedure

5.2.1 Fan Pressurization Tests

Fan pressurization tests were performed to determine the leakage characteristics of the exterior envelope of the attic, the ceiling, and the houses. The attic tests were carried out using two separate fans, one connecting the attic with the interior of the house and the other connecting the interior the house with the outdoors as shown in Figure 5-7. The attic fan was connected through the plexiglass ceiling panel (shown in Figure 5-6) which had been temporally removed for these tests. The flowrate through each blower was obtained by measuring the pressure drop across a laminar flow element which was in series with the fan and pressure difference measurements were taken with calibrated diaphragm transducers (Validyne).

Because ceiling leakage is very important in calculations to find the flow of air and moisture into the attic, it was measured separately from the rest of the attic leakage. To determine the background leakage area of the exterior portion of the attic envelope (not including the ceiling) the attic was pressurized relative to the outdoors and the fan connected to the interior of the house was adjusted until the

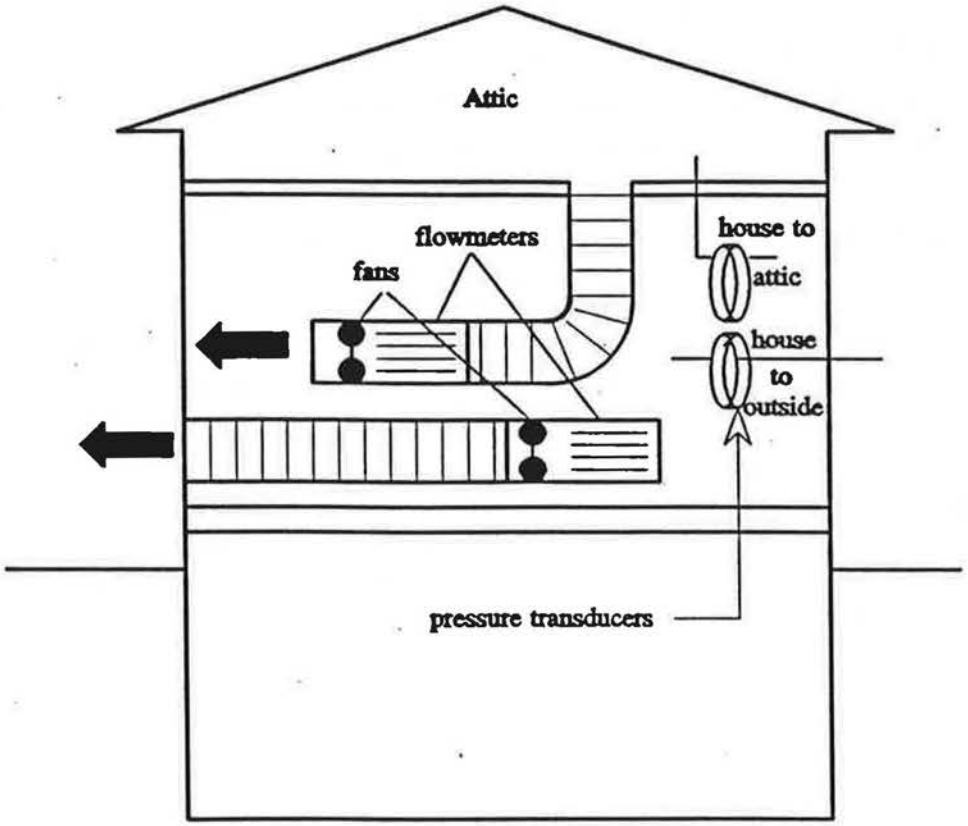

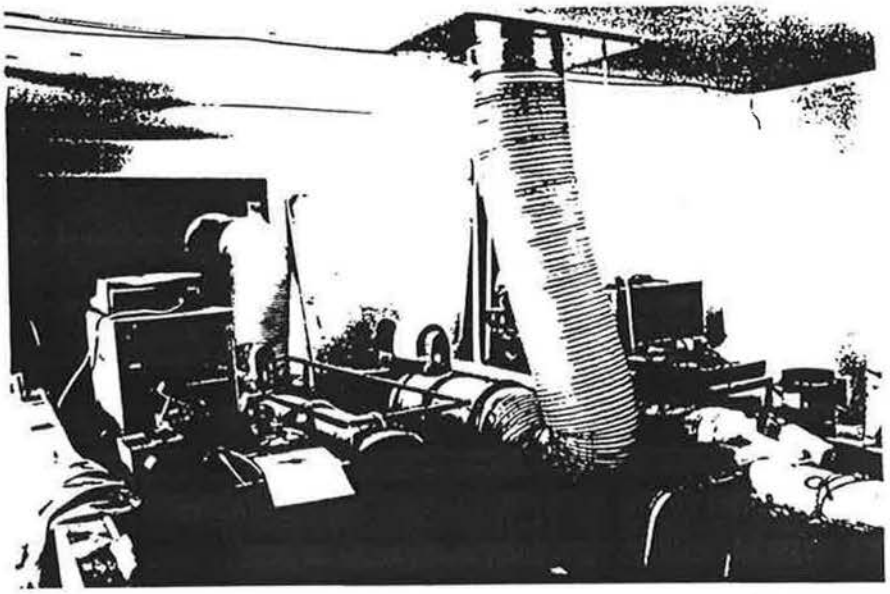

Figure 5-7. Blower Apparatus for Attic Leakage Testing.

attic-indoor pressure difference was zero. Making the pressure difference across the ceiling zero means that there will be no flow through the ceiling, in which case the measured flowrate will not include the ceiling leakage. This procedure required careful manipulation to maintain zero pressure difference across the ceiling because of fluctuations in ceiling pressure difference even at low wind speeds. The measurements were repeated at several attic to outdoor pressure differences to obtain a complete flow-pressure difference characteristic.

The results of these tests are shown in Figures 5-8A and 5-8B for attic 5 and 6 respectively. For these tests, the two roof vents on attic 6 were sealed so that only the background leakage area was being measured. In order to reduce the scatter in these data caused by wind pressure fluctuations, all fan pressurization tests were carried out only when the wind speed was less than 1 m/sec. The figures show the individual data points as well as a linear least squares fit to the data. The linearity of the data indicates that the flow characteristic follows a power law where

$$Q = C\Delta P^{n} \tag{5-1}$$

where Q is the flowrate [m^3/s], ΔP is the pressure difference across the attic envelope [Pa], C is the flow coefficient [$m^3 s Pa^n$] and n is the flow exponent. Building leakage is often expressed in terms of equivalent leakage area. Equivalent leakage area is the area of an orifice that would have the same flowrate as that given by Equation 5-1 at a given pressure difference. By equating 5-1 to an orifice flow relationship, Equation 5-2 may be found. Equation 5-2 is the same as Equation 3-48, but with the four pascal reference pressure substituted, and is used to convert C and n to equivalent leakage area, A_{L4}.

$$A_{L4} = C\sqrt{\frac{\rho}{2}}4^{(n-1/2)} \tag{5-2}$$

where ρ is the air density. The reference pressure of four pascals is chosen because it is the standard pressure used by ASHRAE (1989) (Chapter 23, p.14) in calculating equivalent leakage areas of building components.

The pressure difference range for attic 6 was 3 to 7 Pa whereas, attic 5 was tested from 7 to 30 Pa. These pressure ranges were dictated by the maximum flow capacity of the attic fan (approximately 0.7 m^3/s) and the leakage area of the attic. Because the leakage area of attic 6 was substantially larger than attic 5 (mainly due

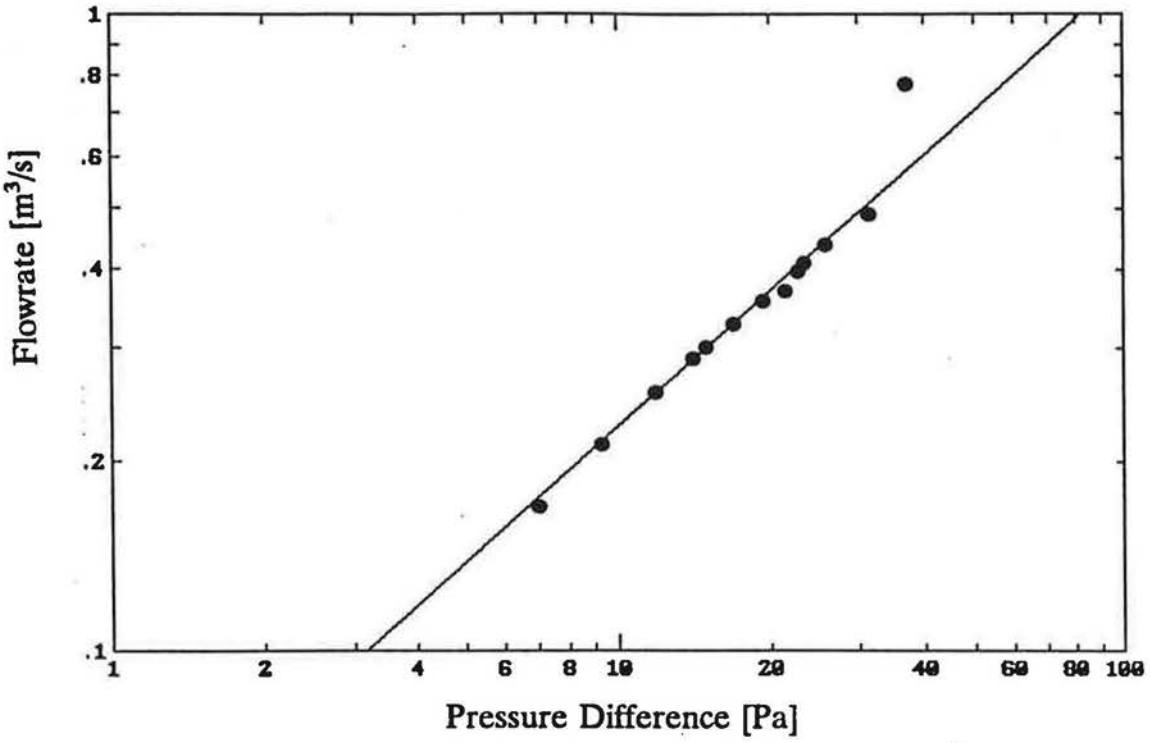

Figure 5-8A. Fan pressurization test results for attic 5.

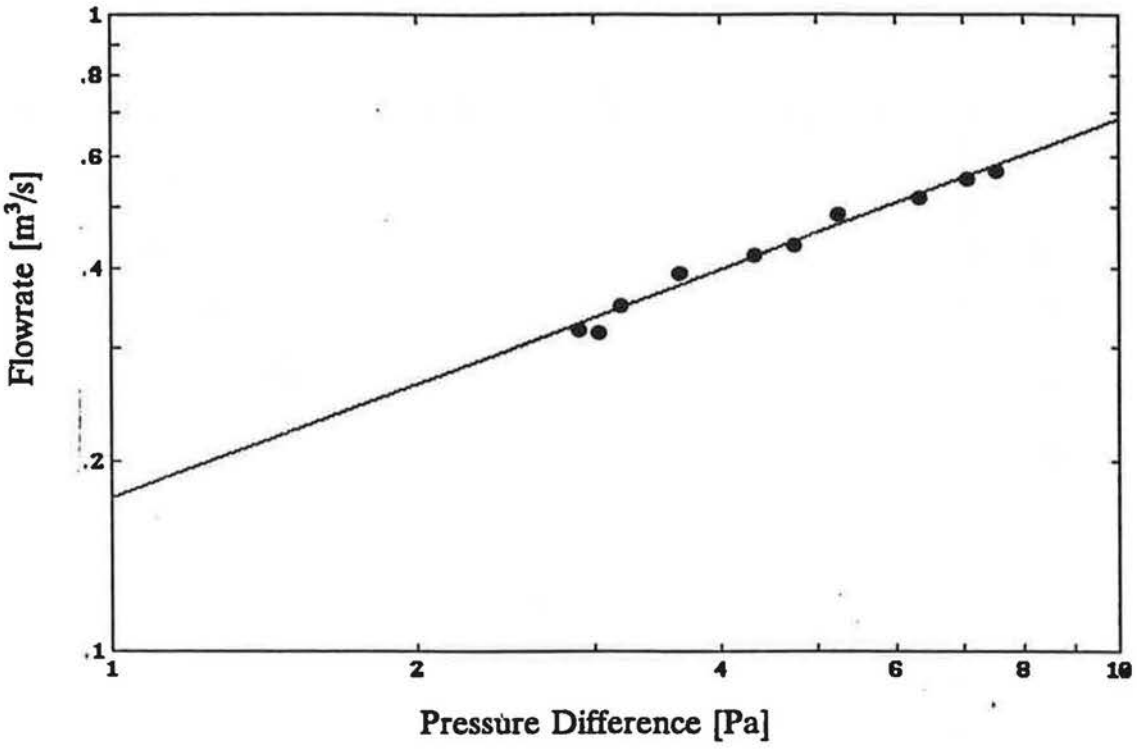

Figure 5-8B. Fan pressurization test results for attic 6.

to the soffits), the maximum pressure difference that could be reached in attic 6 was much less than in attic 5. The values of C and n found by fitting to the data (shown in Figures 5-8A and 5-8B) for the exterior portion of each attic envelope is given in Table 5-2 together with the equivalent leakage area based on a pressure difference of 4 Pa.

Table 5-2. Leakage Characteristics of Attic, House and Ceiling in Houses 5 and 6

House Zone	Flow Coefficient $m^3/sec.(Pa)^n$	Flow Exponent n	Leakage Area @ 4 Pa cm^2
Attic 5 - exterior envelope	4.416×10^{-2}	0.707	456
House 5 - ceiling uncovered	9.842×10^{-3}	0.583	85
House 5 - ceiling covered	8.446×10^{-3}	0.580	73
Attic 6 - exterior envelope	1.740×10^{-1}	0.597	1542
House 6 - ceiling uncovered	6.903×10^{-3}	0.737	74
House 6 - ceiling covered	5.730×10^{-3}	0.766	64

The results show the large difference in leakage areas of the two attics due to the extra soffit leakage in attic 6. Attic 6 has approximately four times the leakage area of attic 5. The differences in flow exponent, n, are due to the different leaks in each attic. The leakage in attic 5 is dominated by small cracks that arise from the construction of the attic envelope and flow through these cracks is probably developing flow because the cracks are short compared with their width. The value of n = 0.707 is close to values measured for the envelopes of houses. Attic 6, on the other hand, includes soffit and roof vents which behave as orifice flow (with n close to one half). The measured value of n = 0.597 for attic 6 supports this observation.

The ceiling leakage area was not included in the above set of measurements since the attic-indoor pressure difference was maintained at zero by the indoor fan. The simplest method of measuring the ceiling leakage characteristics, was to carry out a pressurization test on the interior of the house with the ceiling exposed and repeating the test with the ceiling leakage covered. For both houses 5 and 6 almost

all the ceiling leakage was concentrated in the intentional openings in the ceiling panel and the unintentional openings around the light fixtures, which made covering the ceiling leakage easy to do. In a more conventional house, there would tend to be other leakage paths (such as plumbing stacks and gaps between the flue pipe and the duct leading up to the attic) that are inaccessible and would make this method impractical. The ceiling leakage would then have to be estimated as a fraction of the total house leakage.

Fan pressurization tests on the houses were performed by an automated system that also only carried out the tests when wind speeds were below 1 m/s. A polyethylene sheet was placed over the central portion of the ceiling to seal the ceiling leakage. The sheet covered the ceiling panel and the two light fixtures and was sealed by taping along its edge. Pressurization tests were then performed over a range of pressures from 1 to 100 Pa. Depressurization tests were not performed because the plastic sheet would be blown off the ceiling even when small pressure differences are applied. The fan pressurization test system and measurement methods are described in detail by Modera and Wilson (1989). The most important features of the fan pressurization test system are as follows:

- The tests cover a large range of pressure differences from 1 to 100Pa. This more than covers the range required by ASTM (1982) and CGSB (1986) standards. Testing at windspeeds below 1m/s allows extension of the low pressure range down to 1 Pa, which is much lower than either of the above standards.
- Pressures across the envelope due to wind and stack effects are corrected by taking a reference pressure at zero flow rate for every data point. This reference pressure is the pressure measured across the envelope with the fan off and a closed damper sealing the fan duct system.
- Outdoor pressures are spatially averaged by having a pressure tap outside each of the four walls of the building.

Figures 5-9A and 5-10A show the test results with the ceiling leaks uncovered for houses 5 and 6 respectively. Figures 5-9B and 5-10B show the results of the tests with the ceiling covered for houses 5 and 6. From a least squares fit to the data (solid lines in these figures), values of C and n were obtained. From these the leakage area, A_{L4}, was calculated using Equation 5-2. The fan pressurization test results for the houses are given in Table 5-2. The fraction of leakage in the ceiling can be estimated from the difference between the house pressurization tests with the

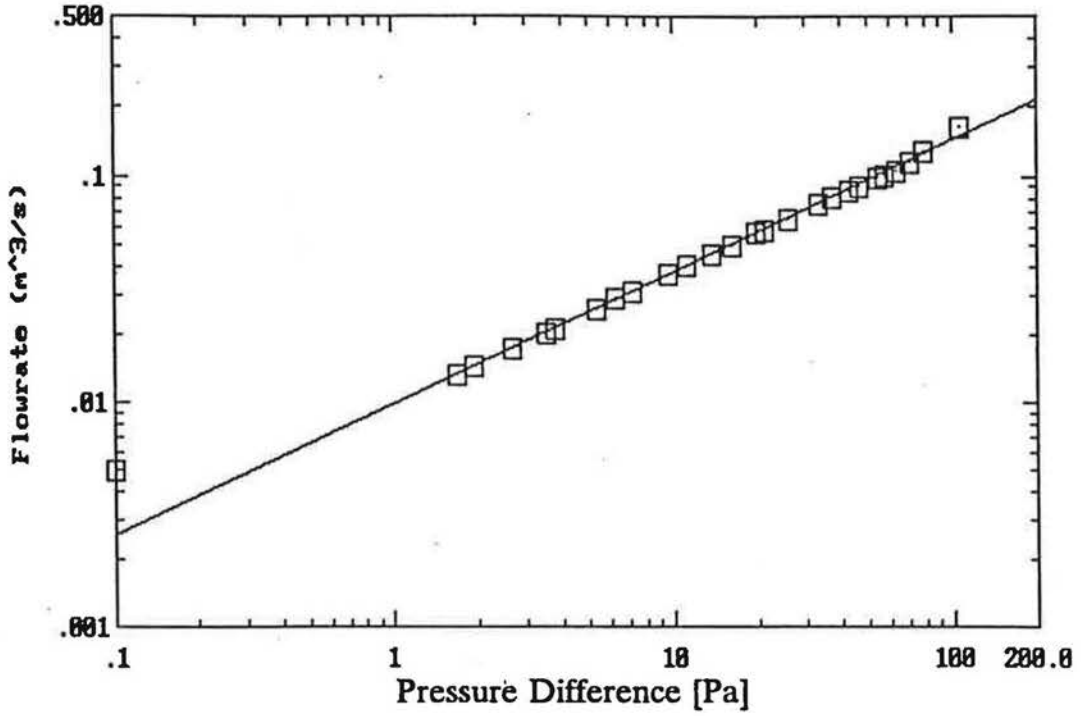

Figure 5-9A. Fan pressurization test results for house 5 with ceiling leaks uncovered.

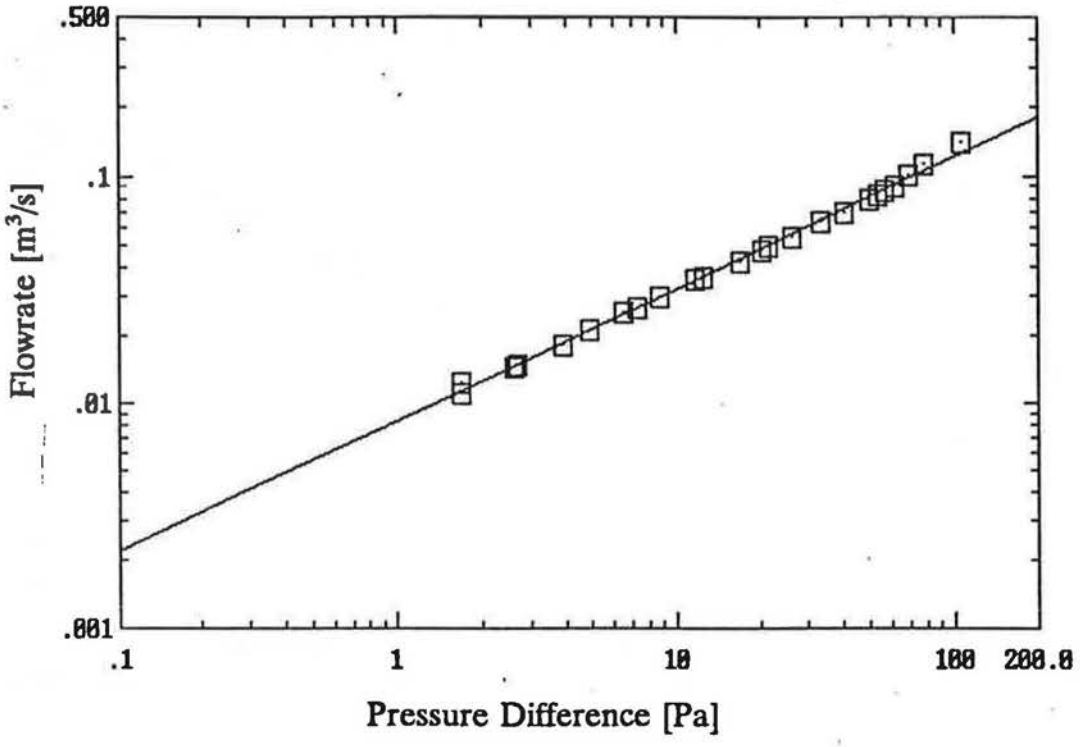

Figure 5-9B. Fan pressurization test results for house 5 with ceiling leaks sealed.

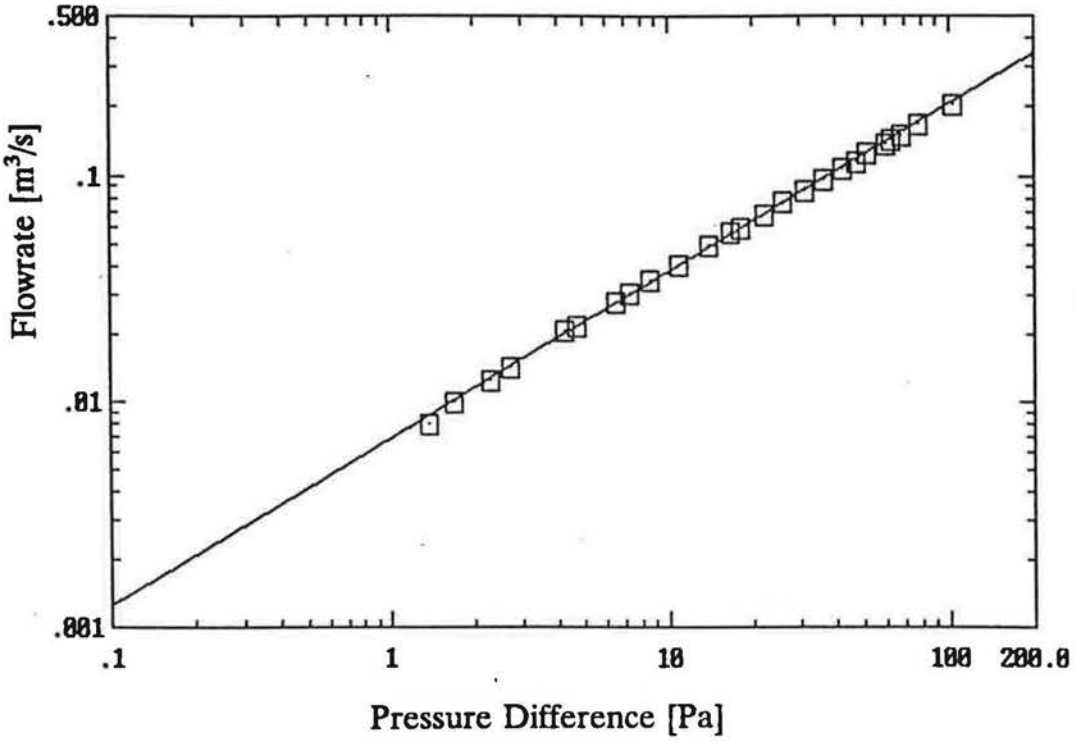

Figure 5-10A.Fan pressurization test results for house 6 with ceiling leaks uncovered.

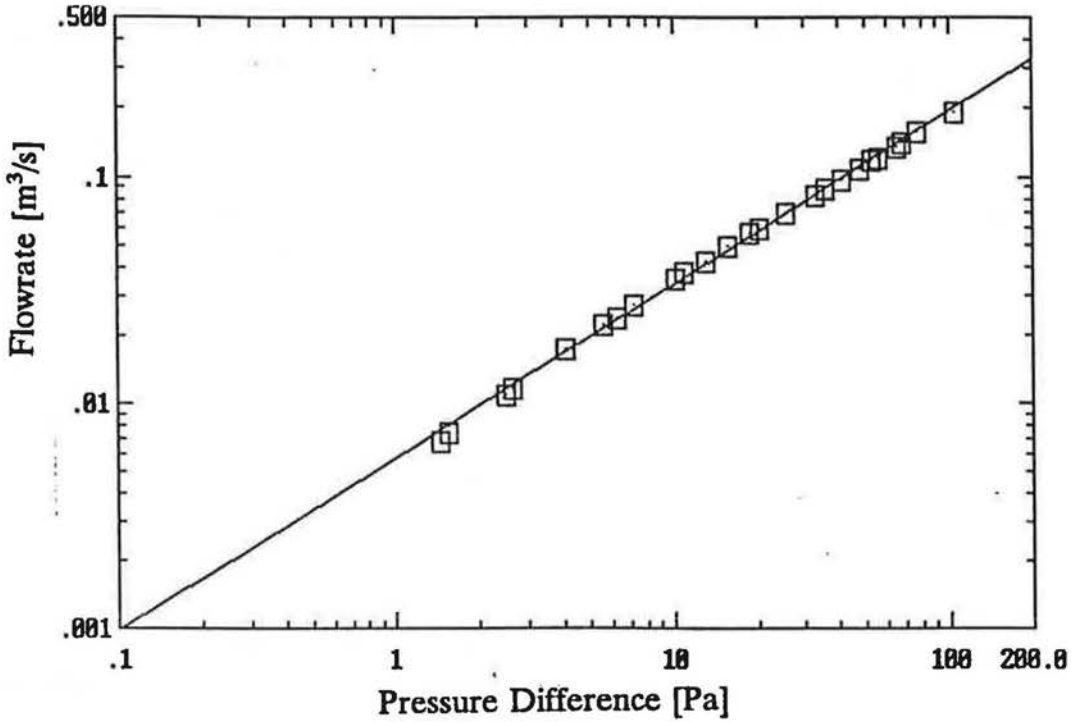

Figure 5-10A.Fan pressurization test results for House 6 with ceiling leaks uncovered.

ceiling covered and uncovered. The ceiling leakage areas (at 4 Pa) for house 5 and 6 were estimated to be 12 and 10 cm^2, respectively. These leakage areas can be compared with the area of the 7.6 diameter orifice flowmeter in the ceiling panel, which is 26.5 cm^2. This area together with the additional leakage of the light fixtures corresponds to a considerably larger gross area than the measured values. The discrepancy is due to the additional flow resistance of the 89 mm thick glass fibre batt ceiling insulation above these leaks resulting in smaller effective ceiling leakage areas. These results show that actual leakage areas are quite different from visible leakage areas and fan pressurization tests are required to accurately measure these areas.

5.2.2 Ventilation Rate Measurements

The ventilation rates of attics 5 and 6 were measured using a tracer gas injection system that measured the amount of tracer gas required to maintain a constant concentration within the attic space. The data acquisition system measured tracer gas concentrations with an infra-red gas analyzer (Wilkes MIRAN 1A) that had the capability of measuring concentration of different tracer gases by adjusting the wavelength of the infra-red radiation. This capability was necessary because two different tracer gases were used to separately measure the indoor ventilation rates (using sulphur hexaflouride SF_6) and the attic ventilation rates (using a refrigerant gas, R22). The house ventilation rates were monitored by a separate system that has been operating for the past ten years at AHHRF. In the houses computer controlled gas injections maintain the gas concentration inside the house at a nominal value of 5 ppm. Ventilation rates were calculated from the amount of gas injected into the interior space. Details of the house ventilation measurement system can be found in Wilson and Walker (1991a).

Attic ventilation rates were monitored separately from the indoor ventilation rates using R22 as the tracer gas for the attic. The R22 concentration in the attic was maintained at a nominal concentration of 5 ppm. Both attics used two small fans to mix the attic air and the tracer gas. these fans are shown in Figure 5-11. The fans provided a combined flow of approximately 10 attic air changes per hour. The mixing of the attic air is important because, as will be shown later, high attic ventilation rates above 20 ACH lead to incomplete mixing of the tracer gas that results in overprediction of attic ventilation rates. A four point sampling system and manifold was used to draw equal volumes of air from distributed locations in the attic in order to obtain a more representative average sample of the tracer gas concentration. All

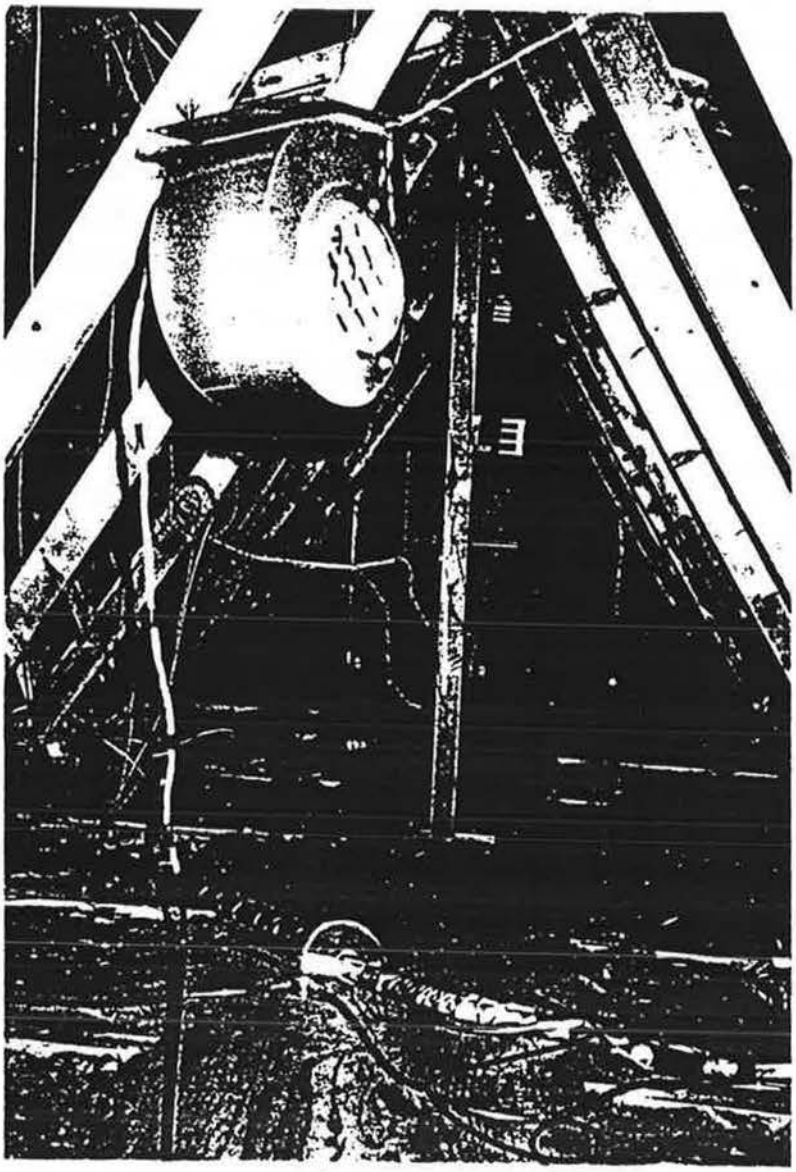

Figure 5-11. Attic interior showing mixing fans.

air samples were drawn through a heated water bath to remove the effects of the sensitivity of the gas analyzer to temperature fluctuations. The gas analyzer was used to measure the concentrations of both R22 and SF_6 in air samples drawn from both attics and both houses. By measuring concentrations of both tracer gasses, attic ventilation rates and indoor-attic exchange rates were measured. The gas analyzer was calibrated by filling it with prepared mixtures of R22 and air and SF_6 and air of varying concentrations in from 0 to 5 ppm. This calibration procedure has been repeated four times over the course of the past two heating seasons.

Tracer gas to maintain the 5 ppm nominal concentration in each attic was injected from a bottle of pure R22. Each injection was provided by pulsing a pair of closely spaced solenoid valves in series to produce puffs of tracer gas. The injector volumes, V_{inj}, for attic 5 and 6 were 5.0 and 7.4 ml of R22 gas (at room temperature and pressure) respectively. These injector volumes were calibrated by counting the number of pulses required to produce 1 litre of gas which was measured by bubbling the gas through water and collecting the gas in an inverted graduated cylinder. These injector volumes are converted to volumes at attic temperature by using the ideal gas law. The volume at attic temperature is used when calculating the attic ventilation rates (as will be shown later in Equation 5-3).

The attic system took 12 to 13 samples from each of the two attics and houses per hour. At the end of each hour, all measurements were averaged and stored by the data acquisition system. At midnight, the first 5 minutes of the hour was used to take a sample of outdoor air to provide a continuous check on the gas analyzer drift. This sample was used to monitor the drift in instrument zeros and on the presence of background contaminants (such as ammonia from fertilizers that are applied in the surrounding area during certain times of the year) that occasionally produce a false tracer gas reading.

The attic ventilation rate is calculated assuming that the tracer gas and attic air are well mixed and using the hourly mean attic and indoor temperatures. The mean attic ventilation rate for each hour is given by

$$Q_a = \frac{N\, V_{inj}}{\Omega^a_{R22}\, 3600} \frac{T_a}{T_{in}} \qquad (5\text{-}3)$$

where Q_a is the attic ventilation rate [m^3/s], N is the number of tracer gas injections during the hour [$hour^{-1}$], V_{inj} is the injector volume [m^3] and Ω^a_{R22} is the average R22 tracer gas concentration over the hour. The factor of 3600 converts the ventilation

rate to be m/s instead of m^3/hour. The ratio of the attic temperature, T_a, to the house temperature, T_{in}, corrects the injector volume from the house, where the injector solenoid pair are located, to the attic where the tracer gas is released. Neglecting the difference between house and attic pressures, which is small compared with atmospheric pressure, Equation 5-4 gives the indoor to attic exchange rate:

$$Q_c = \frac{T_{in}}{T_a} \frac{\Omega^a_{SF6}}{\Omega^{in}_{SF6}} \qquad (5\text{-}4)$$

where Q_c is the flowrate through the ceiling [m^3/s], Ω^a_{SF6}, is the hourly mean attic concentration of SF_6 [ppm] and Ω^{in}_{SF6} is the hourly mean concentration of SF_6 in the house [ppm].

The resolution of the tracer gas measuring system is due to the discrete nature of the injection system, and the resolution of the data acquisition system. For the injection system, the resolution is one injection volume which corresponds to a resolution of 0.017 and 0.025 ACH for attics 5 and 6, respectively, based on an attic volume of 61 m^3 and a nominal concentration of 5 ppm. The resolution of the data acquisition system is limited to 1 bit which corresponds to 1 mV in measuring the gas concentration. Since the voltage output of the gas analyzer at a nominal R22 concentration of 5 ppm is approximately 240 mV, the resolution of the concentration measurement (and hence, ventilation rate) is 0.4%. Thus, for each measurement of the ventilation rate, the combined error is approximately 0.6%. Other sources of error include the hourly resolution of the injection system, the quantity of R22 released per injection and the variation in mean concentration during the hour. An error analysis accounting for these factors was performed by Wilson (unpublished) for the house SF_6 tracer gas system. The same procedure has been followed in this study for the attic tracer gas system. The error analysis for the attic tracer gas ventilation monitoring system is given in detail in appendix B. An example calculation is also given in appendix B that shows that the estimated error is 6% of the measured ventilation rate.

Adequate tracer gas mixing and air sampling introduce other systematic errors. At high ventilation rates above about 20 ACH the fans in the attic can no longer mix the air completely. As shown in the results of the ventilation measurements (section 5.3.1) the samples that are taken contain air that is short circuiting the mixing fans

resulting in an artificially low mean concentration and too high a calculated ventilation rate using Equation 5-3.

5.2.3 Other measurements

Temperatures and wood moisture contents were measured at six locations in each attic. A schematic of the sensor locations is shown in Figure 5-12. Four of these measuring points were placed on the inner surface of the roof sheathing in the middle of the NE, NW, SE, and SW quadrants of the sloped roof. Two sets of thermocouples and moisture pins were placed near the large opening in the ceiling panel. One set was located on the upper end of the horizontal ceiling joist next to the opening, while the second set was placed directly above this location in the roof truss.

5.2.3.1 Wood moisture

At each measurement location a thermocouple was glued to the wood surface and wood moisture content was measured with a pair of stainless steel metal pins imbedded in the wood. The electrical resistance across the pins was measured and moisture contents inferred from the calibration of the resistance readings. The pins measured 6.4 mm in length and 3.2 mm in diameter and were spaced at a distance of 31.8 mm, centre-to-centre. The pins were inserted into pre-drilled holes so that the top of each pin was flush with the surface. The top exposed surface of each pin was sealed by applying a thin coat of epoxy glue. This was done to prevent surface condensation from creating a low resistance path between the pins and produce a false reading. In this way, each pair of pins was recording the moisture content of the underlying layer of wood. The resistances were measured with a wood moisture meter (Lignometer) which had been calibrated on small samples of roof sheathing and joist sections. These samples had been pre-soaked to known moisture contents (determined gravimetrically). In addition to the resistance measurement, the measured temperature at each location was used to correct the wood moisture content reading using the correction factors given by Pfaff and Garrahan (1986).

5.2.3.2 Temperature

Temperatures were measured using type K thermocouples. The thermocouples were epoxied to the wood surface at every wood moisture pin location. In addition the attic air, house interior air and the outside air temperature were monitored. The outside air temperature was measured inside a ventilated box on the north wall of house 6.

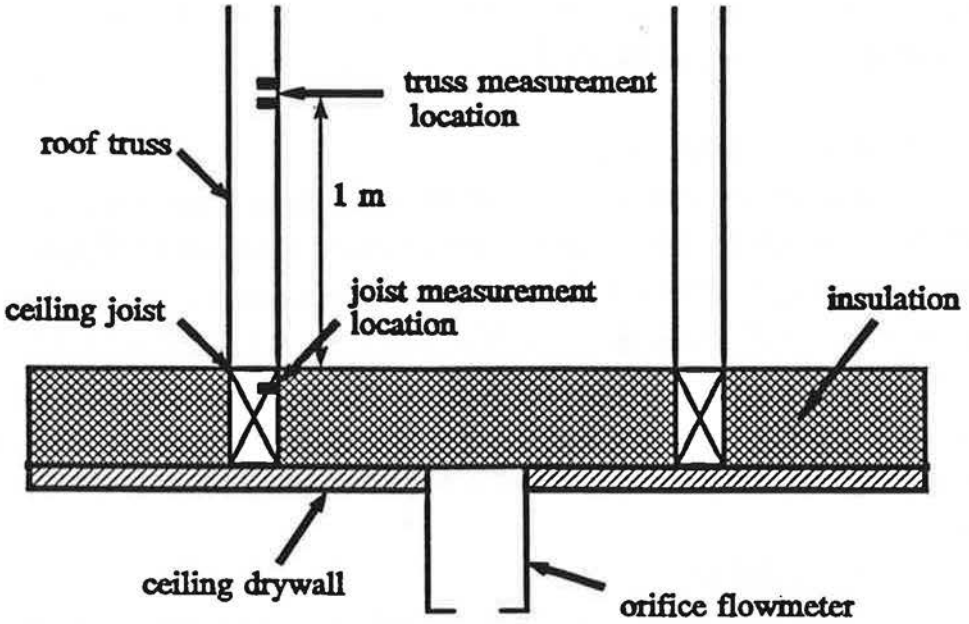

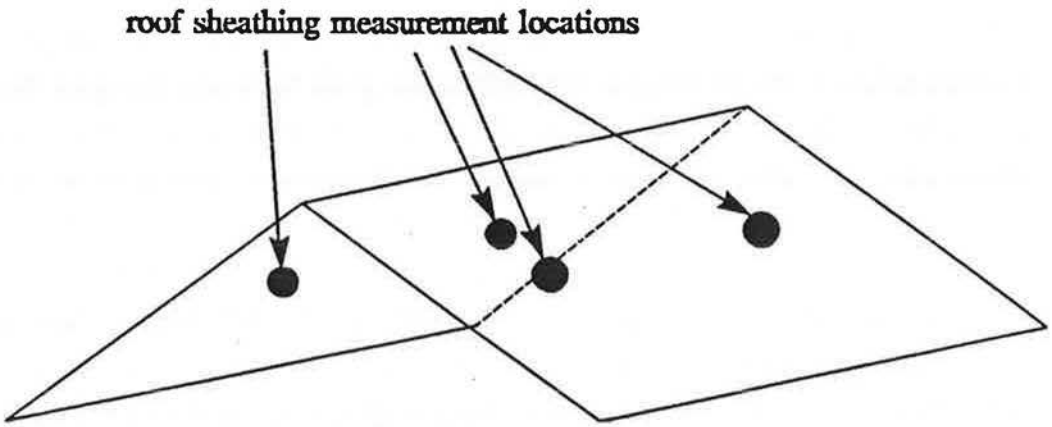

Figure 5-12. Schematic of the attic space showing locations of moisture pins.

5.2.3.3 Relative humidity

A polymer film capacitance sensor (General Eastern) was used to measure the relative humidity. Air vapour pressures were calculated based on these relative humidity measurements and the saturation pressure based on the air temperature. The relative humidity sensors were calibrated over three different saturated salt solutions which spanned a relative humidity range from 12% to 98%. The relative humidity of the air in both attics and houses was measured in addition to the outside air.

5.2.3.4 Wind speed and direction

The sensors for wind speed and direction were placed on top of a 10 m tall tower located midway along the row of houses and approximately 30 m north of the houses. Wind speed was measured with a low-friction cup anemometer which had been calibrated in a low speed wind tunnel while wind direction was measured with a rotating vane (Windflow 540 - Athabasca Research Corp.). The data acquisition system recorded the average wind speed and east and north vector components for each hour. These east and north vector components were used to calculate the true average wind direction.

5.2.3.5 Solar radiation

Incoming solar radiation on the north and south facing sections of the roof was measured with two pyranometers (Kipp and Zonen), one on each of the sloped roof sections of attic 6. One was placed on the north and the other on the south section of the pitched roof surface. The two pyranometers are oriented parallel to the roof slope so that the measured values can be entered directly to the heat transfer model without geometric conversion.

5.3 Results

Prior to presentation of a comparison of measured results and predictions (this will be done in Chapter 6), some initial results of attic ventilation rates and indoor-attic exchange rates are presented in this section in order to identify certain trends in the data.

Data binning procedure

In several of the figures presented in this chapter and the following chapter on model verification the measured and predicted data is binned so that trends may be revealed in the data that is otherwise obscured by scatter. In all cases the binning procedure is the same. For each bin the mean and standard deviation are calculated.

In the figures the measured data is represented by a square for the mean value and error bars representing ± one standard deviation. The predicted values are shown by a line connecting the mean values of each bin. The variables on both the horizontal and vertical axes are averaged so that sometimes the points representing the mean values will not appear in the centre of the bin.

5.3.1 Ventilation Rates

Attic ventilation rates were found to be dominated by wind speed, increasing as wind speed increased. Ventilation rates in attic 5 varied between 0 ACH up to approximately 7 ACH at average wind speeds of 9 m/sec, while ventilation rates in attic 6 varied from 0 ACH up to 50 ACH. With inferred ventilation rates approaching 50 ACH there may not be sufficient mixing of R22 tracer gas in the attic by the two attic fans to yield accurate values of ventilation rate. In order to investigate this effect, ventilation rates in attic 6 were plotted on a log-log scale. When the data are plotted in this way, a straight line should result i.e. there is a power law-type dependence of ventilation rate on wind speed. A power law exponent of 2n is expected because the wind driven pressure difference is proportional to wind speed squared and the flowrate is proportional to pressure difference to the power n. This assumes that leakage paths are not changed by valving action due to increased pressure differences and flowrates. If valving action increased or decreased the flow area with increasing pressure difference then the power law dependence of ventilation rate on windspeed would be obscured. In addition, a single wind direction must be chosen to reduce the effects of shelter that change wind pressures at the same wind speed. Results for attic 6 with southeast winds only (in the range of 120° to 150°) are shown in Figure 5-13 where the measured data has been binned every 1m/s and the mean value plotted with the error bars showing one standard deviation within the bin. The dashed line in Figure 5-13 simply connects the average values of ventilation rate in ascending order to compare with a straight line. The results for attic 6 generally follow a power law that is linear in this figure up to an average wind speed of approximately 6 m/sec where the mean ventilation rate is about 20 ACH. Beyond this wind speed, there is a significant deviation in ventilation rates from the power-law relation.

If the problem is one of incomplete mixing of tracer gas in the attic then more gas would be injected than is necessary to maintain a constant concentration of 5 ppm. This would yield higher inferred ventilation rates than the true values. Since

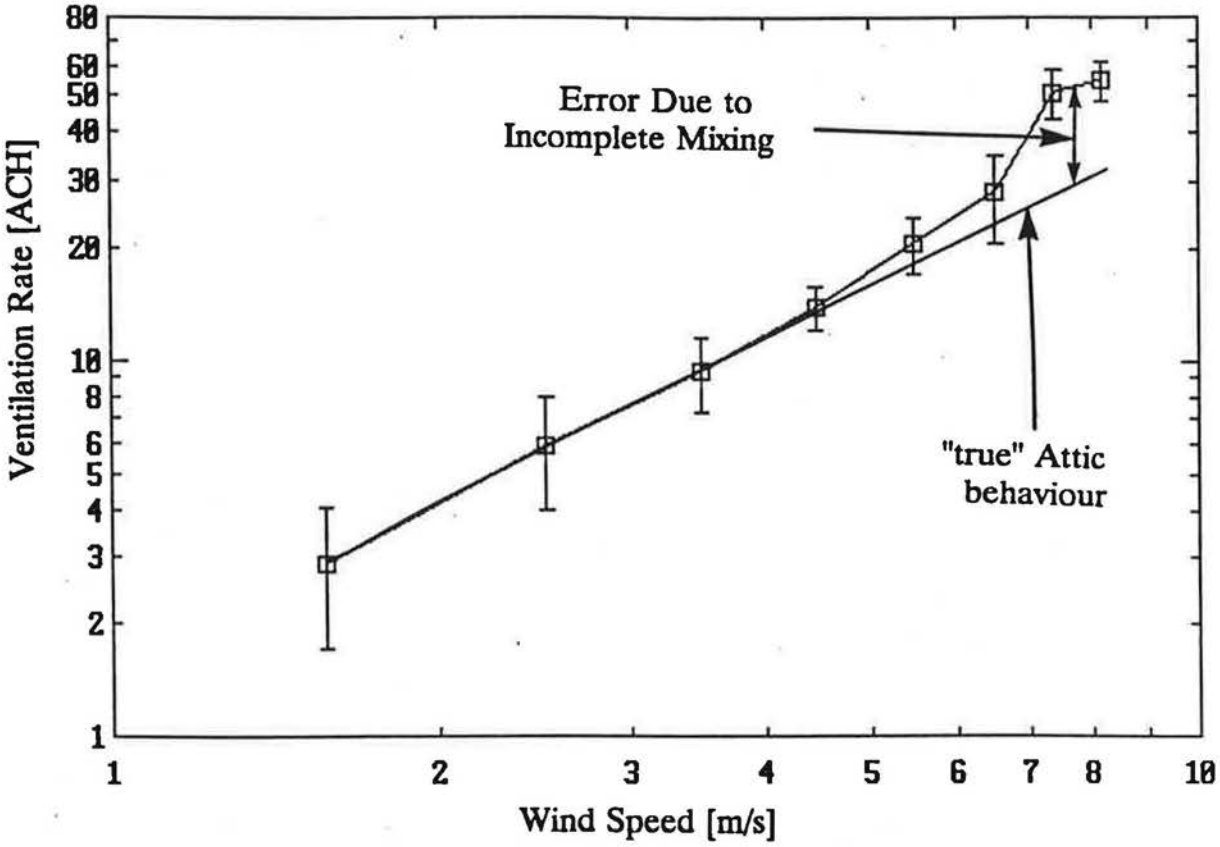

Figure 5-13. Measured ventilation rates in attic 6 as a function of windspeed for south-east winds between 120° and 150° (with 0° being north).

this is what is observed in the data and the attic leaks are not of type that would experience a valving action, the conclusion is that this must be the limit for accurately measuring ventilation rates in the attics with the current measurement technique. One possible method of increasing this limit would have been to increase the flow rate of the mixing fans in the attic. Larger fans may have created pressures on the attic interior surfaces which would affect the ventilation rate. It was decided not to alter the measurement technique but invoke a simple criterion to stop ventilation rate measurements if the wind speed was greater than 6 m/s. This corresponds to a maximum ventilation rate in attic 6 of about 20 ACH. The same criterion of a 20 ACH maximum was applied to attic 5.

The ventilation of an attic is driven by a combination of wind-induced pressures on the attic envelope and the attic stack effect that depends on the attic-outdoor temperature difference. Figures 5-14A and 5-14B show the ventilation rates in attic 5 and 6 as a function of wind speed. These figures have a large range of ventilation rates for any given wind speed because they include wind from all directions and all attic-outdoor temperature differences. For all wind speeds, the ventilation rates in attic 5 are much less than in attic 6 and reflect the difference in leakage areas. Attic 5 has approximately one quarter the leakage area of attic 6 as shown in Table 5-2. Both sets of data show a general increase in ventilation rate with wind speed although there is considerable scatter in these data. A large part of this scatter is due to the variation in wind direction which alters both the shelter and pressure coefficients on the attic envelope. Both attics are essentially unsheltered for winds from the north or south and would therefore have relatively large ventilation rates when the wind is from these directions. Strong shelter occurs for east and west winds producing lower ventilation rates. An example of this is shown in Figures 5-15A and 5-15B where attic 5 ventilation rates are shown as a function of wind speed for south and west winds, respectively. Each data set only includes wind directions $\pm 22.5°$ about the nominal direction. For west winds, the ventilation rates are about a factor of three less than for south winds showing that attic 5 is sheltered by the other houses in the east-west row.

The dependence of attic ventilation on stack effect is shown in Figures 5-16A and 5-16B for attics 5 and 6 respectively where attic ventilation rates are plotted versus the attic-outdoor temperature difference. In these two figures each point represents an hour of measured data. To show the trend in these figures more clearly the data has been binned every 5°C of attic-outdoor temperature difference. The

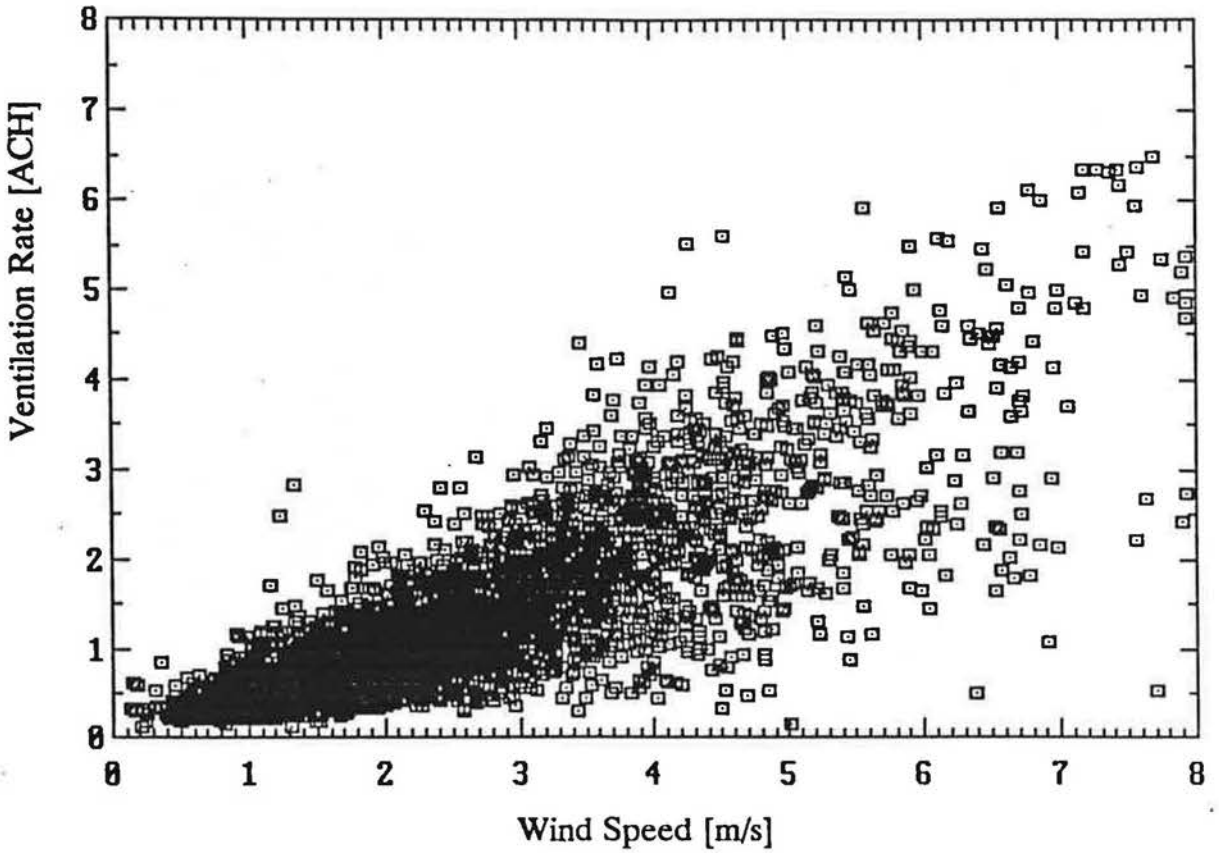

Figure 5-14A. Measured ventilation rates in attic 5 for all windspeeds and temperature differences (3758 data points).

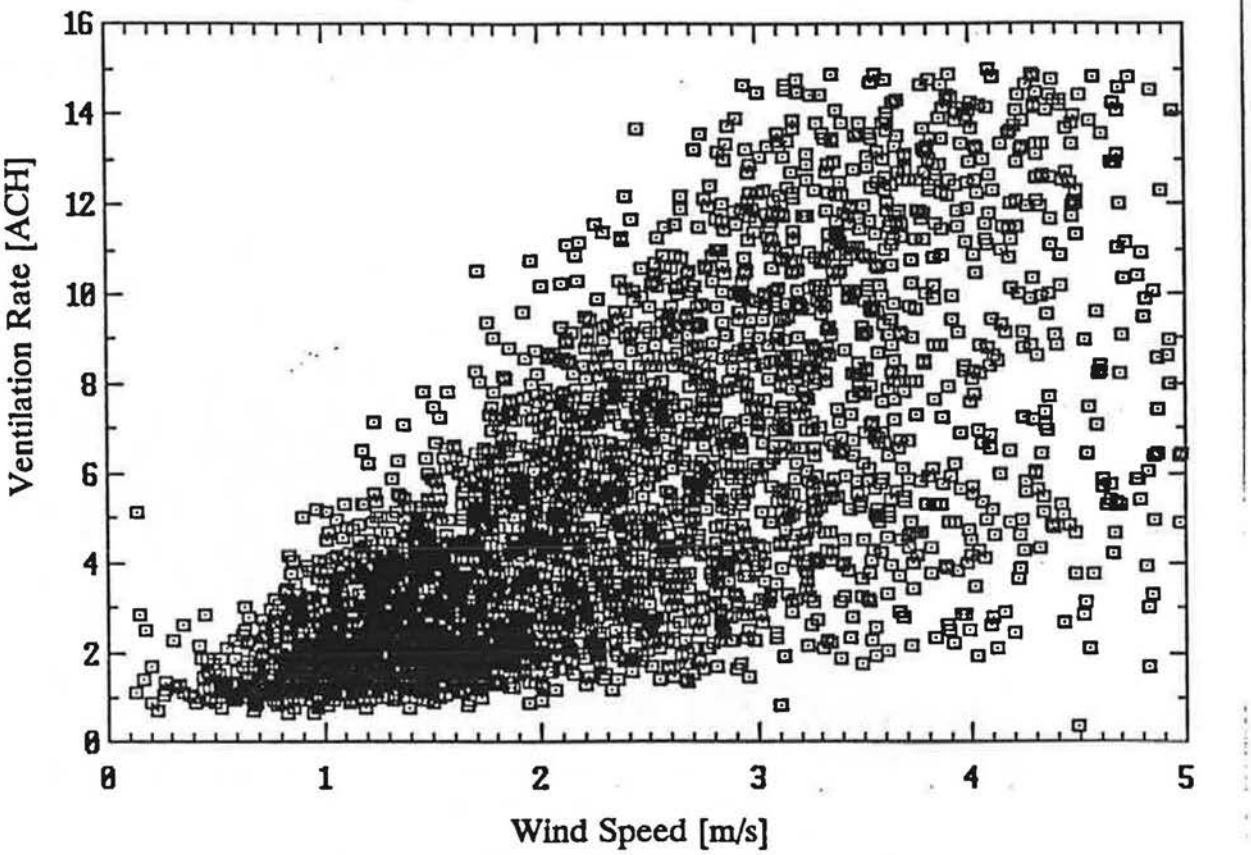

Figure 5-14B. Measured ventilation rates in attic 6 for windspeeds up to 5 m/s and all temperature differences (3522 data points).

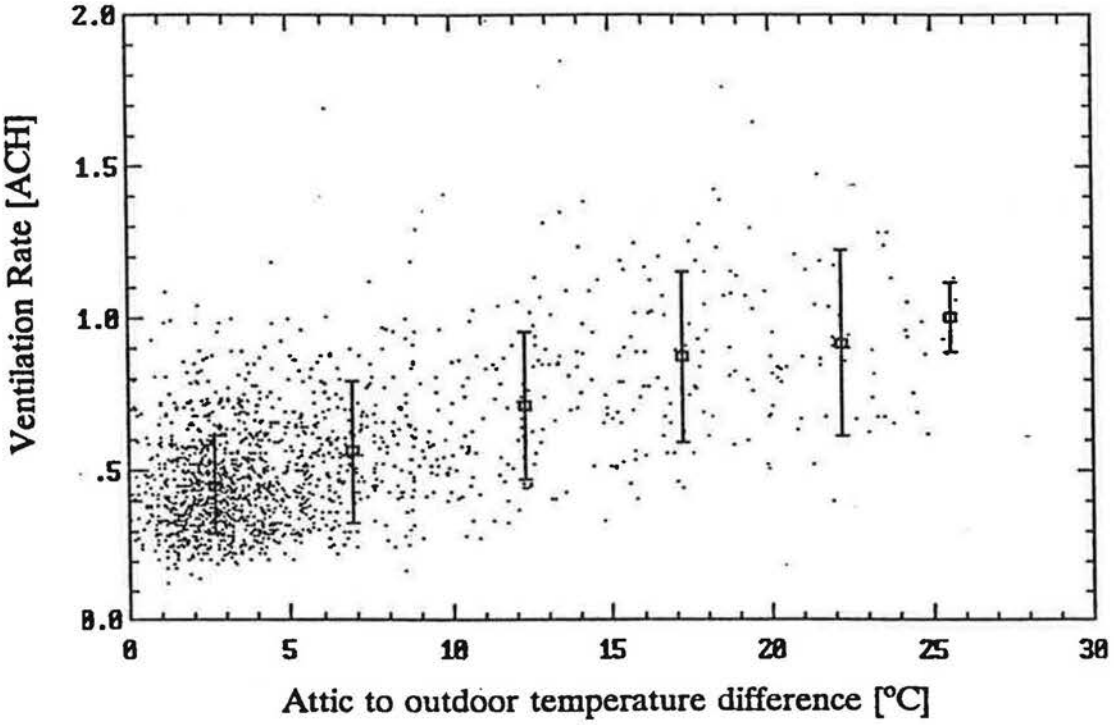

Figure 5-16A. Temperature dependence of measured ventilation rates in attic 5 for windspeeds less than 2m/s (1573 points).

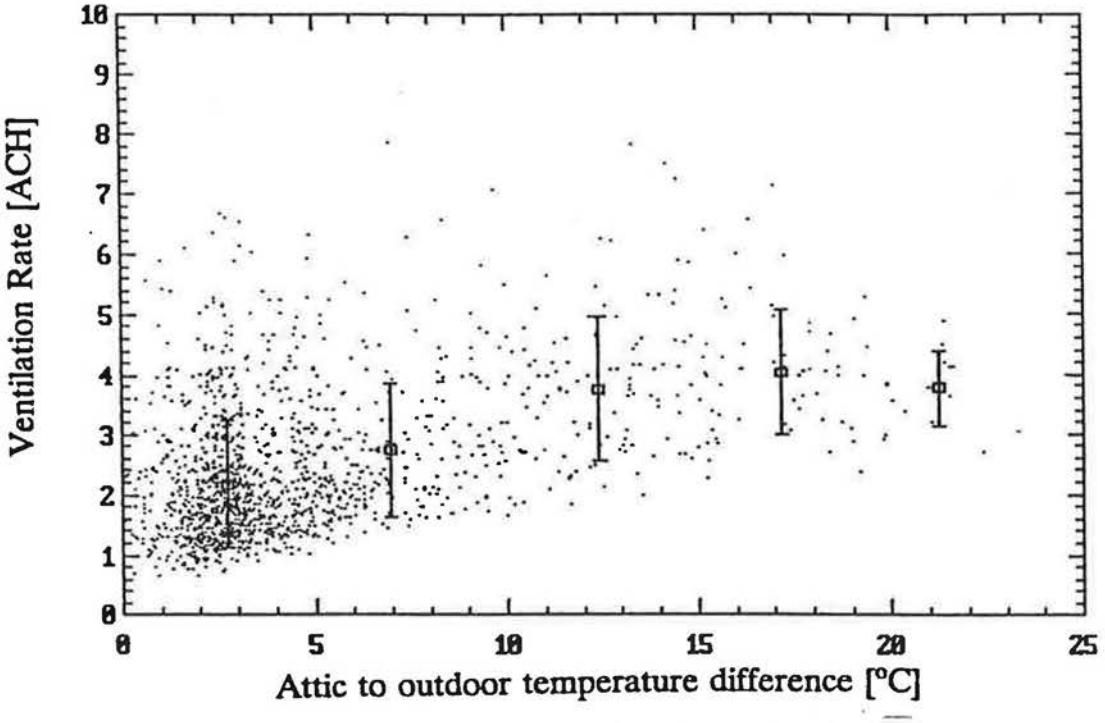

Figure 5-16B. Temperature dependence of measured ventilation rates in attic 6 for windspeeds less than 2m/s (1444 points).

mean is shown by the squares and the error bars represent the standard deviation in each bin. These data have been selected from the time period between December 1, 1990 and October 31, 1991 and include only those hourly-averaged ventilation rates when the wind speed was below 2 m/sec. Although the data show considerable scatter, there is a weak dependence of ventilation rate on attic-outdoor temperature difference with stack effect driven ventilation rates reaching approximately 1 ACH in attic 5 and 4 ACH in attic 6. Comparing Figure 5-14 to 5-16 for both attics indicates that stack effect driven ventilation is much less than ventilation generated by wind-induced pressure on the attic envelope.

One of the observations from the data presented in Figure 5-14 is that to see the expected increase in ventilation rate with increasing wind speed, a large number of measurements need to be taken. Figure 5-14A for attic 5 contains 3758 hourly averaged data points and Figure 5-15A contains 3522 data points. Data sets that contain a limited number of measurements could display any type of variation with wind speed, increasing, decreasing, or constant. To uncover true trends in the data a large number of measurements are therefore required. For this study over 5000 hours of attic ventilation data have been accumulated. With a large data set it becomes possible to sort for low windspeeds in order to examine the stack driven ventilation for the attic shown in Figure 5-16.

The effect of wind direction on ventilation rates was partially illustrated in Figure 5-15 for attic 5, where data was selected for sheltered and unsheltered wind directions. To better observe the effect of wind direction on ventilation rates, the data has been plotted as a function of wind angle (0° being north and positive angles measured in a clockwise sense). The measured results for attics 5 and 6 are presented in Figures 5-17 and 5-18, respectively. In each figure the upper plots show individual data points, while the lower plot shows the average and standard deviation of the measurements when data was sorted into 22.5° wind angle bins. This helps to accentuate the dependence of ventilation rates on wind direction and remove some of the scatter that can make the data difficult to interpret. To further reduce the considerable scatter that is evident in the figures, the data is normalized to factor out the variation of ventilation rate with wind speed for a given direction.

The range of ventilation rates at a given wind direction is mostly caused by the range of wind speeds. To remove the wind speed dependence each ventilation rate measurement is divided by windspeed to the power 2n because (as discussed earlier) ventilation rate is proportional to wind speed to the power 2n. This is done for each

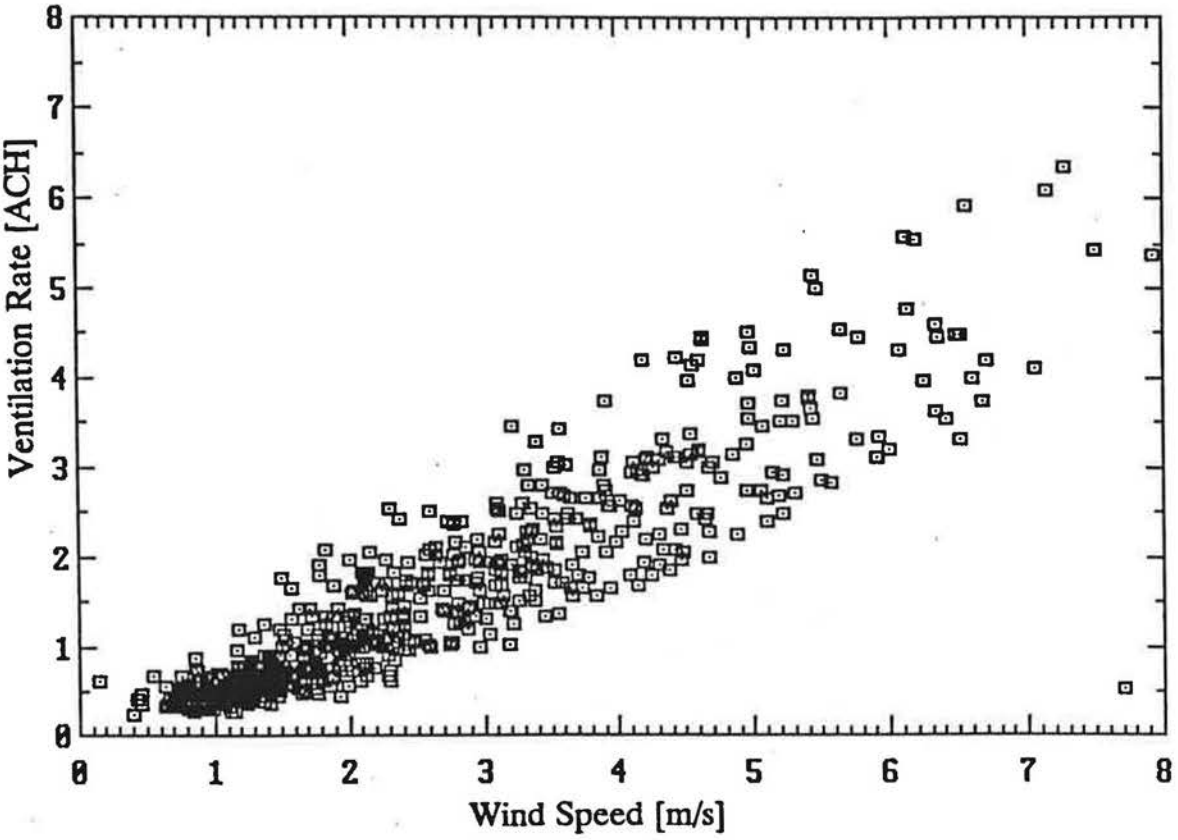

Figure 5-15A. Measured ventilation rates in attic 5 for south winds only (unsheltered) (641 data points).

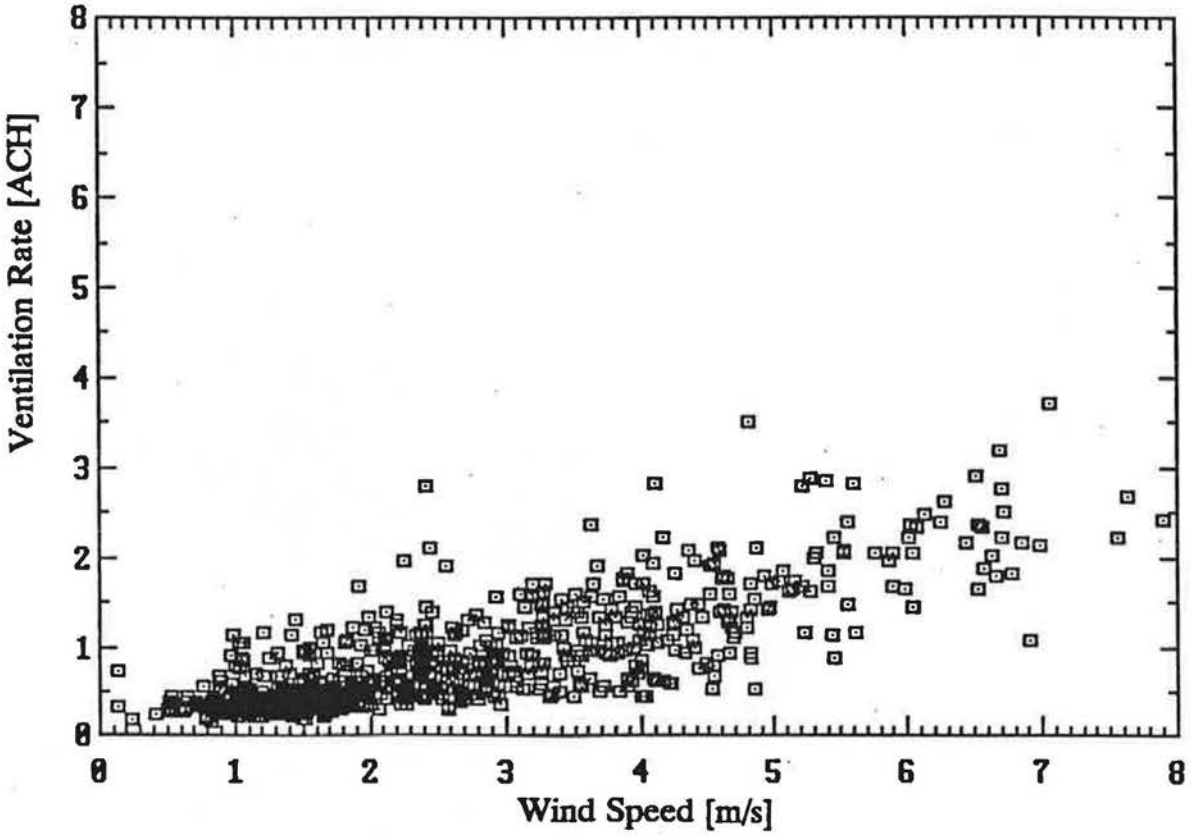

Figure 5-15B. Measured ventilation rates in attic 5 for west winds only (sheltered) (784 data points).

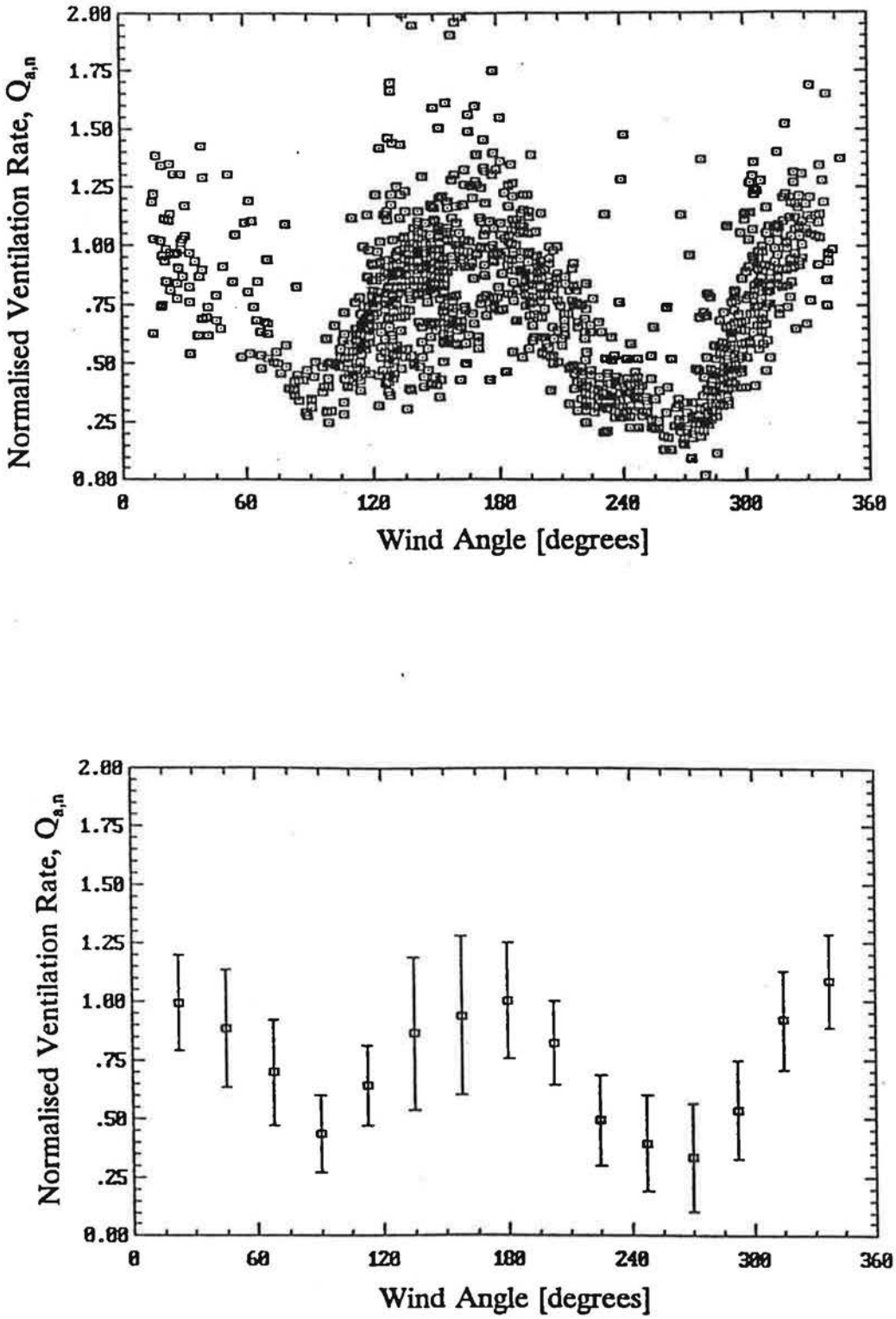

Figure 5-17. Effect of wind direction (wind shelter and pressure coefficients) on ventilation rate for attic 5 (1302 points).

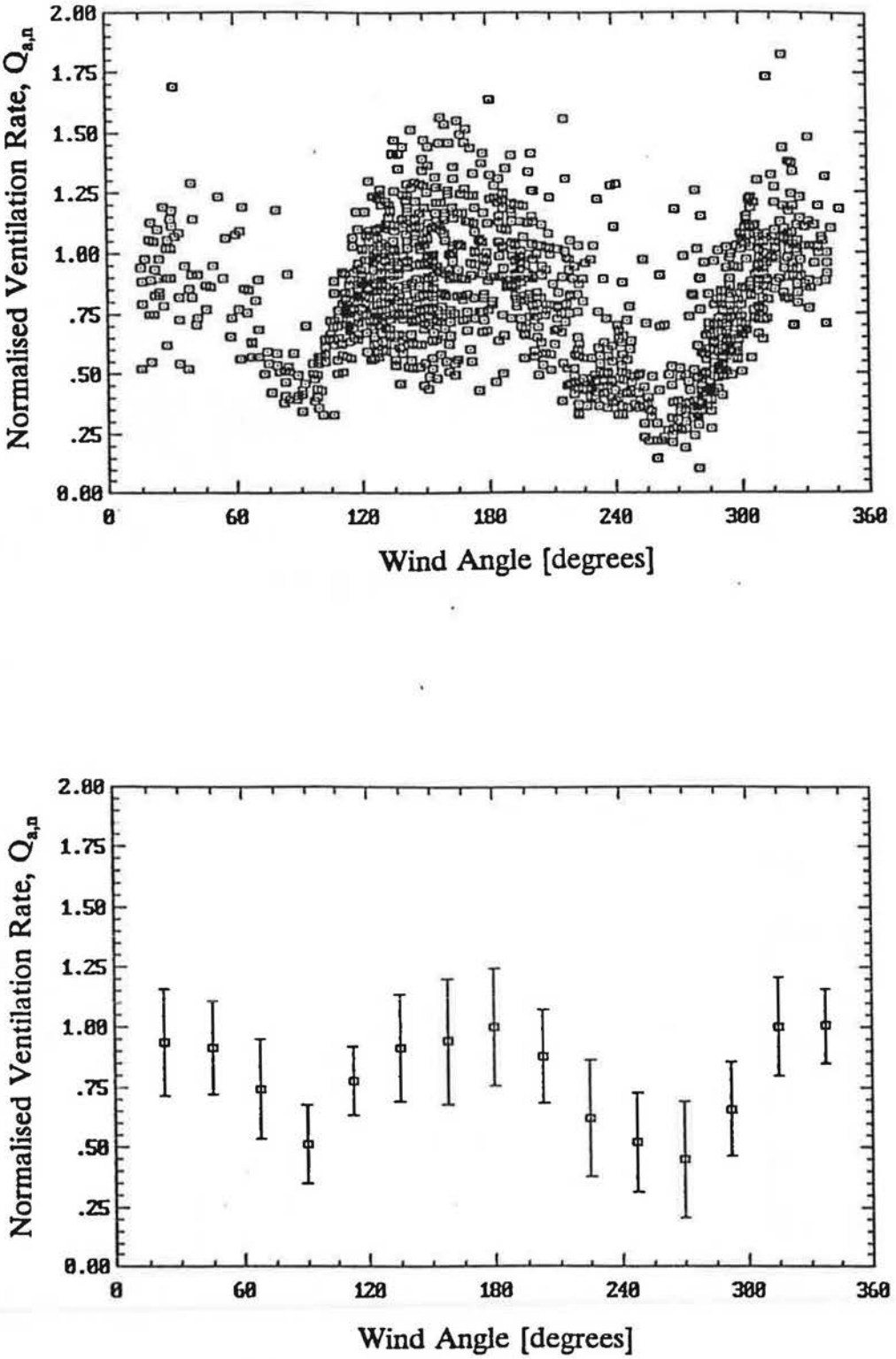

Figure 5-18. Effect of wind direction (wind shelter and pressure coefficients) on ventilation rate for attic 6 (1302 points).

individual data point, not the binned averages. These wind speed normalized ventilation rates are then divided by the mean wind speed normalised ventilation rate from the bin for south winds (180°). So the ventilation rate normalised for both wind speed and wind shelter effects, $Q_{a,n}$, (shown in Figures 5-17 and 5-18) is given by

$$Q_{a,n} = \frac{Q_a}{U^{2n}} \frac{1}{Q_{180}} \qquad (5\text{-}5)$$

where Q_{180} is the mean wind speed normalised ventilation rate for south winds. The southerly direction (180 degrees) was chosen because this direction contained a large amount of data and the houses experienced the least wind shelter.

Both data sets for attics 5 and 6 show a reduction in ventilation rate of approximately 50% for easterly winds (90°) and 70% for westerly winds (270°). The reduction in ventilation rates for westerly winds was slightly larger than for easterly winds and this small asymmetry is due to the air flow pattern over the houses which affects the surface pressure coefficients. For westerly winds, both attics 5 and 6 are sheltered by four identical houses. For easterly winds, attic 5 is sheltered by house 6 and attic 6 is only partly sheltered by the windbreak shown in Figure 5-1. The exact nature of the differing flow patterns and their effect on pressure coefficients would require detailed experimentation in a wind tunnel (or perhaps numerical simulation) and is beyond the scope of this study. Figures 5-17 and 5-18 show that the neighbouring houses provide a large amount of shelter for attics 5 and 6 that reduces ventilation rates by about a factor of three.

5.3.2 Attic fan ventilation

During the second year of testing, a ventilating fan was installed in attic 6 and tests were carried out for two modes of operation. The fan was operated depressurizing the attic (standard installation procedure) and then pressurizing the attic. As mentioned previously in section 5.1, the fan provided a maximum flow rate of 9.6 ACH and was cycled on between 10:00 am and 4:00 pm and off for the remaining portion of the day. The effect this has on ventilation rates in attic 6 can be seen in Figure 5-19A which covers a three day period from November 20 to 22, 1991. This period was selected because the ventilation rates for the first two days were relatively constant, while ventilation rates increased significantly on the third day due to increased wind speeds. For comparison purposes, the ventilation rates in attic

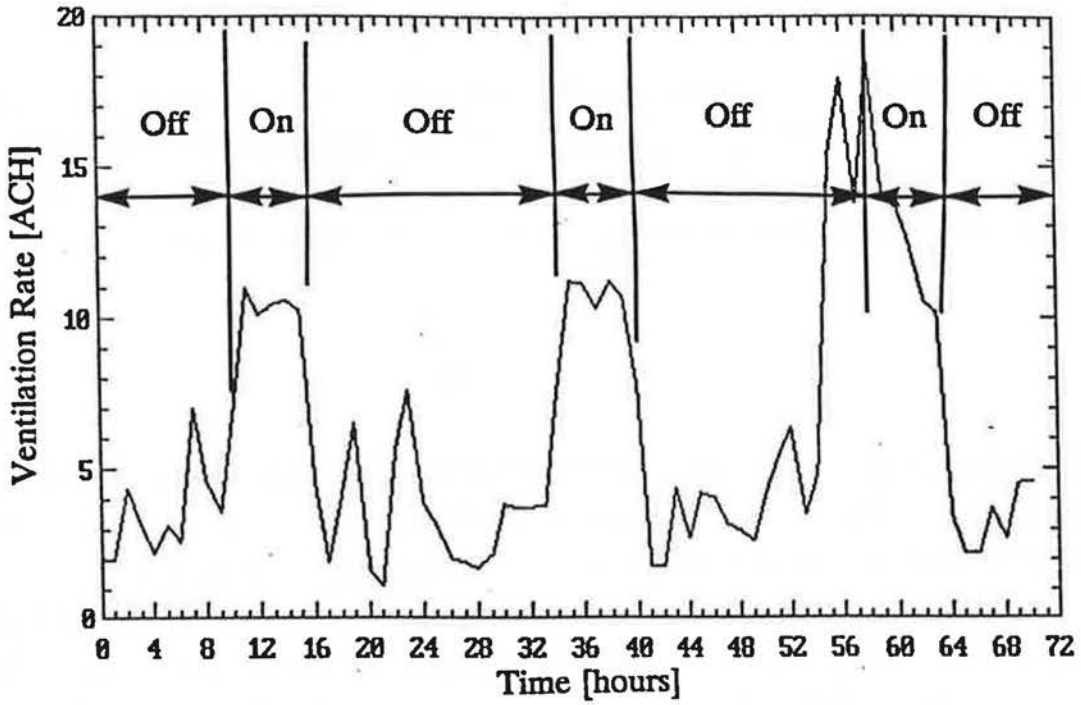

Figure 5-19A. Effect of ventilation fan on attic 6 ventilation rates.

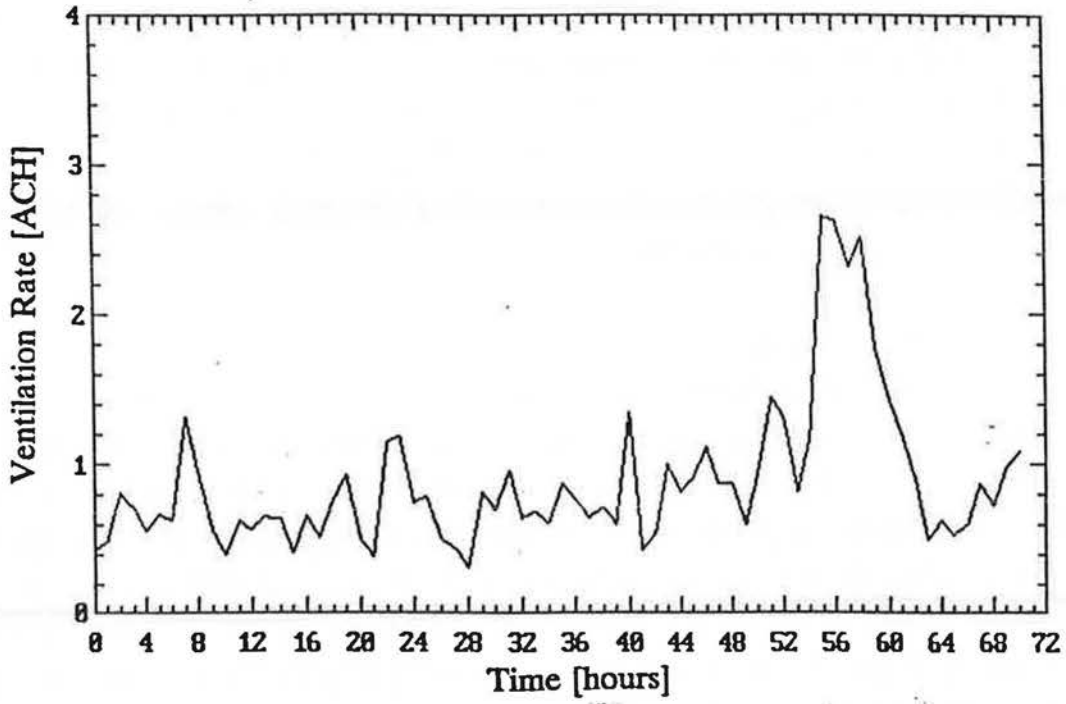

Figure 5-19B. Ventilation rates in attic 5 for the same time as Figure 5-19A, showing the increase in ventilation rates for the third day caused by increased wind speed.

5 over the same period are shown in Figure 5-19B and indicate relatively calm conditions the first two days with low ventilation rates and increased ventilation on the third day. When ventilation rates are low, the attic fan creates pressure differences across the attic envelope that are much larger than wind or stack effect pressure differences and for these situations attic ventilation rates are dominated by the fan. Over the first two days, the ventilation rates with the fan on averaged approximately 11 ACH and with the fan off, approximately 4 ACH. The fan contribution was therefore about 7 ACH, which is close to the maximum capacity of the fan. On the third day, the wind speed increased during the day resulting in an increase in the background ventilation rate to approximately 13 ACH while the measured rate was approximately 16 ACH. In this case, the fan did not increase the ventilation rate to the same extent as on the previous days because the wind-induced pressures on the attic envelope were relatively large.

5.3.3 Indoor to attic exchange rates through the ceiling

One of the important measurements obtained during the field monitoring program was the magnitude of the indoor-attic exchange rate and its dependence on outdoor weather conditions. Moisture is transported into the cool attic space when there is a sustained exchange of air from indoors to the attic and the interior heated space has a large relative humidity. During cold weather this moisture may deposit as frost which steadily accumulates. A sudden thaw will melt the frost with resultant water damage to the ceiling and an increase in sheathing and joist wood moisture content. Despite its importance, there are very few field measurements of the magnitude of this flow or its dependence on ambient weather conditions.

Measured indoor-attic exchange rates (expressed as ACH based on the attic volume) in attics 5 and 6 are shown in Figures 5-20A and 5-20B, respectively and are correlated with the indoor-outdoor temperature difference. As with previous temperature driven ventilation rate figures, the measurements have been selected for wind speeds less than 2 m/s to reduce the scatter. The individual hourly averages are shown as dots together with the average and standard deviation in each 5 °C wide bin. During extremely cold weather, there is a large sustained pressure difference across the ceiling due to the stack effect which results in exchange rates, on the order of 0.2 to 0.25 ACH (12 to 15 m^3/hr). This is approximately 60% of the total house ventilation rate (at the low ventilation rates induced by stack flow only). For stack dominated ventilation rate in the attics the ceiling flow rate represents about 10% of

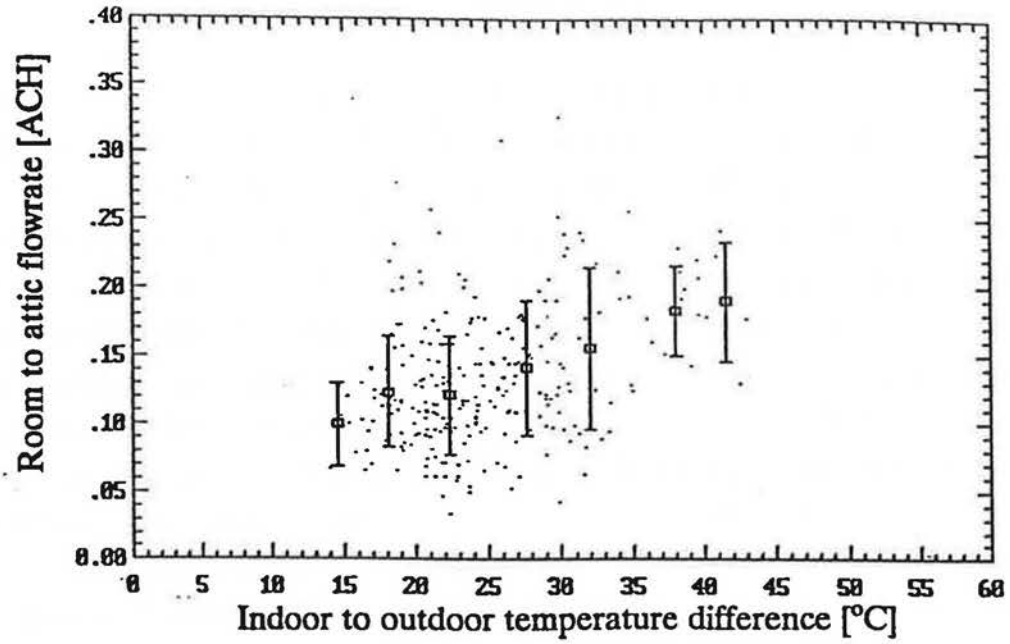

Figure 5-20A. Indoor-outdoor temperature difference effect on measured indoor to attic exchange rates for attic 5 for windspeeds less than 2m/s.

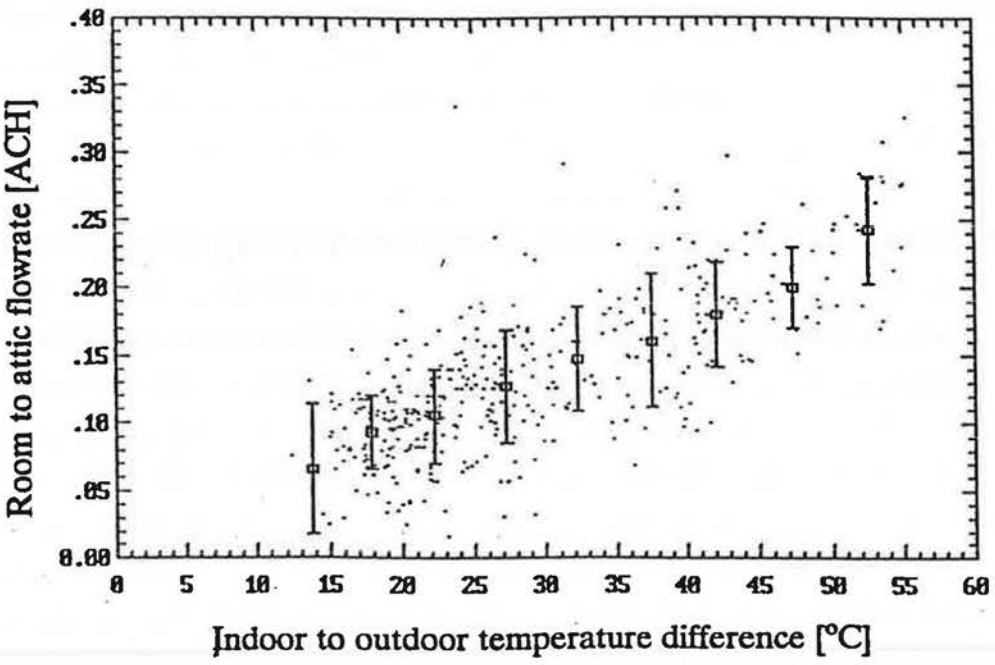

Figure 5-20B. Indoor-outdoor temperature difference effect on measured indoor to attic exchange rates for attic 6 for windspeeds less than 2m/s.

the total for attic 5 and only 2% for attic 6. When the wind speed is greater than 2 m/s the attic ventilation rates increase and the ceiling flow rate becomes difficult to measure because the attic concentration of SF_6 is too low. The ceiling flow rate is not a large fraction of the attic ventilation rate and results in the two zones for the ventilation model being only weakly coupled.

At the house interior conditions of 20°C and relative humidity of 40%, this maximum leakage flow will convect on the order of 100 grams of water per hour. The magnitude of the ceiling flow rates depends on the total ceiling leakage area and therefore these measured values are characteristic of test houses 5 and 6 at AHHRF. The indoor-attic exchange rates may also be correlated with wind speed. To look for this effect a typical set of measurements is shown in Figure 5-21 for attic 5 exposed to winds from the south (180°±45°). A relatively large wind angle bin was selected to provide enough data points. The data suggests that there is no obvious correlation of exchange rates with wind speed. The large scatter in the data probably obscures any correlation that may exist.

In a previous study by Cleary (1985), the room to attic exchange rates were measured on a single occasion. Cleary measured an exchange rate through the ceiling that was 25% of the total house ventilation rate and 3% of the total attic ventilation rate. Cleary's measurement shows that measured ventilation rates in other attics are similar to those found in this study.

5.3.4 Attic air and wood temperatures

The measured attic temperatures exhibit a strong diurnal cycle due to daytime solar gains and night time radiative losses. Figure 5-22 shows a spring day, where hour 1 is midnight, for attic 5. The south facing sheathing is heated the most and is more than 30°C higher than the outdoor temperature at its peak value at 2 p.m. (hour 15) in the afternoon. The truss and attic air temperatures are less than the sheathing temperature because they are not directly exposed to the radiative gains. The peak values do not occur at the same time due to the thermal masses involved and the attic air and the trusses lag behind the sheathing by approximately two hours. In addition, after the sun has set at about 7 p.m. (hour 19) the low thermal mass of the sheathing and its exposure to the cold sky temperature means that it cools faster than the attic air and the trusses. This is important because it implies that a steady state model of heat transfer that does not account for the thermal masses will not predict the correct magnitude or time variation of attic temperatures.

The night time cooling of attic sheathing due to radiation to the sky is

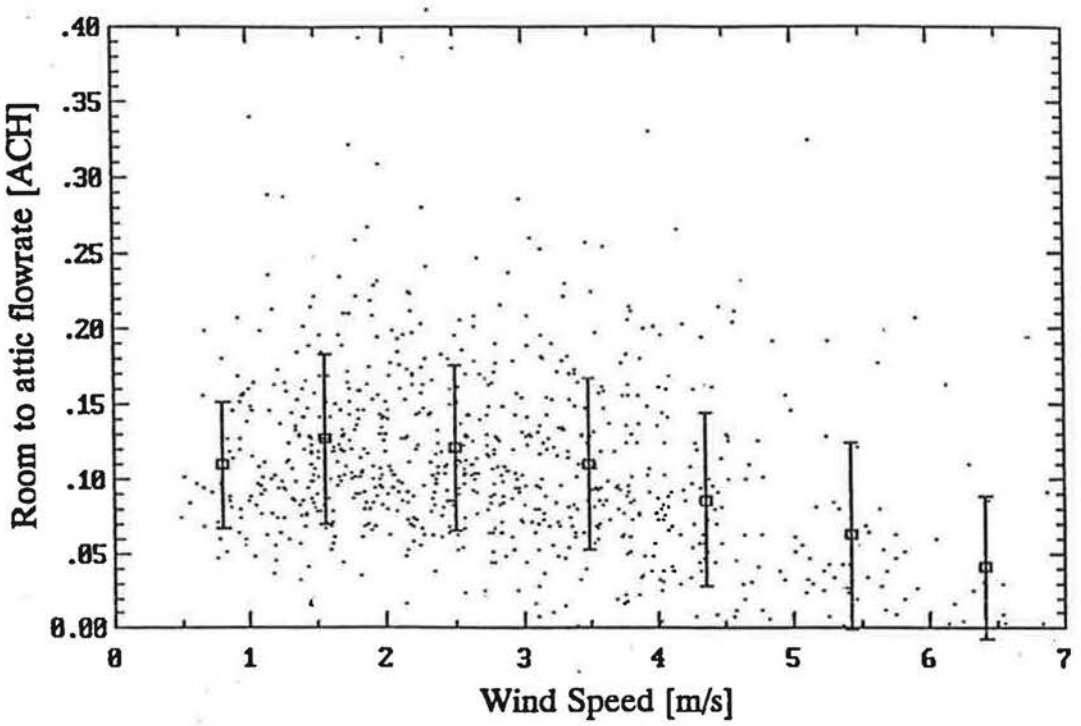

Figure 5-21. Effect of winsdpeed indoor to attic exchange rates for attic 5 for south winds (180°±45°).

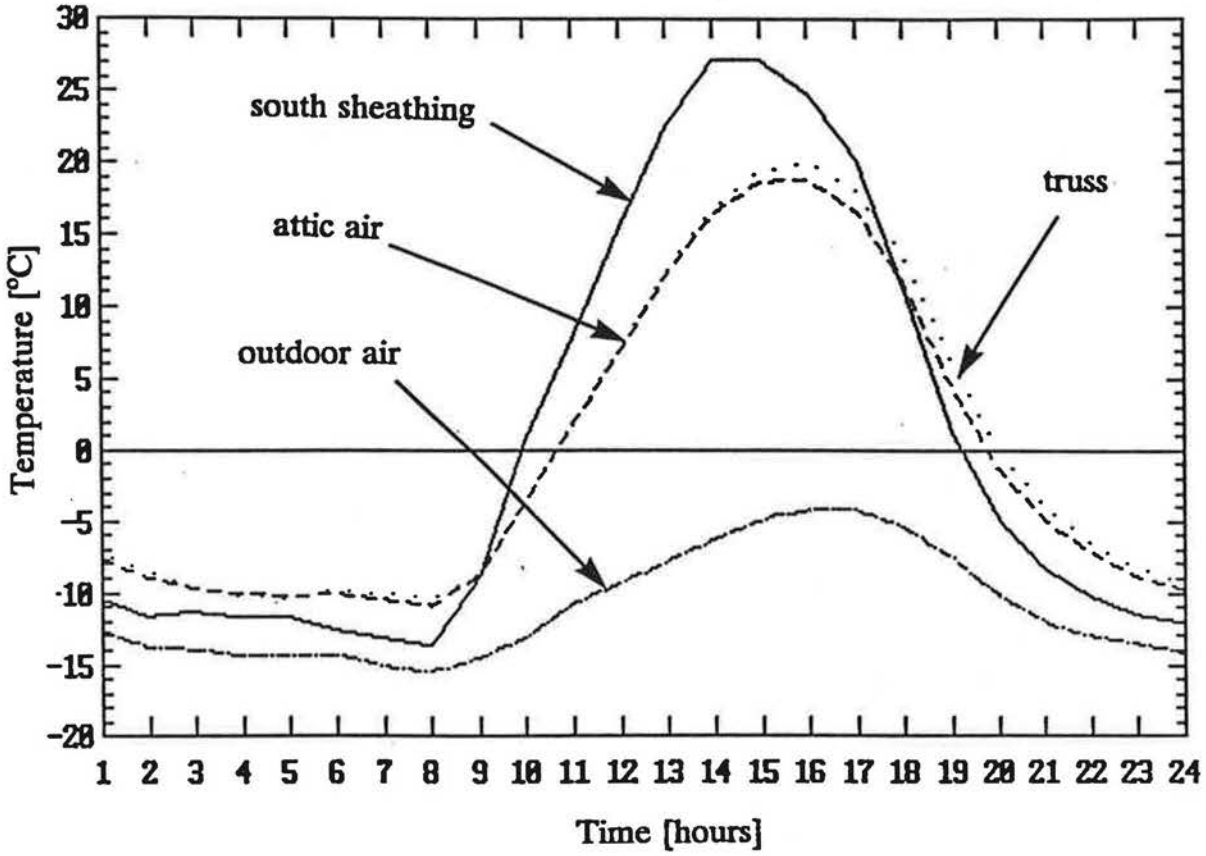

Figure 5-22. Diurnal variation of temperatures in attic 5 for March 12th 1991.

illustrated further in Figure 5-23 on a spring day for attic 6, where hour 1 is noon. The outer sheathing temperature drops 3 to 4 degrees below the ambient temperature and 4 to 5 degrees below the attic air. The inner sheathing shows less temperature depression of about 2 degrees below the attic air but is still the coldest attic surface. This is important for night time moisture deposition on the sheathing surfaces.

5.3.5 Wood moisture content

Typical results for wood moisture content are shown in Figure 5-24 for a heating season (5 months). The results shown in Figure 5-24 are for the north and south sheathing in attic 5. At the low values (below 7%) of wood moisture content shown in Figure 5-24, the wood moisture meter is at its operating limit and therefore all that can be realistically inferred about the measured values is that they are at or below about 7%. Because of the uncertainty in these low values of wood moisture content the small rise and fall of about 2% over the heating season does not imply any seasonal moisture storage in the sheathing. These low values are because the measuring pins for measuring wood moisture content are sealed below the surface and do not see the larger changes in moisture content at the wood surface. These measurements are useful for verification of the model predictions of the inner wood moisture contents as they should indicate that the wood remains dry as shown by this data. These measured values do not give any information about the moisture content of the surface layer. Therefore, it will not be possible to verify model predictions for the surface layer, except to see if moisture is condensed as frost (as was occasionally observed by visual inspection of the attics during winter months).

5.4 Summary of measurement program

The measurement program for this study was undertaken in order to find the range of factors influencing moisture transport in attics and to provide data for verification of the ventilation, heat transfer and moisture transport models developed in the preceding chapters. The measurements were hourly averages made in two attics at the Alberta Home Heating Research Facility. Attic ventilation rates were measured using a constant concentration tracer gas system. House to attic exchange rates were measured by the same system using two different tracer gasses for the house and the attic (SF_6 and R22 respectively). Temperatures were measured in both houses and attics using thermocouples. Relative humidity sensors monitored the moisture content of the air inside the houses and attics and outdoors. Wood

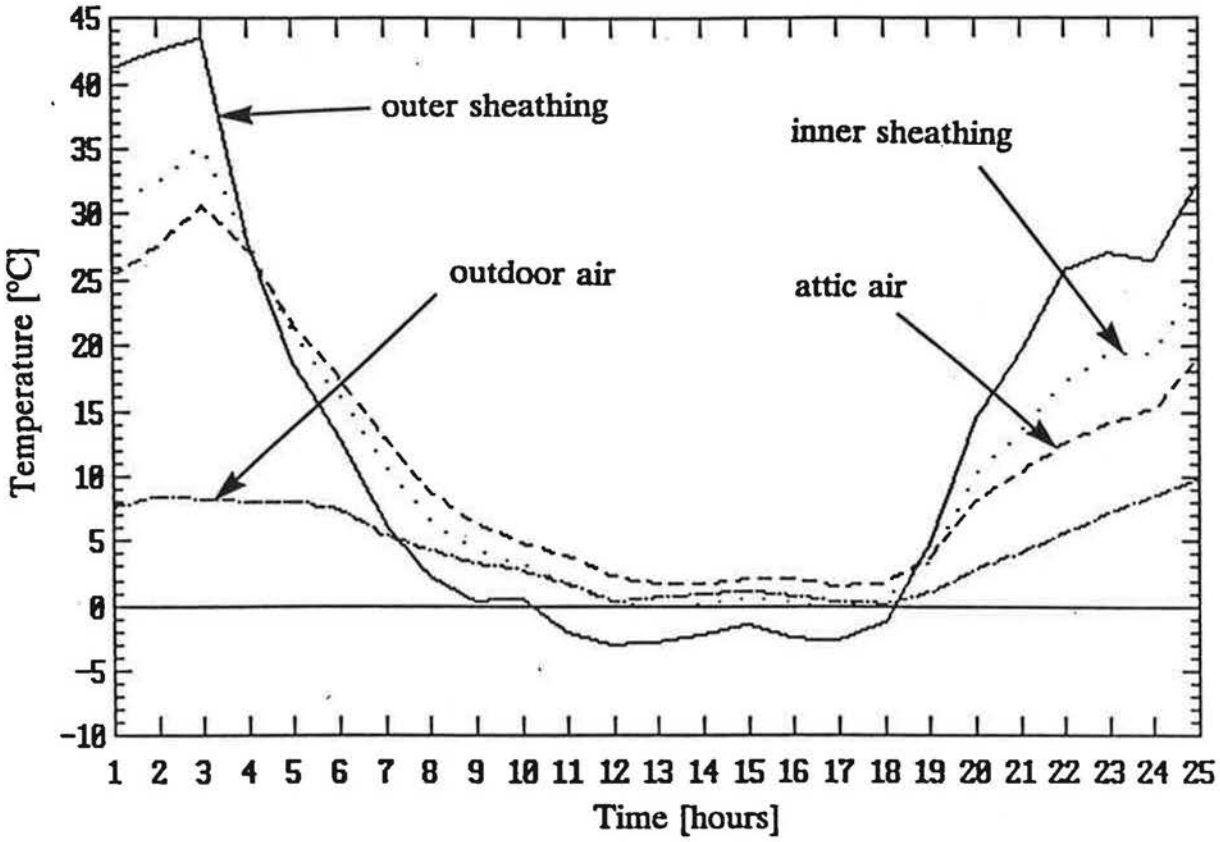

Figure 5-23. Diurnal variation of temperatures in attic 6 for April 9th and 10th 1991.

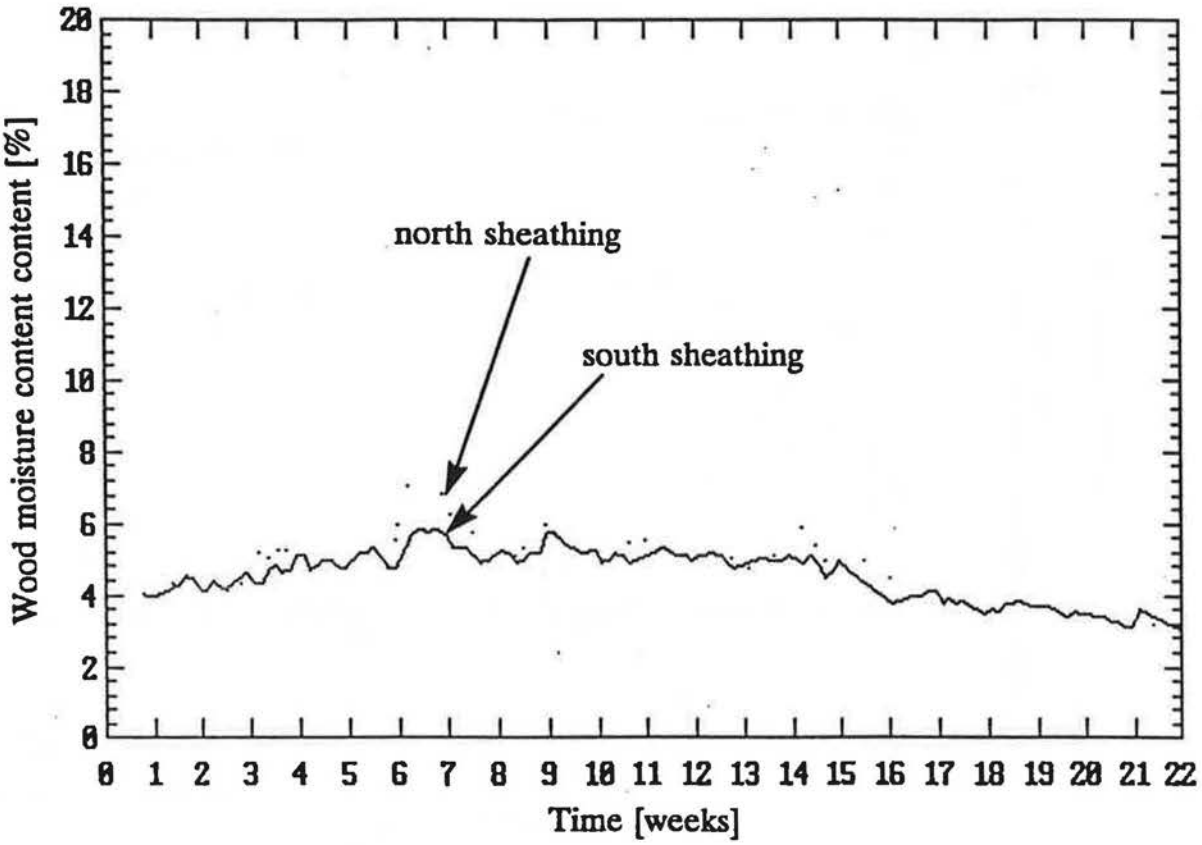

Figure 5-24. Measured wood moisture content in attic 5 over the heating season from December 1991 through April 1992.